DEVELOPMENT OF A THERAPEUTIC TRANS – SCLERA ILLUMINATED LASER DELIVERY DEVICE FOR RETINAL PATHOLOGIES

TEO KENG SIANG RICHARD

NATIONAL UNIVERSITY OF SINGAPORE

2008

DEVELOPMENT OF A THERAPEUTIC TRANS – SCLERA ILLUMINATED LASER DELIVERY DEVICE FOR RETINAL PATHOLOGIES

TEO KENG SIANG RICHARD

(M.B.B.S, NUS)

A THESIS SUBMITTED FOR

THE DEGREE OF MASTERS OF SCIENCE

DEPARTEMENT OF OPHTHALMOLOGY

NATIONAL UNIVERSITY OF SINGAPORE

2008

ACKNOWLEDGEMENTS

TABLE OF CONTENTS

SUMMARY

Laser photocoagulation has been the corner stone of treatment for various retinal pathologies such as diabetic retinopathy. Much has progressed since the 1960s and the technological breakthrough in photonics, optics, hardware processors and software programmes has contributed to the advancement of laser emission, optical lenses and the imaging of the fundus. However, one component of the treatment protocol has remained very much unchanged: the laborious 'mammoth' task of manually delivering hundreds to thousands of laser shots to the retina in a piecemeal fashion. Such procedures are tedious, operator dependent and the inconsistency compromises the efficacy and safety of the treatment process. The long duration and multiple episodes of such laser delivery have made the procedure uncomfortable and dreaded by patients.

This thesis describes the design of a computer assisted laser delivery for the treatment of diabetic retinopathy. The proposed model takes into account of both clinical and engineering issues such as the treatment criteria, safety considerations and usability factor. Some of these challenges include the limited slit-view of the retina, fatigue experienced by the ophthalmologists due to prolonged handling of the fundus lens with concurrent manual delivering of laser and the need for patient to keep their eye still during the procedure. Various existing solutions are analyzed and their relevance investigated. These consisted of ophthalmic imaging methods, laser delivery systems, lens refractory techniques and eye fixation devices.

The proposed novel integrated system consists of a trans-sclera illumination imaging device that is equipped with an eye stabilizing vacuum fixation ring. A second optomechanical component consists of a beam steering and laser source sub-system. These systems combined to provide the ophthalmologist a global view of the entire retina while the computer controls the positioning of the laser beam on the retina, the spot size and regulates the power accordingly with minimal human intervention during the procedure.

LISTS OF FIGURES

LIST OF TABLES

1   INTRODUCTION

1.1   Introduction to Diabetic Retinopathy

Diabetic retinopathy, a complication of diabetes, is one of the main causes of blindness for adults aged 24 to 44 years old, and the second most common cause of blindness in people who are 45 to 74 years old[1]. Nearly all patients suffering from type 1 diabetes and 60% of patients with type 2 diabetes develop symptoms of diabetic retinopathy after the first 20 years of the disease[2]. Studies have shown that up to 21% of patients with type 2 diabetes had retinopathy at the time of diagnosis of diabetes[3, 4].
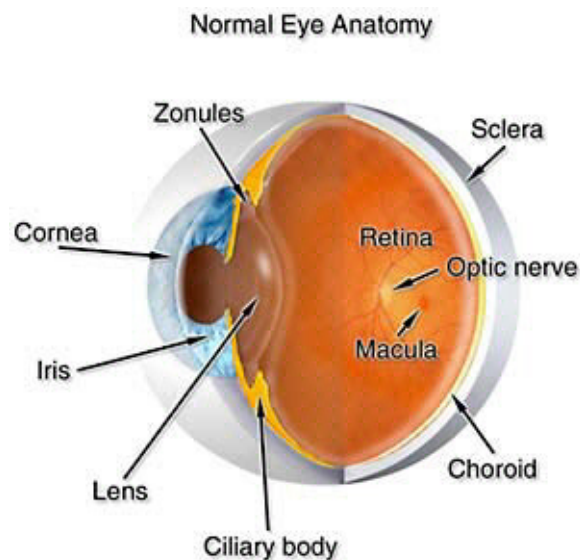
Figure 1.1: An eye anatomy showing both the anterior and posterior portions of a human eyeball
(Adapted from: http://www.maculacenter.com/images/illustrations/eye.jpg)

In the earliest phase of the disease, the arteries in the retina begin to weaken and leak, forming small, dot-like hemorrhages. These leaking vessels often lead to swelling or edema in the retina and decreased vision[5].

The next stage is known as Proliferative Diabetic Retinopathy (PDR). In this stage, circulation problems cause areas of the retina to become oxygen-deprived. In an attempt to maintain adequate oxygen levels within the retina, a process called neovascularization takes place. Due to the nature of diabetes, the blood vessels

formed are fragile and hemorrhage easily. Blood may leak into the retina and vitreous, causing spots or floaters, along with decreased vision.
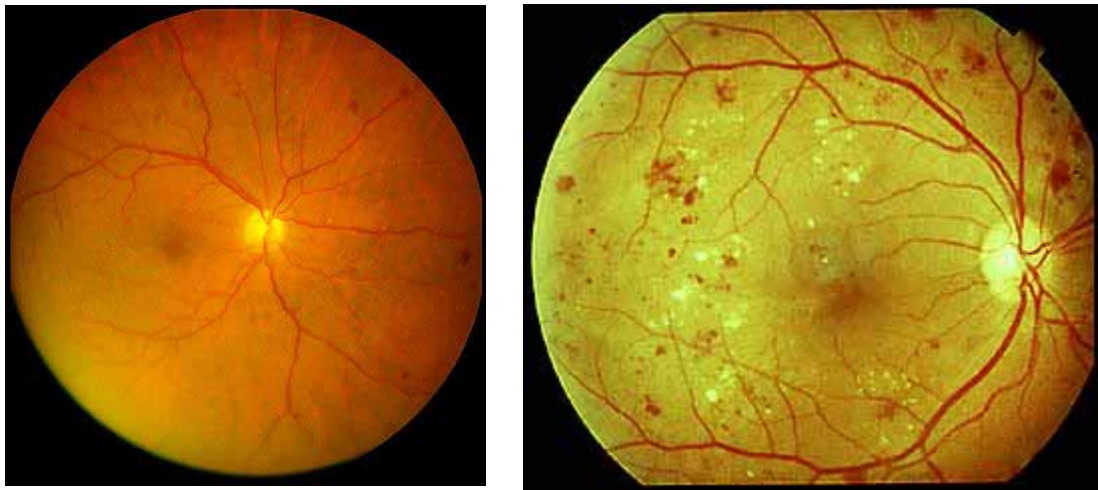
Figure 1.2: A comparison of a normal retina (left) with a retina of a patient suffering from diabetic retinopathy
(Adapted from: http://www.medibell.com/images/retina.jpg and http://www.retinaphysicians.com/images/supplied/june/134-K40-diabetic-hard-exuda.jpg)

In the later phases of the disease, continued abnormal vessel growth and scar tissue may cause serious problems such as retinal detachment and glaucoma. Eventually a total loss of vision would occur.

Thus, vision loss due to diabetic retinopathy results from several mechanisms. Central vision may be impaired by macular edema or capillary non-perfusion. The development of new blood vessels due to PDR and contraction of the accompanying fibrous tissue can distort the retina and lead to tractional retinal detachment, producing severe and often irreversible vision loss. Moreover, the new blood vessels may bleed, adding the further complication of pre-retinal or vitreous hemorrhage.

In 2007, Singapore has about 275,000 diabetics. Another 500,000 have impaired glucose tolerance, which is also called pre-diabetes[6]. In a screening program involving 13,296 diabetic patients over a two-year period, 22% of patients were found to have retinopathy and 11% had sight-threatening retinopathy that required treatment[7]. As one in 10 diabetics suffers from diabetic retinopathy, this disease is

prevalent in the society. Hence continual improvement in the efficiency of the treatment methods as well as the usability of the treatment apparatus is necessary.
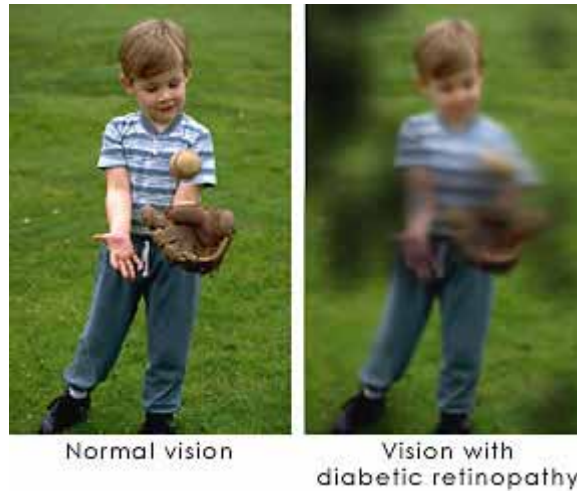
Figure 1.3: Effect of diabetic retinopathy on vision.

(Adapted from: http://www.stlukeseye.com/Conditions/DiabeticRetinopathy.asp)

1.2   Literature Review

1.2.1   Rationale of the Laser Photocoagulation Treatment

Retinal photocoagulation has been the definitive treatment in the management of diabetic retinopathy over the last three decades. The Early Treatment Diabetic Retinopathy Study (ETDRS)[8,9] and Diabetic Retinopathy Study (DRS)[10] demonstrated the overwhelming benefit of scatter photocoagulation for proliferative retinopathy, while focal photocoagulation was shown to reduce moderate visual loss from clinically significant macular edema. However in recent years, there has been much research and advancement in the medical treatments. The use of new agents such as anti-angiogenics, vascular endothelial growth factor inhibitors, protein kinase C inhibitors, aldose reductase inhibitors, advanced glycated end-product inhibitors and growth hormone antagonist have shown interesting and promising results[11-13]. Furthermore, treatments to manage blood pressure and lipid levels have improved the management of diabetic complications; such innovative therapies that directly target the microvascular complications are on the horizon[14,15]. But as promising as the on going medical treatment trials may sound, it has been generally accepted that they are being considered complimentary to, and not replacement for, the best practices now being applied. Retinal photocoagulation will remain a corner stone and important component of the management of diabetic retinopathy.

Photocoagulation for the treatment of diabetic retinopathy was first performed by Meyer-Schwickerath in the 1960s. He made the initial attempts to inhibit new growth of vessels in the proliferative form of diabetic retinopathy by cauterizing them with heat from a xenon arc imaged on the retina. Subsequent invention of the ruby laser replaced the xenon arc as it was able to increase the energy available at the retina with a smaller but more discrete lesion. Early attempts to coagulate specific retinal vessels with the ruby laser were not successful although Aiello et al[12]. did manage to treat cases of proliferative retinopathy with scatter ruby laser photocoagulation and yielding satisfactory results. L'Esperance[17] pointed out the emission of the ruby laser was poorly matched to the absorption spectrum of hemoglobin and that the blue / green emission spectra of the argon laser was well absorbed by hemoglobin. Thus the argon laser was thought to have the potential advantage in the treatment of

proliferative diabetic retinopathy by causing the blood within the retinal vessels to clot easily. However the concept of direct coagulation of the new vessels was challenged after the National Eye Institute conducted a large, double-blind, randomized prospective clinical trial – The Diabetic Retinopathy Study (DRS) has demonstrated convincingly that pan retinal photocoagulation with the argon laser was indeed effective in the management of proliferative diabetic retinopathy. This study also showed that xenon arc photocoagulation was effective, and previous studies with ruby laser (as mentioned above) were similarly effective. Furthermore it appeared that the success of any photocoagulation was proportional to the amount of retina treated. This led to the proposed model that photocoagulation is effective in inhibiting retinal neovascularization in proliferative retinopathy because it facilitates oxygenation of the inner retina by diffusion from the choroid. This appears to occur through the photic destruction of the major oxygen consuming cells in the retina, the rods and cones. The photocoagulation energy is mainly absorbed by the retinal pigment epithelium (RPE) with subsequent thermal conduction and destruction of adjacent photoreceptors. These receptors have the majority of the mitochondria in the retina (almost 90%) and responsible for more than 50% of the oxygen consumption in the retina. Furthermore, the major targets of the laser treatment – the RPE and photoreceptors, are not supplied by the retinal vessels but the choriocapillaries. With

Figure 1.4: Fundus Images of the retina before and after laser treatment.
(Adapted from: http://www.medibell.com/images/retina.jpg and
http://www.medibell.co.il/clinical/im_gallery.asp)

this in mind, Wolbarsht explains how the choroidal circulation regulates the retinal circulation and thus the rationale of photocoagulation therapy for proliferative

retinopathy. The destruction of the oxygen consuming photoreceptors leads to a higher oxygen tension from the choroidal supply to the inner retina. This could possibly lead to constriction of the retinal vessels circulation with subsequent atrophy.

1.2.2 History of Laser Photocoagulation System Development and Attempts at Automation

Since its introduction in the 1950s, the laser photocoagulation method of treatment had evolved in its choice of treatment laser[16,17] and the coupling of a slit lamp with articulating arms containing mirrors to deliver the laser beam[18].

In the 1970s, a system comprising of a contact lens, aiming beam and a control joystick was used to place the laser beam on the retina. This system, which is still used today, brings about a higher degree of precision in positioning the laser and allows for the varying of laser spot size, power and pulse duration during the course of treatment.

There had been many attempts at developing an automated system that would track and deliver laser shots to the retina since the early 1970s. One of the first applications of a video camera to track the retina was discussed by C. Berkley at the Workshop on Television Ophthalmology in 1965[19].He suggested that the retinal image could be held steady by fixing on a portion of the retinal image with feedback signal. Kelly and Crane analyzed the fundus tracker issues in 1968[20] and proposed the use of a circular scanning technique instead of the usual X-Y scanning technique. They demonstrated how picture registration could be performed with just a single scan around the optic disc, in a complete circle. However the tracker was never built as the means to accomplish registration in real time was not available. Crane continued researching with Cornsweet and Steele and designed a three-dimensional eyetracker[21,22]. This device uses two purkinje-images (the reflected images from the surface of the cornea and lens) to track the anterior part of the eye. Timberlake and Crane used this device to develop a stabilized laser for photocoagulation of the retina in 1985[23]. Once the operator positions the laser, the system monitors small movements of he anterior surface of the eye and adjust the two mirrors such that the laser remains locked at one location on the retina. It has an accuracy of one minute of arc and has a response time

of 1ms. It has been shown to track the retina relatively well in a controlled, experimental setting although the equipment setup was expensive and the optics involved was complicated. There are other current systems that track the anterior segment of the eye, but tracking the anterior part of the eye does not necessarily track the posterior part of the eye. This is in part due to the fact that eye movement is not strictly rotational and that small error at the anterior segment is magnified in the posterior segment. Furthermore the computational time taken for real time translation of anterior segment tracking to the posterior region reduces the reaction time of the system such that it is not clinically applicable. Thus it is inevitable that direct tracking of the retina has to be in place for accurate and automated practical application of laser in the posterior segment. There exist other methods of retina tracking such as scanning laser opthalmoscopy[24,25] but such setup becomes clinically not applicable once the laser delivery component is incorporated.

However much that these early works have contributed towards laser delivery to the retina, it was not until researchers at the University of Texas at Austin started work in 1984 towards the development such an automated laser system that we have come closed to realizing a clinically useable system. In 1987, Markow detailed a plan for a 'robotic laser system for ophthalmic surgery'[26]. This conceptual system controls lesion parameters and placement on the retina for the treatment of diabetic retinopathy, tears and macular degeneration. Although it was limited by available technology, Marlow demonstrated the feasibility of such a system. His work provided a framework for subsequent researchers that followed.

The early works of this group of researchers involve the transformation of what were previously immeasurable lesion parameters to measurable lesion reflectance. Yang[29], a fellow researcher of Markow's, extended the work of Bringruber et al[27]. and Weinberg at al[28]. and demonstrated how a two dimensional reflectance image could be used as a feedback signal to control lesion parameters. She was able to control the diameter of the lesions to within six percent of the desired dimension; however lesion depth varied from 15 to 38 percentage of that desired[29]. Jerath went on to investigate the use of central lesion reflectance as a feedback signal to produce uniform lesions despite variation in tissue absorption or changes in laser power *in vivio* on pigmented rabbits. She used the average gray level from the five central pixels of the forming

lesion as a signal to control lesion depth[30]. Recent attempts by Maharajh to correlate other lesion reflectance related parameters include lag time between laser onset and lesion formation, the rate of lesion reflectance intensity increase, and the initial slope of the increase as a measurable indicator of lesion depth[31]. This was an extension of the work began by Inderfurth et al. The confocal reflectometer used to collect this reflectance data during laser irradiation was developed by Ferguson[32].

A system to compensate for retina movement was developed by Barrett[33]. This helps to stabilize the irradiating laser on a specific retinal lesion site. The main component of the system is a tracking algorithm that uses six vessel templates locked together to form a two-dimensional 'fingerprint' of the retinal surface. A limited exhaustive search technique is applied to the algorithm to find the blood vessel 'fingerprint' pattern on video images of the retina. This information serves to update the positioning of the irradiating laser and thus help 'locked' the laser on a specific retinal coordinate. Barret was able to demonstrate the capability to control lesion placement in vivo on pigmented rabbits[34]. This system was able to provide accuracy within a 100 micron target radius for retinal movement of less than two degrees per second. This concept / prototype system was further improved and transformed into a clinically significant system by Wright[35,36]. He rewrote the tracking algorithm and upgraded some of the hardware and was able to achieve retinal tracking speed of 70 degrees per second. This setup was able to maintain an error radius of 100 microns while tracking up to ten degrees per second. More significantly, Wright also quantified the engineering requirements for a clinically practical system: retinal tracking speed of more than 10 degrees per second, laser pointing resolution of 100 microns, system response time of less than 5ms, and reproducibility of uniform lesions of specified parameters.

Due to the limitation of technology and affordability at the point in time, Ferguson and Wright[37-39] combined the analog confocal reflectometer with the digital tracking system for a hybrid analog-digital tracking system named CALOSOS for Computer Aided Laser Optics System for Ophthalmic Surgery. This was necessary as the digital system provides global tracking of the retina at the expense of response time. Although it could maintain lock on retinal velocities up to 70 degrees per second,
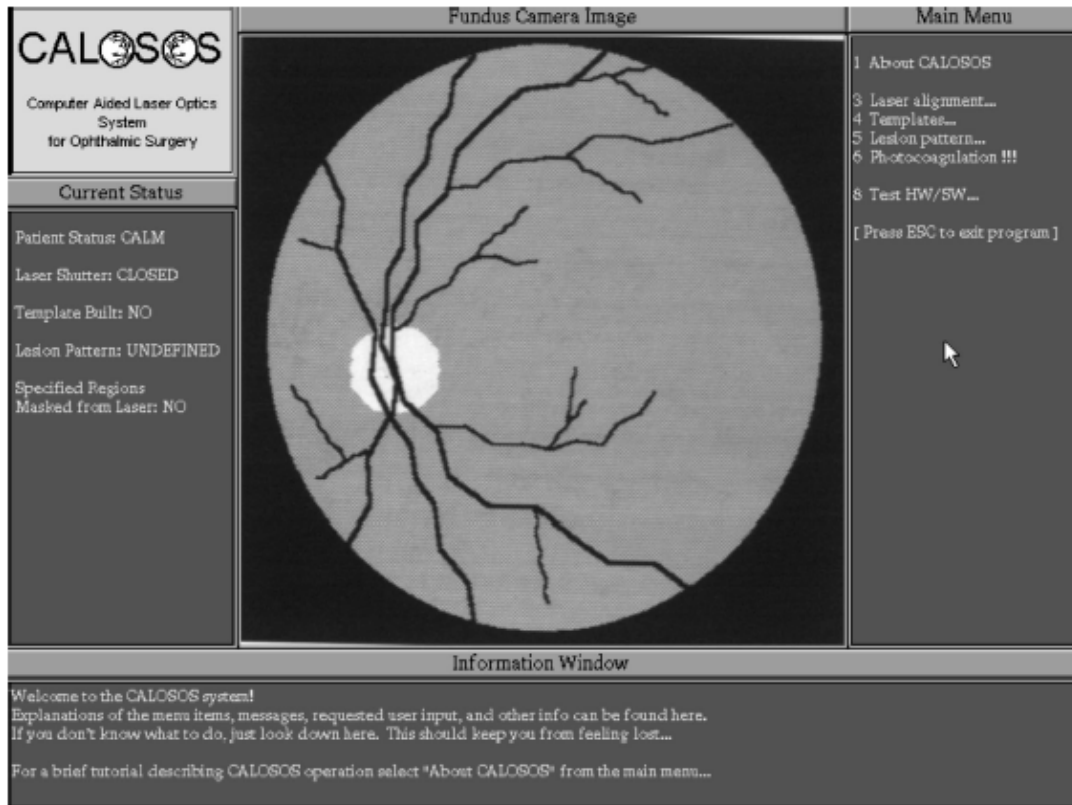
Figure 1.5: An example of the user interface for CALOSOS. The fundus camera signal shown is a simulated retinal image.
(Adapted from Wright CH et al[38])
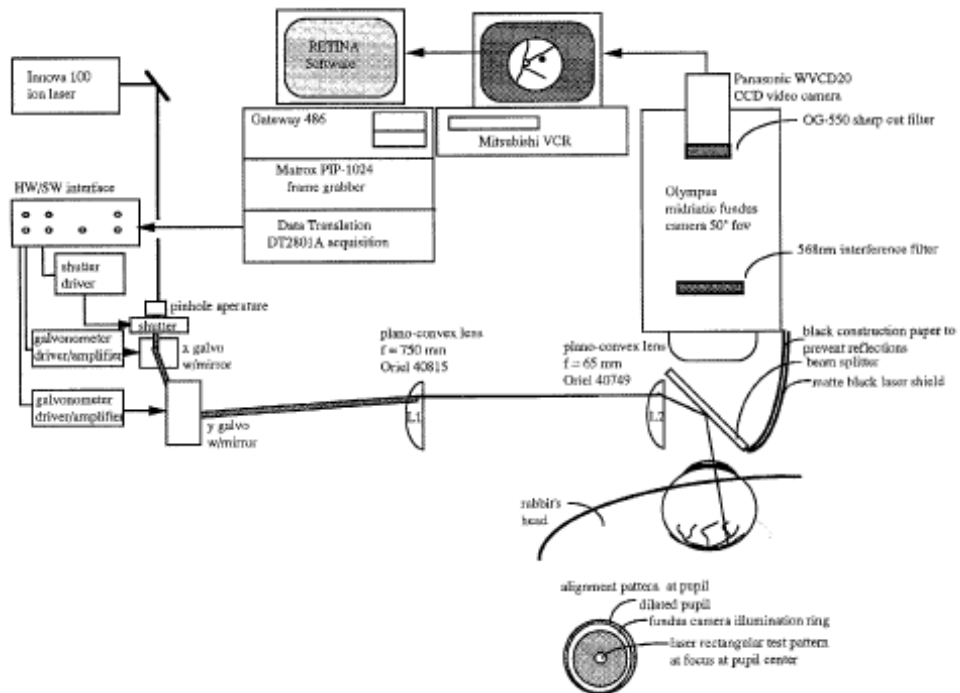
Figure 1.6: The schematic diagram showing the CALOSOS set-up
(Adapted from: Barrett SF et al[34])

factoring the need to localize the irradiating laser to a 100 micron error radius reduces the tracking speed to 10 degrees per second. The digital based system is limited by the standard video frame rate of 30 fps, which translates to a response time of 33ms. Whereas the analog system is able to maintain local lock on a formed lesion within a 100 micron error radius and has a response time of 5ms but once it loses lock, it would not able to 'relocate' itself and hence the requirement for the hybrid analog-digital system.

Limitation of CALOSOS

Although there is on going work in improving the above system, it is directed towards a non contact, small field of view and a piece meal approach to the delivery of laser to the retina. This approach has its limited practical application as it assumes patients to be consistently co operative and well trained to follow commands. More significantly, the decrease field of view with piece meal approach would result in an extremely complex integration of the tracking and processing of the entire retina image such that the response time would not be clinically viable. Such a system also does not allow delivery of laser to the anterior aspect of the retina, such as beyond the equator or pars plana. Thus it is not surprising that given this approach, there is no single successful attempt in automated delivering of a complete therapeutic dose of laser shots encompassing the entire retina of interest in any experimental animal model.

Furthermore, the fundus imaging systems used in the above mentioned research are designed to photograph the posterior pole of the fundus in fields of view that range from 20° to 60° and are limited to providing piecemeal view of the posterior pole of the eye. Technically fundus photography is somewhat challenging because of the small size of the pupil through which the fundus can be observed. This influences both ability to illuminate the fundus properly and the ability to collect the light reflected from it. Current fundus imaging systems illuminate the retina through the pupil by a light source that is located in the region of the camera and is directed into the posterior segment of the eye. This limits the illumination within the immediate macula region. Thus these conventional fundus cameras depend strongly on a dilated pupil and clear ocular media. Furthermore they are limited to a maximum of 60° field of view at any one time. In addition, these systems suffer from the reflections of the

illuminating light off the cornea, crystalline lens, pseudophakic lens and its interface with the vitreous cavity. Attempt to increase the illumination would create 'hot spots' and result in poor quality of the image captured. Even with ideal illumination, without any direct contact of lenses or prism with the eye, the field of view would be limited to about 60°.

1.2.3 Review on Current Laser Photocoagulation System

The current laser photocoagulation system comprises of a laser delivery and beam steering system which is coupled together with an illumination system. The vision system is arranged confocally with the beam delivery and illumination system. All three system components will passes through the fundus lens and the cornea, enter the eye through the pupil and reaches the retina (Figure. 1.8).
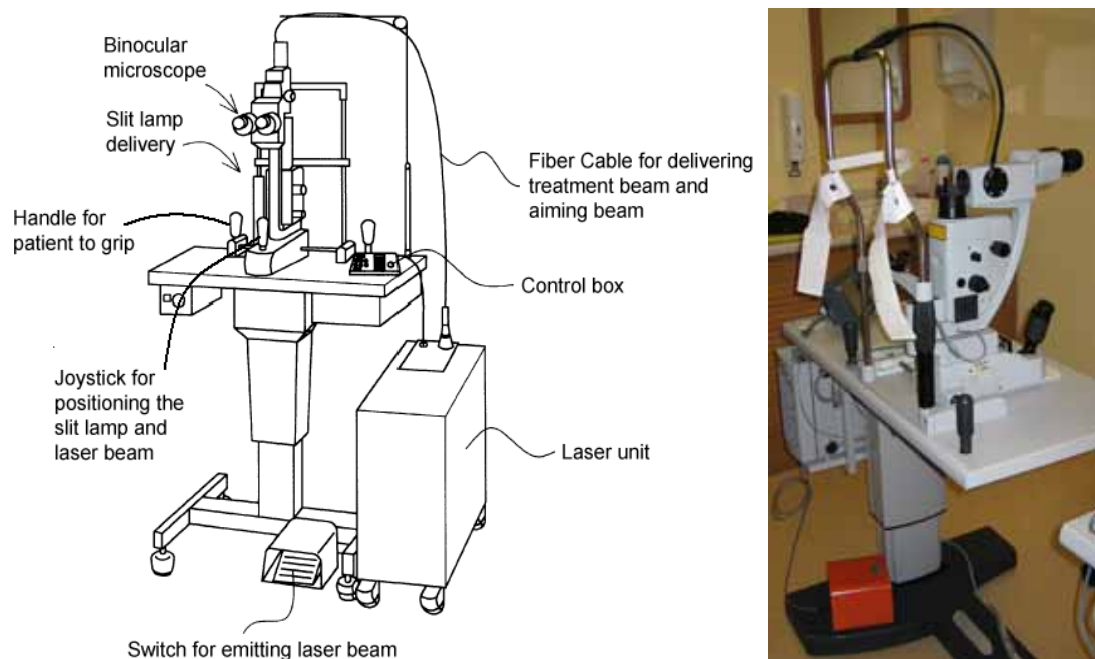
Figure 1.7: Current laser photocoagulation treatment apparatus used for treatment of Diabetic Retinopathy.
(Picture taken at: Eye Clinic, National University Hospital, Singapore)
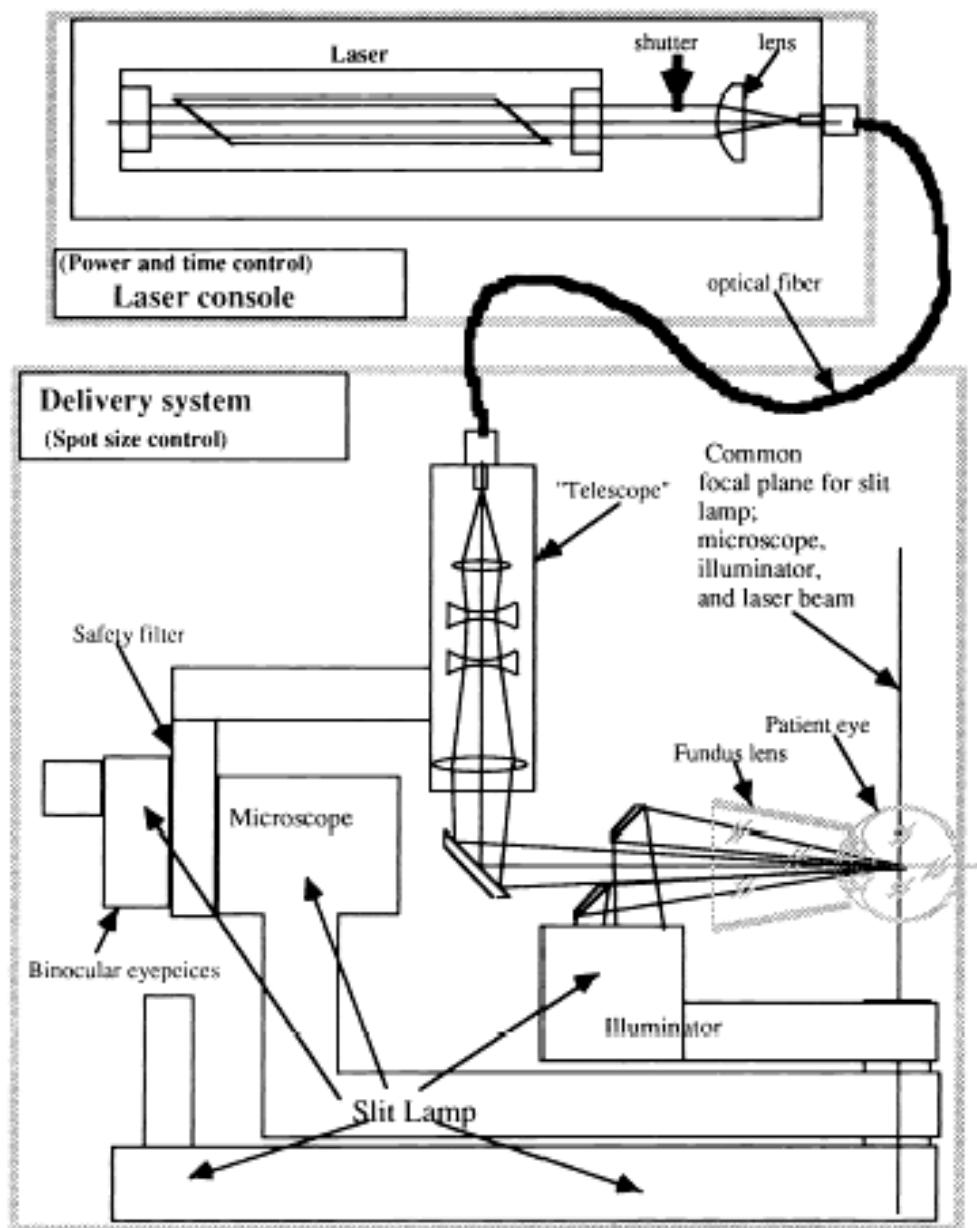
Figure 1.8: Schematics of a laser delivery system.
(Adapted from: Dewey D. (1991). Corneal and retinal energy density with various laser beam delivery systems and contact lenses. SPIE Ophthalmic Technologies. Vol. 1423: 105-116.)

Current laser photocoagulation system consists of a slit lamp biomicroscope and a compatible laser console (Figure 1.9)

Laser system integrated

Laser system detachable
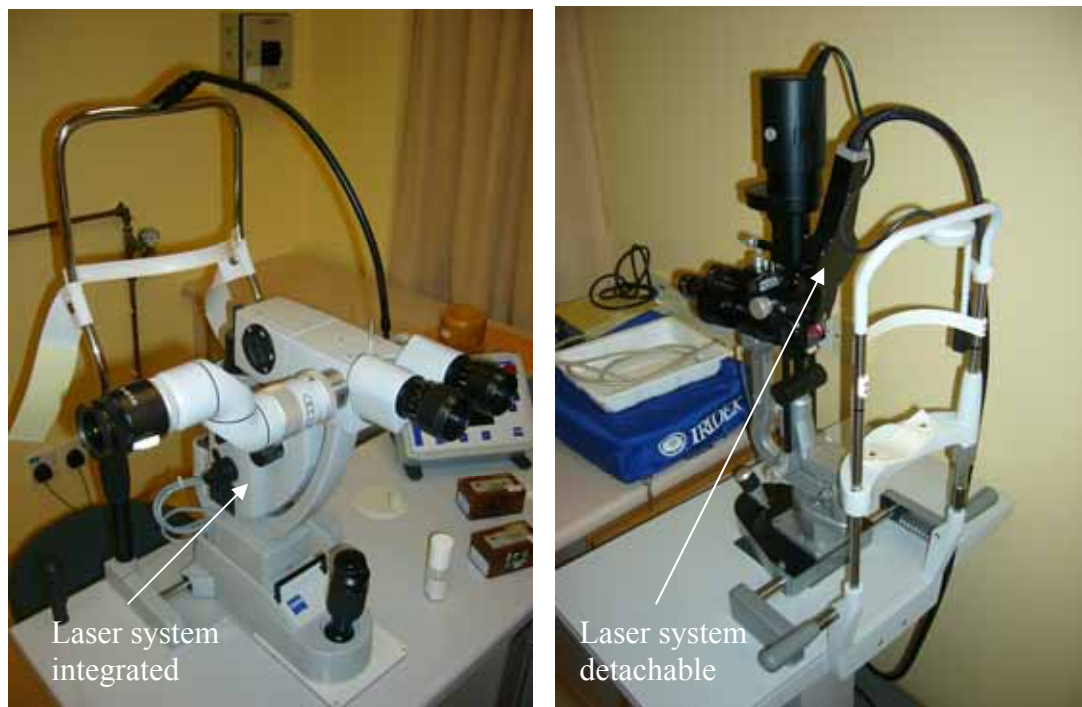
Figure 1.9: Variations of Slit Lamp Biomicroscope / Laser combination systems used for photocoagulation treatment
(Picture taken at: Eye Clinic, National University Hospital, Singapore)

Description of a typical photocoagulation system: Carl Zeiss® Visulas 532

- o Solid State, Diode-pumped
- o 532nm wavelength providing 1.5W of power
- o Visible, grey white burns appearing on the retina surface

To patient

Laser Path

Slit lamp camera (With light source and magnification). For observation of patient's eye

Rotation of laser tower for wider angle to reach extreme end regions of the retina
Normally, it is aligned with the slit beam camera in a same path

Laser Tower
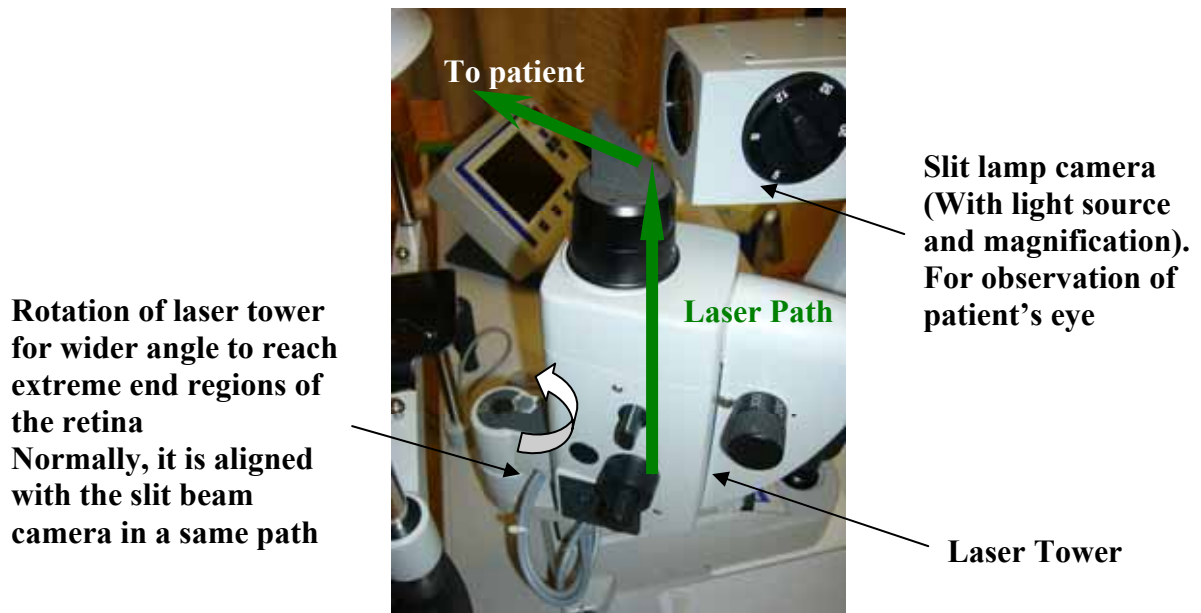
Figure 1.10a: Carl Zeiss® Visulas 532 (Integrated with slit lamp camera SL150)

Power

Display screen

Navigation buttons for selection, incre/decrement of magnitudes

Buttons for selecting different modes
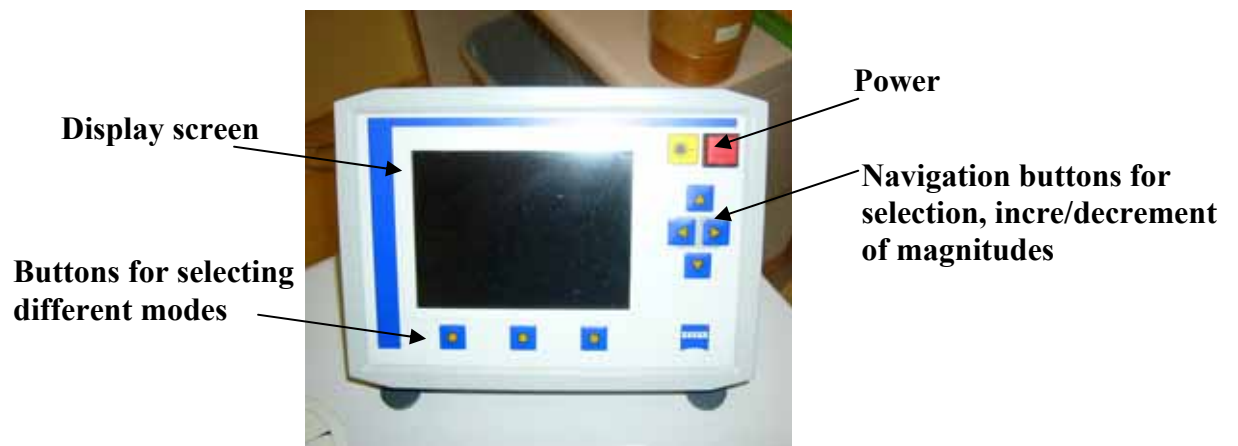
Figure 1.10b: Carl Zeiss® Visulas 532 (Control panel for laser conFiguration)

Pictures taken at: Eye Clinic, National University Hospital (NUH), Singapore

The system uses a joystick to direct the laser beam through a fundus lens and into the patient's eye. The movement of the slit lamp is illustrated in Figures 1.10c and 1.10d.

Slit lamp pivoting axis

Laser emitted from the slit lamp

Slit lamp's laser tower can rotate about the axis for coarse positioning before treatment commence
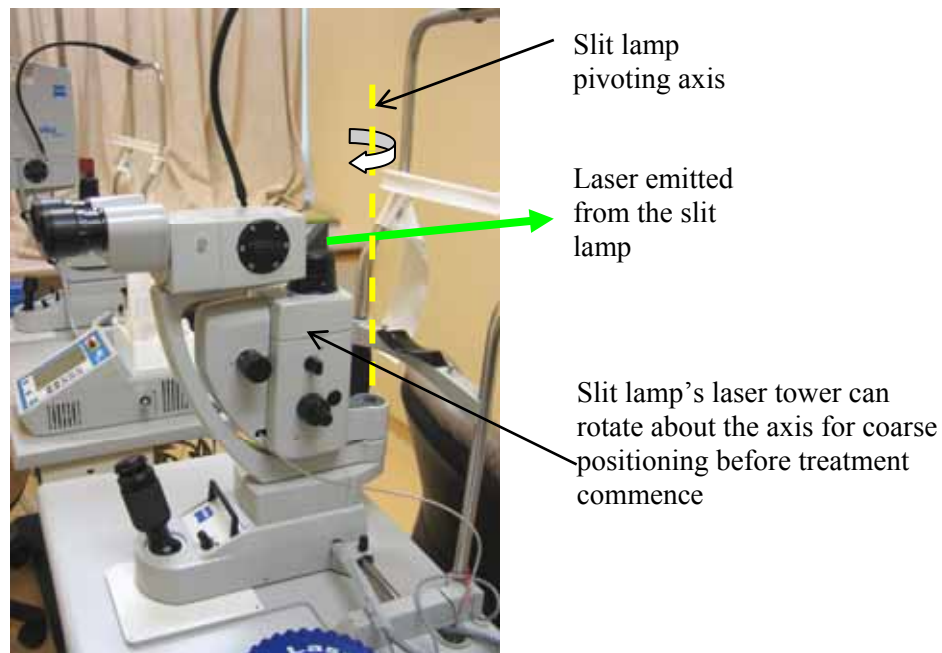
Figure 1.10c: Current method – Source of laser emission and pivoting axis of a slit lamp laser photocoagulator.

Rotate Clockwise – Translate downward
Rotate Anti-clockwise – Translate upward

Translate left

Translate backward

Translate forward

Translate right
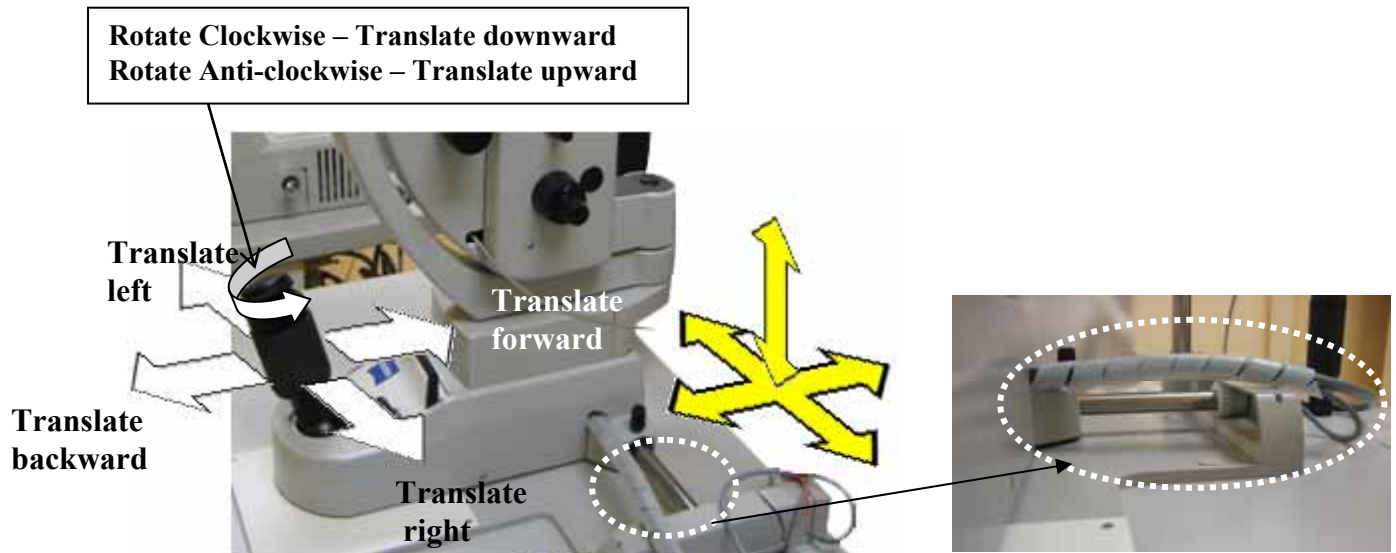
Figure 1.10d: Current method – Translational motion of the slit lamp laser photocoagulator for beam steering and focusing.
Pictures taken at: Eye Clinic, National University Hospital (NUH), Singapore

The ophthalmologist holds the fundus lens with one hand and manipulates the joystick with the other. (Figure 1.11)
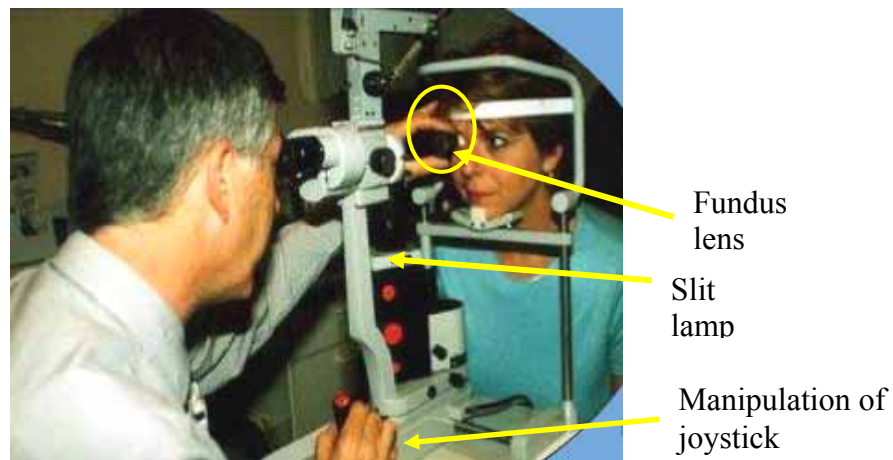
Figure 1.11: Manipulation of a typical slit lamp biomicroscope for eye examination – Dual hand task.
(Adapted from http://www.avclinic.com/eyeconditions.htm)

In laser photocoagulation, the procedure is carried out as shown in the Figure below:

Figure 1.12: Laser photocoagulation in progress
(Adapted from: http://www.avclinic.com/Laser_at_slit_lamp.jpg)

With the patient in a sitting position, the ophthalmologist views the retina using a slit lamp device, which provides the illumination source and a secondary magnification of 30X. In conjunction with the viewing of the retina, the ophthalmologist has to manually hold a magnification lens (or fundus lens) which provides the primary magnification of up to 50X. As the field of view of the slit lamp device is small (a 'slit' vision as the name implies), the ophthalmologist has to adjust and focus the image in order to view and orientate the different sectional view of the patient's retina.

Due to the nature of the optical properties of the lens in the slit-lamp and fundus lens, the retinal image viewed by the ophthalmologist will be inverted. Hence it is of the ophthalmologist's concern to coordinate the laser movement accordingly to ensure the correct delivery of the laser on the intended retina regions during treatment.

A section of the magnification lens
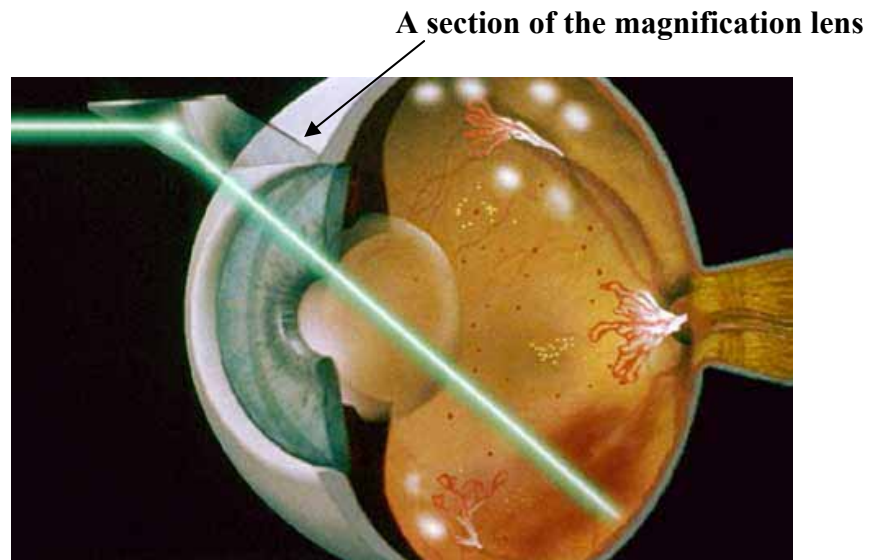
Figure 1.13: Refractory path of the laser in tandem with the optical path of the magnification lens
(adapted from:
http://www.eyesondiabetes.org.au/upload/1655839281_diag&mgt12.jpg)

Typically, the amount of laser spots being delivered per eye can be more than 1000 and stretching over several treatments, depending on the severity of the condition.

Besides providing the primary magnification for the observation of the retina, another function of the lens is its refractive capability in directing laser paths precisely on the patient's retina.

With reference to Figure 1.13, the laser beam will be refracted in tandem with the optical path of the magnification lens. Hence, manipulating of the lens (in a conical path pattern as defined in Figure 1.14) not only allows the ophthalmologist to view the different regions of the patient's retina, it also provides the appropriate refractory index for the laser beam to be delivered accurately at spots targeted by the ophthalmologists.

Central axis of the magnification (Fundus) Lens

Magnification (Fundus) Lens

Manual adjustment of the lens in a conical motion by the ophthalmologist
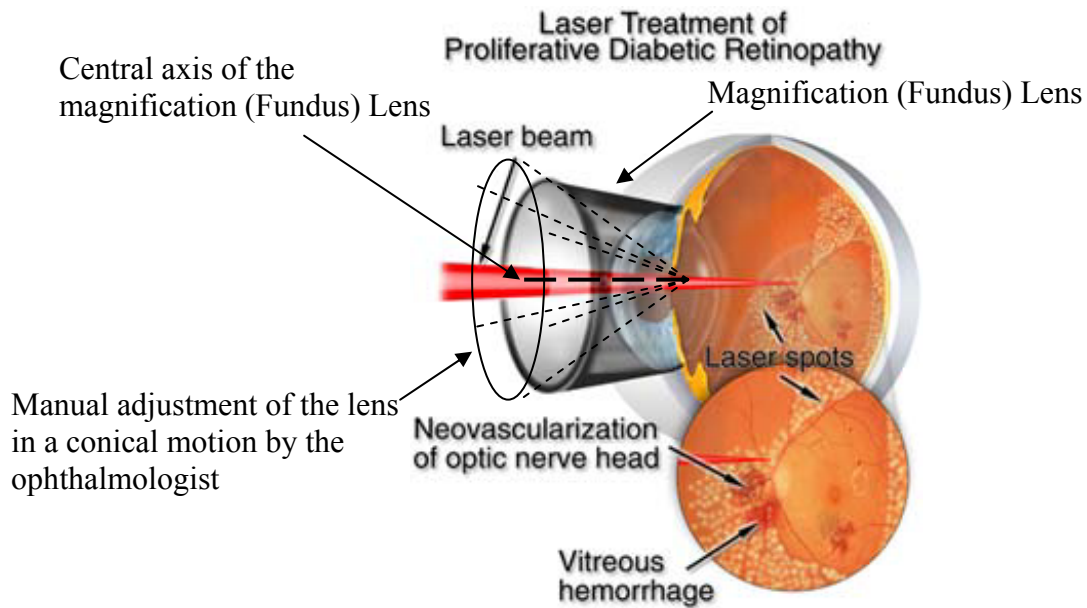
Figure 1.14: An illustration on the laser photocoagulation procedure
(Adapted from: http://www.eyemdlink.com/images/illustrations/small/prp_inset.jpg)

The fundus lens is designed with a concavity which is shaped to fit the anterior region (cornea) of the patient's eye. The concavity is filled with a layer of coupling gel (Methelcellulose) before the lens is held in a vertical plane and place on the patient's eye for observation (Figure 1.15). This serves as a medium of improved comfort and safety for the patient's eye during the procedure which requires manipulation of the lens. However, there is a need for repeated refilling of the cavity with the gel throughout the treatment as the gel tends to be discharged through the interface between the cavity and the cornea layer of patient's eye due to gravity.

Placement of the coupling gel in the concavity of the lens before vertical placement on the patient's eye for observation
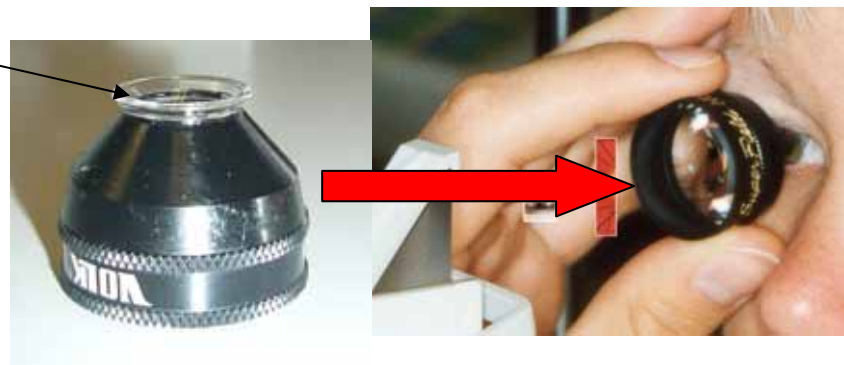
Figure 1.15: Fundus lens (VOLK®) used for laser photocoagulation operation
Picture taken at: National University Hospital (NUH), Eye Clinic, Singapore

18

1.2.4 Current Treatment Analysis/ Problems Identification

Current techniques of laser delivery to the posterior segment of the eye do not use the conventional fundus camera for image capturing due to the limited field of view. Instead, the laser device is integrated with a slit lamp and positioned such that the laser shot coincides with the observed retina image viewed through the slit lamp. With the assistance of contact magnification (fundus) lenses, the field of view of the retina is increased by many folds and the image of the retina is also magnified. However due to the interference of illuminating and collecting light rays and internal reflection of the contact lenses, 'hot spots' are created and thus resulting in limited illumination and field of view. Although such contact lenses could view more than 100° field of view in theory, the light interference and 'hot spots' limit the view to somewhat piecemeal in nature so that only a small part of the magnified retina could be seen through the slit lamp (Figure 1.16). Laser shots are delivered to portions of the retina one at a time and the operator has to maneuver the slit lamp and the contact lens continuously to treat the entire relevant portion of the retina. Furthermore the quality of the image is very much dependent on the presence of vitreous opacity, cataract and other anterior segment abnormality.

The current process of laser delivery to the posterior segment of the eye is tedious, tiring and cumbersome and the outcome varies from operator to operator depending on his or her experience and alertness. Each session of laser therapy for diabetic retinopathy could vary between 15 minutes to half an hour or more depending on the cooperation of the patient and quality of image captured by the contact lenses and slit lamp. This translates to increase discomfort for the patients who have to maintain a fixed eye position for long period of time in a sitting position. In addition, patients would have to put up with long exposure of relatively bright light and have the lenses kept in contact with their eyes. Such patient's discomfort coupled with the tedious and tiring operation process could compromise the consistency and safety of laser delivery to the posterior segment of the eye. With a somewhat slower reflex of the hand foot coordination of a tired or less than alert operator relative to the reflex eye movement of an uncomfortable patient, it is not unexpected that there is a real danger of laser being delivered to important structures of the posterior segment such as the macula, major retinal vessels and optic nerve (Figure 1.17).
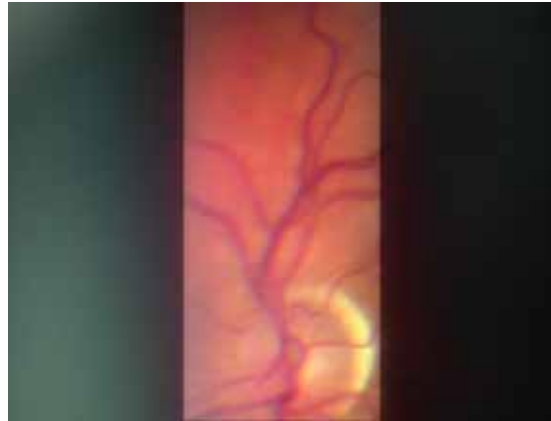
Figure 1.16: Field of view of the retina is limited when viewed through the slit lamp biomicroscope.
(Adapted from: http://www.medmont.com/products/tools/dv2000/e_90d.jpg)

Fovea Centralis within the Macula

Optic Disc

sclera
choroid
retina
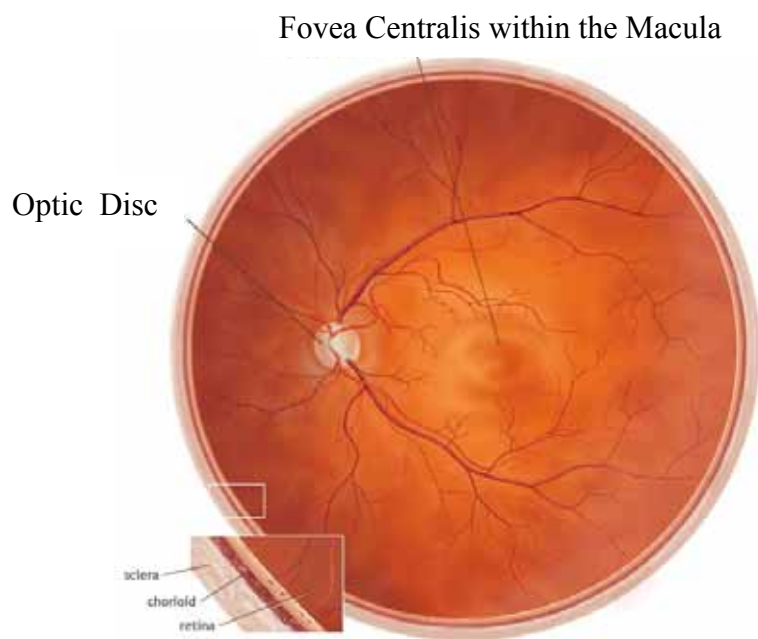
Figure 1.17: Important structures within the retina (posterior region of the eye)
(Adapted from: http://www.amdcanada.com/images/content/4_2_Fig1.jpg)

1.2.5 Recent Development of Laser Photocoagulation System

A new system used by Optimedica in its Patterned Scanning Laser (PASCAL) machine had introduced the concept of delivering a multiplicity of shots in a predetermined pattern with a single depression of the foot switch[40]. The main benefits of this method is the usage of a much shorter pulse rate of 20 milliseconds as compared to 100 milliseconds, allowing the whole treatment to be carried out 5 times faster.

Theoretically, multiple shorts per push of the switch, when delivered in a time shorter than the patients' typical eye fixation time will greatly improve the procedure's efficiency and safety. In addition, by reducing the number of applications per treatment, the independent probability of unintentionally hitting the fovea center is also reduced. The smaller total energy used due to shorter pulse duration will also limit the thermal spread to the nerve system in the choroids, thereby reducing the patient's discomfort.

Part of the intent of this development aims to improve on the achievement of the PASCAL system by automating the delivery of the laser beam to the whole treatment area instead of delivering only a multiplicity of spots at one time.

1.3   Objectives

Current diabetic retinopathy treatment requires the ophthalmologist to use one hand to manipulate the fundus lens to obtain the best field of view, the other hand to aim the laser beam, and one foot to press the switch to emit the laser, while craning their neck to view the retina through the microscope eyepieces. Ophthalmologists had described this procedure as painful and tedious to administer, as typical treatment session takes about 15 to 30 minutes to complete. Patients normally return for 2 or 3 treatments, where about 1000 light burns or more are placed on the patient's retina at each treatment.

As the positioning of the laser on the retina is achieved through manual manipulation of the laser beam and fundus lens, inexperienced ophthalmologist will find it difficult to place the spot evenly and with fine enough spacing in between spots. In Figure 1.18, the lower half of the image shows the result of treatment using a conventional photocoagulation system. The upper half of the image shows the result of treatment using the Pascal method which utilizes a proprietary micromanipulator to carry our laser scanning over a limited area.

The usage of slit lamp, which provides only a slit of light at one time, limits the field of view of the treatment area (Figure 1.16). Furthermore, during treatment, the involuntary movement of the patient's eye may lead to accidental irradiation of the macula or the optic disc which could damage the patient's eyesight.
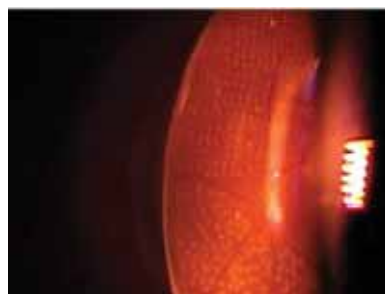
Figure 1.18 Image of the retina demonstrating the difference between manual firing and using the Pascal method of pan retina photocoagulation treatment
(Adapted from http://www.optimedica.com/pascal/images/image-fundus3.jpg)

Therefore to address the issues mentioned above, an improved overall layout of the equipment will be suggested to allow better handling and control of the apparatus

during the procedure, while increasing the level of comfort for the patient. This design will incorporate a trans-sclera illumination system to replace the usage of a slit lamp, a suction system to stabilize the position of the eye, a CCD camera to allow monitoring of the retina and specifically, a computer controlled laser delivery system will be designed to provide for a fast and accurate delivery of laser treatment so as to ease the work of the ophthalmologist and to address the safety concern over involuntary movement of the patient's eye.

1.4 Scope

The main scope of this study is to develop an Observatory device for real-time global view of a stabilized retina and an Optomechanical system to perform laser scanning for treatment of diabetic retinopathy.

The Observatory device encompasses the following:

(1) **Trans-sclera illumination device with fundus lens** – to provide an indirect illumination (i.e. not via the pupil of the eye) of the retina without the creating 'hot spots' when the reflected light and image is received by a camera. A magnified global view of the retina will be possible as compared to the present limited 'slit' view.

(2) **Vacuum suction ring** – to stabilize the eye during the treatment process and negating the need to have subsequent sophisticated tracking equipment

The Optomechanical system consists of these sub-systems:

(3) **Laser Delivery and Laser Source System** – to deliver the treatment and aiming laser at the required **power, spot size and pulse rate**

(4) **Beam Steering System** - to position the laser beam on the patient's retina and to deliver the entire treatment within 5 minutes

(5) **Vision System** – for diagnosis and viewing during treatment

Figure 1.19 shows pictorially the scope and the design of the proposed system, whilst the flow chart that follows summarize this project.

Laser Delivery System

Design of a laser delivery system and laser source using off-the-shelf material

Vision system

Sourcing for a suitable CCD camera which is small and lightweight to fit the design requirement

Beam Steering (Scanning System)

Design of a 2 axis galvanometer scanning system and calculation of the rotation required for steering the beam

Observatory device:

Novel integration of a trans-scleral illumination system, a vacuum suction ring and fundus lens to provide a stable global retina image

Figure 1.19: Summary of the scope of development and the current design objective

The scope of this project can be summarized with reference to the flow chart shown below:

```
                    ┌─────────────────────────────┐
                    │  Computer Assisted Ophthalmic │
                    │    Laser Delivery System      │
                    └─────────────────────────────┘
```

Computer Assisted Ophthalmic Laser Delivery System

Proposed Observatory device

Proposed Optomechanical system

Eye tracking mechanism and central coordinating control system

Trans-scleral Imaging

Fixation Ring for eyeball movement stabilization with Magnification lens coupling gel enclosure

Laser delivery system and laser source

Beam steering system

Vision system

For future integration and development

1.5 PROPOSED OVERALL INTEGRATED SYSTEM DESIGN

By integrating the above mentioned components, a proposed overall system design layout is arrived as shown in the schematic layout:

Optic fibers for laser tower

Feed-back control to motor drive and galvano-mirror to pin-point laser position

Motor drive rotate about z-axis

Image enhancement

Mobile Workstation

CCD camera to capture image X30 with illumination filters.

Laser Tower

Galvano-mirror rotate about y-axis

Beam splitters to co-align camera with laser path

Vacuum pump

z

y

x

Electrical cables to provide light source for transscleral illumination

VOLK® lens

Proposed observation device assembled with suction chamber and illumination ring of light

Eyeball

Figure 1.20: A schematic diagram showing the proposed system design layout

Damping Arm for ease in manipulating observatory device and internal housing of:
-Vacuum tubing (suction pump)
-Optic fibres (image and transmission by CCD camera)
-Power cables (transscleral illumination)

Display of retinal image

Processors for image enhancement

Vacuum pump and controls

Proposed Observatory Device

Laser generator box and power supply

Patient (Lying down position)

Ophthalmologist

Workstation is designed to be movable

Figure 1.21: A 3D illustration model showing the proposed system design

Mobile workstation:
- **For easy movement of the entire setup between different operating wards.**
- **For easy adjustment of the setup to the most comfortable position for both the patient and the ophthalmologist during treatment.**

Vacuum pump and controls for the suction/fixation ring

Detachable clamp of damping arm for adjustability during usage (Eg: Left or Right-handed conFiguration for the ophthalmologist.)

Ophthalmologist

Patient

Damping arm envelope
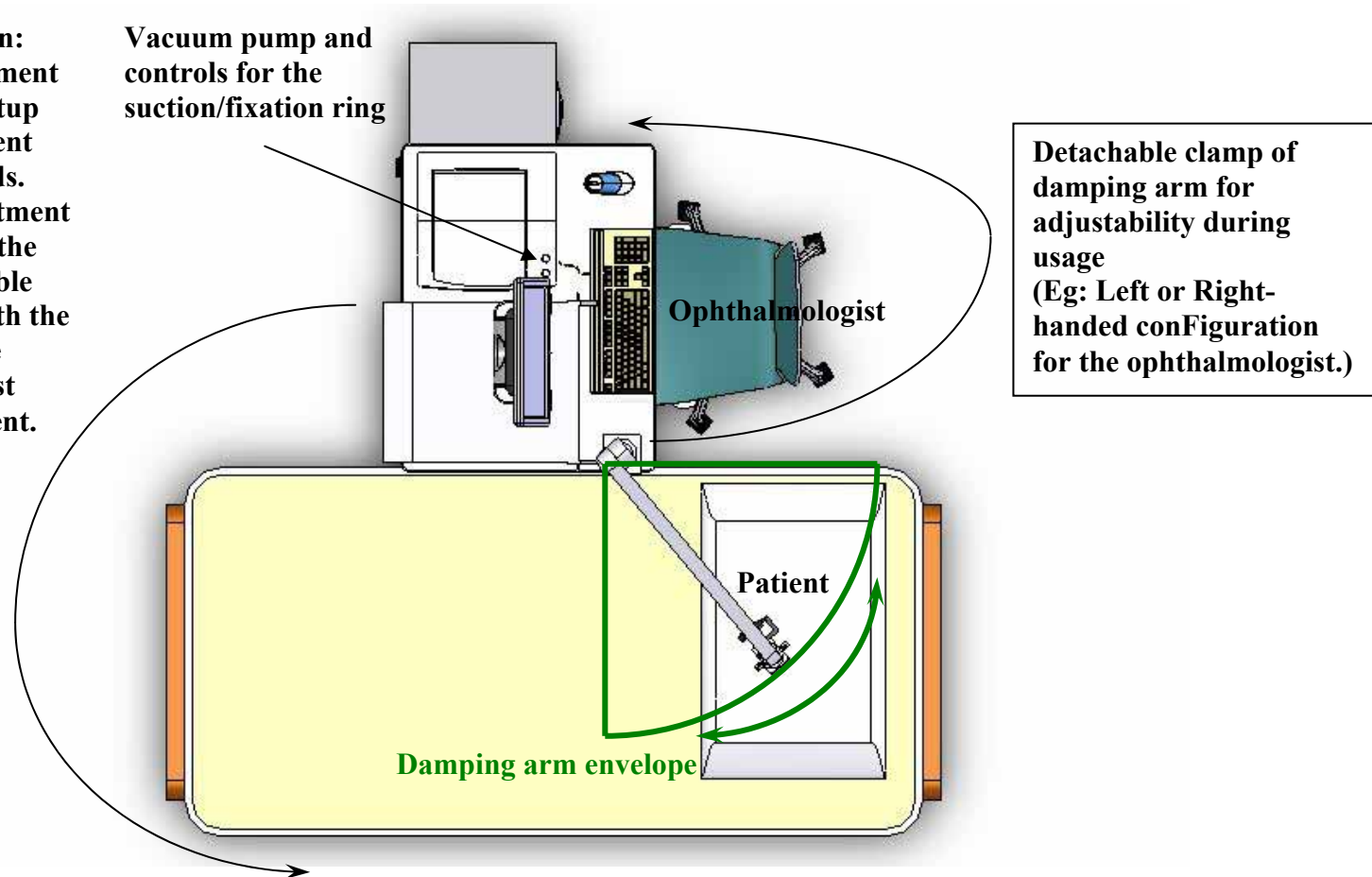
Figure 1.22: The proposed system design workspace description

In summary, an overall system design and layout has been conceptualized. However, the scope of this project will be limited to the development of a multi-functional observatory device for stabilization, illumination and image capturing of the eye and an optomechanical system to provide laser delivery to the retina. Future integration of eye tracking mechanism and a central coordinating system will be required for a complete system setup.

2 PROPOSED OBSERVATORY DEVICE

2.1 REVIEW OF EXISTING TECHNOLOGY AND SOLUTIONS

The eye is in constant motion. Even when it is focused at an object, there is micro saccadic movement that may affect the accuracy of laser delivery in photocoagulation treatment. To overcome such an obstacle would require sophisticated tracking software that are extremely expensive and require large amount of processing power. Thus, an intermediate approach would be to employ an eye stabilizing unit to keep the eye stationary with subsequent integration of a simple eye tracking device to enhance the accuracy of the laser delivery while providing a fail-safe mechanism in the process.

In considering the development of an integrated Observatory device, an assessment of current know-how and market practices would be important. Evaluations of equipment that help reduce eye movement and devices that provide a wide angle view of the retina would have to be made before integrating the individual component.

2.1.1 Eye Movement Restriction

<u>Eyeball Fixation Apparatus</u>

A fixation apparatus minimizes the involuntary movements of the eye and facilitates the tandem coordination between the tracking device and the laser delivery system. This would facilitate the resultant response time between real time eye movement and laser positioning compensation to meet clinical requirement.

There are several products available to restrict the eyeball movement during an ophthalmic procedure. Common to all is the use of a suction force or vacuum pressure on the sclera of the eye via a pneumatic suction ring, hence its ability to restrict its movement. This method is widely used in LASIK surgeries. During the process, the intraocular pressure of the eye is increased, with the suction pressure applying up to 65 mm Hg. However, the application of the negative pressure should not exceed more than a minute so as not to cause potential injuries to the eye. A sclera depressor

mechanism will be used to avoid the application of excessive pressure onto the corneal layer.

2.1.2 Ophthalmic Photography Techniques

The requirement includes an effective imaging technique that provides wide angle field of view of the retina. The images should be of high clarity and provide adequate details for subsequent digitization and easy manipulation using standard software. Furthermore, the imaging technique should be acceptable to the majority of the patients with varying needs. Current ophthalmic imaging systems include:

Fundus Cameras
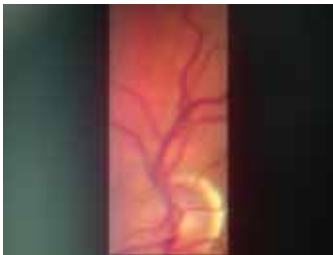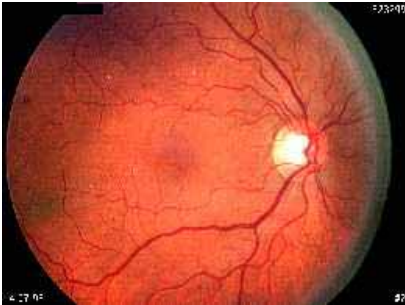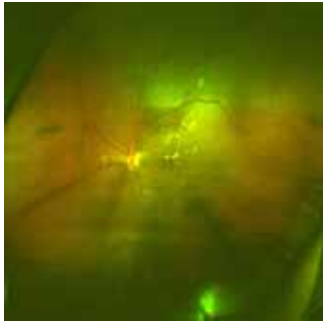
Current fundus cameras provide images of the posterior regions of the eyes by having a field of view between 30º to 60º and a magnification of 2.5 times. It is the most common form of ophthalmic imaging for full colour examination, red-free contrast between vessels and other structures and angiography.

Trans-sclera Illumination

The application of trans-sclera illumination enables real time imaging with 130° field of view of the retina. This concept is introduced by MediBell® Medical Vision Technologies (Panoret 1000). The indirect approach to illumination via the sclera instead of the pupil prevents 'hot spot' formation and thus allows capturing of high quality images with wider angle of view.

Scanning Laser Ophthalmoscopes (SLOs)

The scanning laser system combines two low-powered lasers into a single beam that is then projected onto the patient's retina and manipulated through a 200-degree scan angle. Light reflected from the retina is then returned through the scanning system and then converted to electrical impulses by highly sensitive photo‑diodes. These impulses are in turn digitized and formatted to create the image.

	Slit-Lamp	Fundus Imaging	Scanning Laser Ophthalmoscope (SLO)	Trans-sclera Imaging
Field of View	40mm x 6mm slit	30º to 60º with proportionally less magnification	Up to 200º ultra-wide	Up to 130º field of vision
Technique	Emitting and reflected light source through the pupil of the eye.	Emitting and reflected light source through the pupil of the eye.	Laser scanning on the retina while reflected light digitized to create image	Indirect illumination via the sclera of the eye while image captured through the pupil.
Manufacturers	Carl Zeiss	Canon	Optos Panoramic 200	Medibell Panoret 1000
Laser Delivery Capability	Basic ophthalmic examination. Combines with a laser system to provide the current mode of photocoagulation	Currently the most widely used ophthalmic camera	For ophthalmic screening only No therapeutic laser delivery	For ophthalmic screening only No laser delivery
Examples				

Table 1: A comparison of the various ophthalmic photography methods

The trans-sclera illumination technique is the preferred choice of imaging in view of its wide field of vision, good quality real time images, availably of digitized formats and its existing design potential for integration with an eye stabilizing unit.

2.2.   INTEGRATED OBSERVATORY DEVICE

2.2.1   Integration of Eye Fixation Device with Trans-sclera Illumination Ring

According to US Patent 6,656,197 by Lahaye and 5,009,660 by Clapman (Refer to Appendix 1), the eye fixation device is used to facilitate ophthalmic laser surgical procedures where the eyeball has to be immobilized to a certain extent for precise laser delivery during the operations. The fixation ring is of 10mm in diameter, with guided holes spread within the circular structure. According to LASIK procedures, a vacuum pressure of 65mmHg will be applied, hence creating a suction force on the anterior cornea layer to restrict the movement of the eye. However, this application is kept at a period of less than 1 minute to prevent the elevation of the intraocular pressure of the eyeball that may result in excessive stretching of the ciliary muscles and potential damage to the eye.
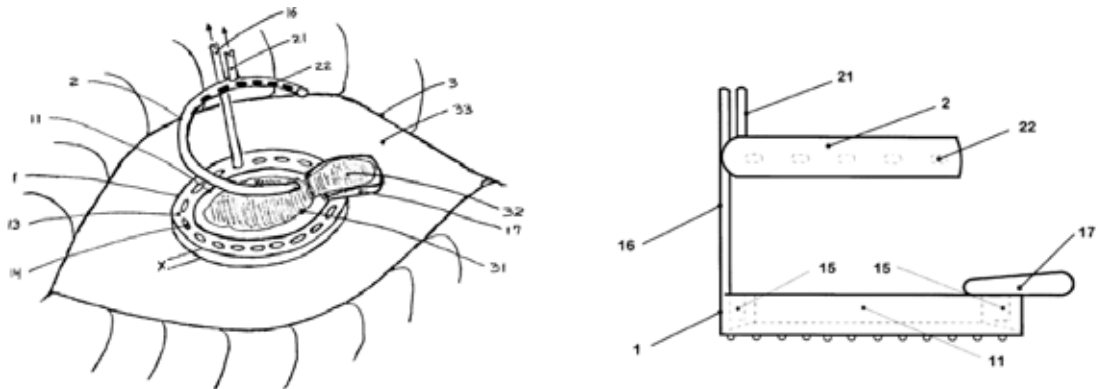
Figure 2.1: Description of the patented eye fixation device.
(See Appendix 1 for detailed description of the drawings)
(Adapted from: United States Patent 6,656,197 B 12/2003 LaHaye)
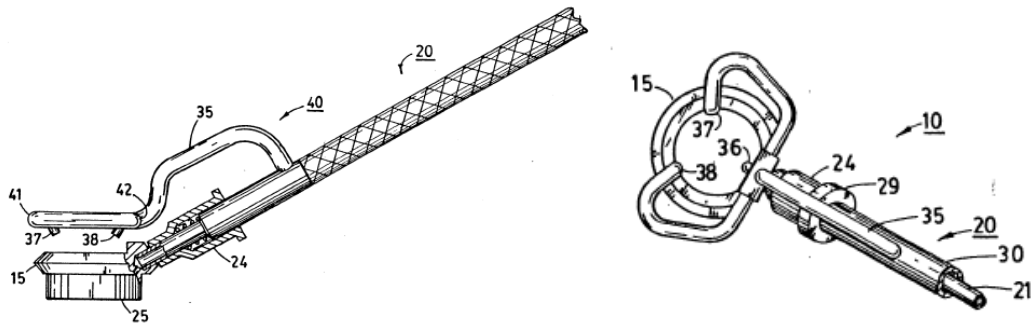
Figure 2.2: Description of the patented eye fixation hand-piece.
(See Appendix 1 for detailed description of the drawings)
(Adapted from: United States Patent 5,009,660 A 4/1991 Clapham)

Figure 2.3: A computer simulation on placement of the eye fixation device on the
cornea region during LASIK surgery
(Adopted from: http://www.amdcanada.com/images/content/4_2_Fig3.jpg)

As the duration of fixation ring application is in the range of 5 - 10 minutes, it would not be suitable to apply similar parameters for the purpose of this project. Although experimental animal studies have found that the eye can withstand an increase in intraocular pressure up to the range of between 80 and 230 mm Hg during and immediately after the suction phase[41], it would be more favorable to apply the suction at a lower pressure to reduce the potential to cause adverse effects to the eye. Taking into account of the readings obtained by Wei-Li Chen et al.[41] as well as the opinions of various ophthalmologists, it would be most appropriate to fix the suction level at 20mmHg for the purpose of this development.

According to US Patent No 6,267,752 by Svetliza (Refer to Appendix 1), an eyelid speculum is coupled with an illumination unit for trans-illumination through the sclera of the interior of the eyeball. The speculum is shaped in a conical manner such that the bottom edges act as eyelid retractors, which the eyeball will be exposed to the maximum state for effective observation. The speculum is also designed with internal chambers to facilitate the irrigation of eye fluids to the eyeball and draining away the excess flow.
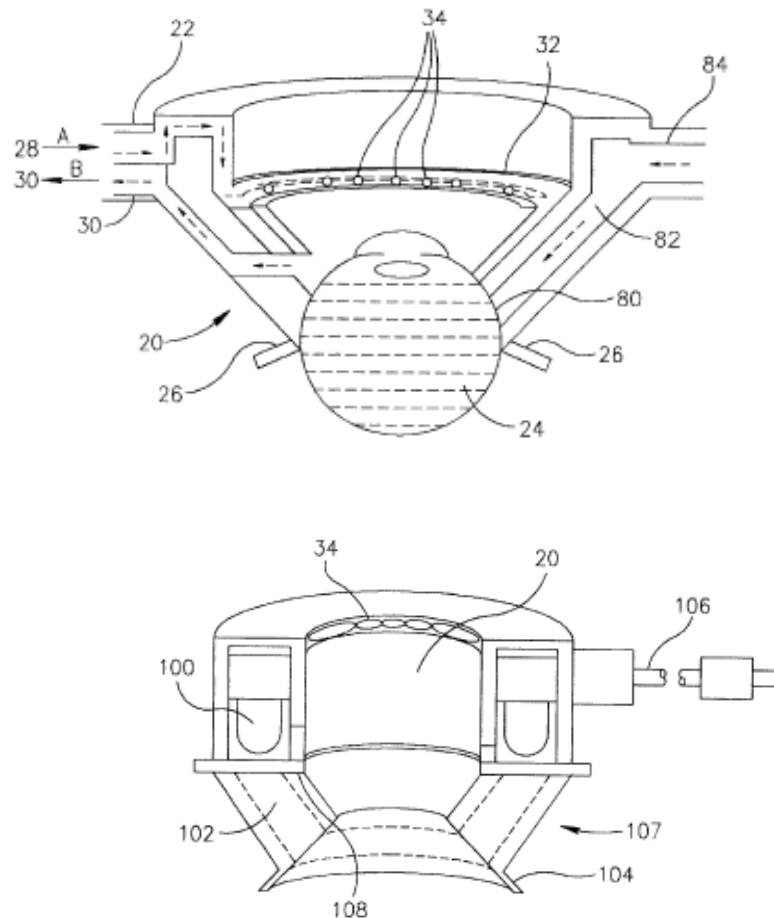
Figure 2.4: Description of the patented trans-illumination device using optic fibres (Top) or direct lighting by light bulbs (Bottom)
(See Appendix 1 for detailed description of the drawings)
(Adapted from: United States Patent 6,267,752 B1 07/2001 by Svetliza)

Using this technique, it is claimed that the indirect illumination reaches the interior of the eye well-diffused and homogeneous, thus providing a good source of background lighting for imaging. In contrast, the illuminating light within conventional fundus cameras and slit-lamp biomicroscope passes through the cornea; pupil, the crystalline lens and reaches the retina before being reflected in a similar path to the observer.

This results in 'hot spots' formation and limits the clarity and field of view of the retinal images due to the interference of both the incident light source and reflected light along the same path. Furthermore, background scattered reflections of the tissue layers traveling in the optical path between the retina and the anterior segment of the eye[42] may further complicate the retinal imaging procedure.

With trans-sclera illumination technique, it uses an indirect approach such that the incident light passes through the entire circumference of the translucent sclera adjacent to the cornea and reaches the retina in a homogenous manner. The reflected light from the retina is transmitted through the crystalline lens, pupil and cornea without any interference of the incident light and thus resulting in an optimized retina image that is clear and has a wide field view.

The light source can be obtained from optic fibres that traverse around the illumination chamber or the integration of LED units within the illumination chamber. If optic fibres are used, considerations have to be made on the potential loss of illumination efficiency along the optic fibre from one end to the other. Thus, the direct installation of LED units within the chamber itself will be more viable in the development of the observatory device.

Standard white LED units will be the lighting of choice in view of its low cost, energy efficiency and installation flexibility. This approach would enable the overall design of the observatory device to be kept simple and manufactured at a low cost.

During the development of this technique, Medibell Medical Vision Technologies launched a high-resolution retina camera to optimize the capturing of images. A pre-clinical study[42] on the safety of this device had been carried out on laboratory animals. Observation of the device's application up to 40 minutes did not demonstrate any adverse effects from heat generated via the lighting source or the increase in intraocular pressure.
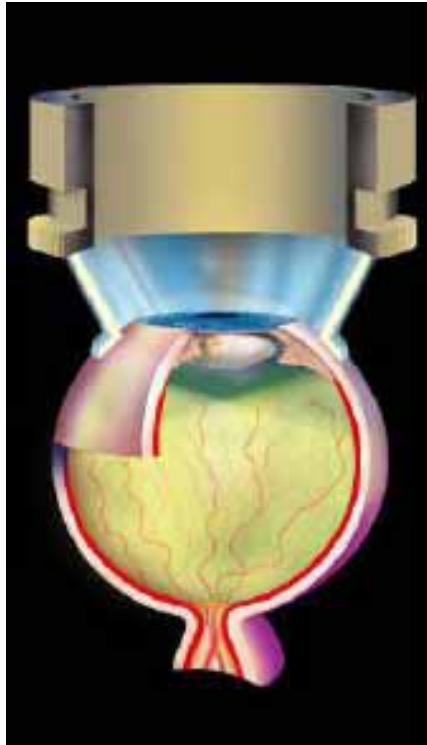
Figure 2.5: An illustration showing the concept of trans-sclera illumination
(See Appendix 2 for detailed description of the drawing)
Picture adapted from:
B.Ben Dor et al.[42]

It was noted that lighting in a typical slit-lamp biomicroscope was adequately provided at 20W by a halogen lamp. By utilizing the specification, the appropriate number of LED units required for the observatory device can be determined accordingly.

2.2.2   Manufacturability and Ease of Fabrication of Observatory Device

To facilitate the ease of fabrication and manufacturing of the observatory device, basic metal sheet-bending was applied to achieve its circular construction. Precision engineering is required for the cutting process and to achieve the tight tolerances specified in the design.
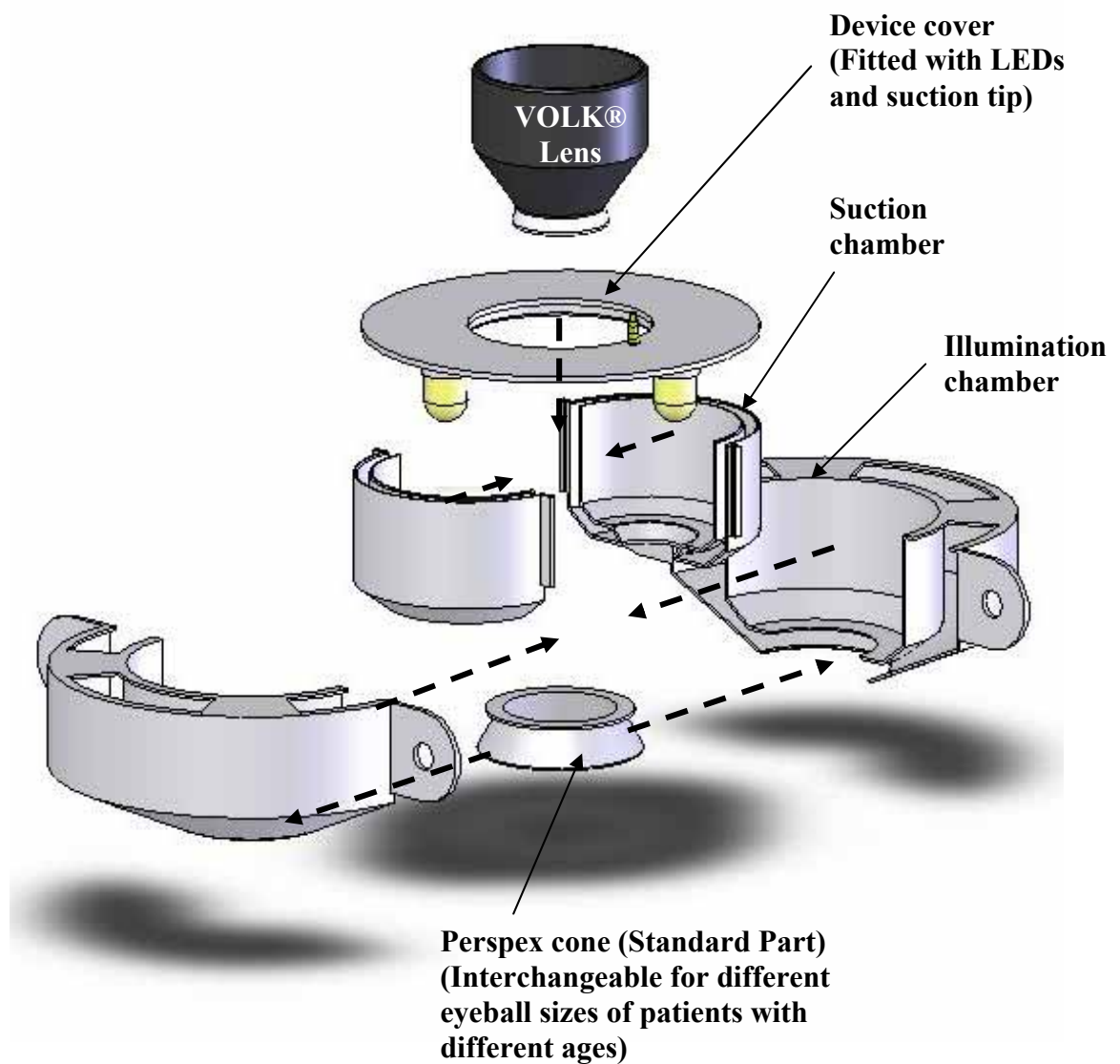
**Figure 2.6: An illustration showing the exploded assembly
of the observatory device
(See Appendix 3 for detailed technical drawings of each assembly part)**
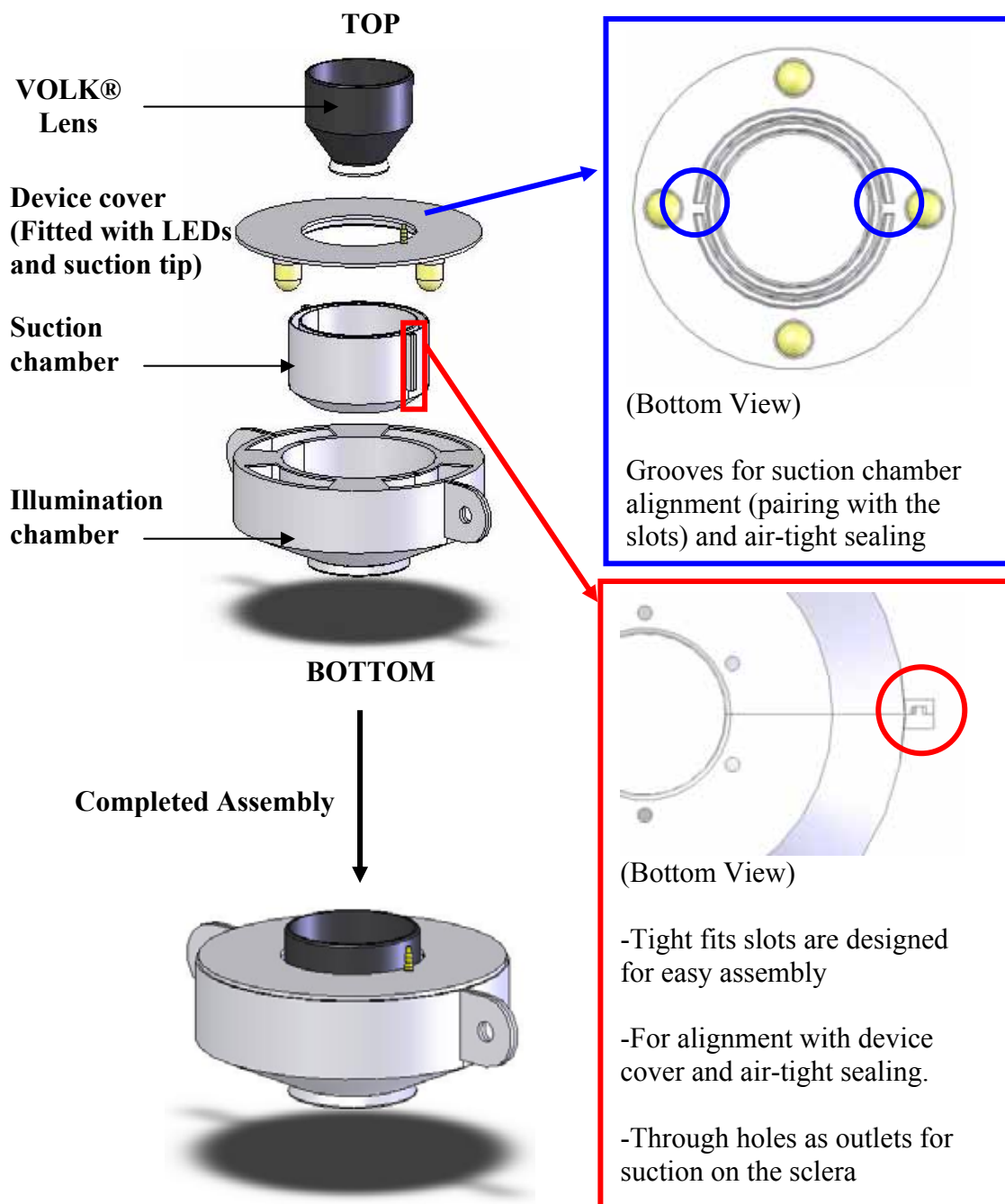
Figure 2.7: An illustration showing the various components of the observatory device.
(See Appendix 3 for detailed technical drawings of each assembly part)

The following labels appear in the figure:

- **VOLK® Lens**
- **Device cover (Fitted with LEDs and suction tip)**
- **Suction chamber**
- **Illumination chamber**
- **TOP**
- **BOTTOM**
- **Completed Assembly**

(Bottom View)

Grooves for suction chamber alignment (pairing with the slots) and air-tight sealing

(Bottom View)

-Tight fits slots are designed for easy assembly

-For alignment with device cover and air-tight sealing.

-Through holes as outlets for suction on the sclera

Suction
chamber

Device cover
(Fitted with LEDs
and suction tip)

Illumination
chamber

Perspex cone
(Interchangeable for
different eyeball sizes)

Figure 2.8: An illustration showing internal (cross-section) of the observatory device.

Illumination
chamber

Suction
chamber

Suction 20mmHg
Light Source 20W

VOLK®
Lens

LED

LED

Perspex cone
(Interchangeable for
different eyeball sizes)

Coupling Gel
enclosure

Average eyeball diameter of 24.5mm
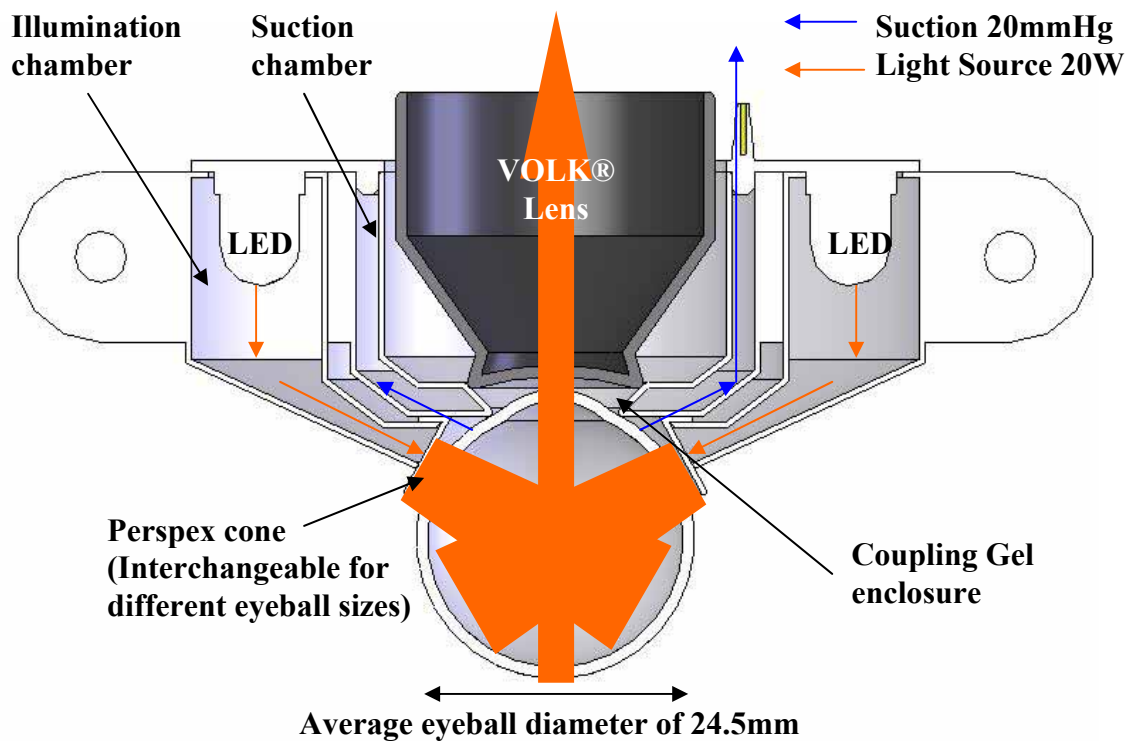
Figure 2.9: An illustration on the proposed observatory device and how it works

3 PROPOSED OPTOMECHANICAL SYSTEM

3.1 SPECIFICATIONS FOR DESIGN

In order to derive the specifications of the laser delivery system, an understanding of existing issues and various requirements for treatment of diabetic retinopathy is essential. These requirements can be categorized as follows:

- (a) Operation and Treatment Criteria
- (b) Patient's safety and comfort
- (c) User requirement

3.1.1 Operation and Treatment Criteria

Treatment Protocol

There exists various treatment protocol performed for different stages of retinopathy. Each has a different treatment zone with varied intensity (power, duration and multitude) of laser burns. The recommendations are as follows:

Treatment Type	Spot Size (μm)	Area of treatment and total number of burns	Pulse Duration (second)
Full Scatter treatment	500	From the oval boundary around disc and macula, extend peripherally to beyond the equator. 1,200 – 1,600 in 2 or more session (No more than 900 in a single session)	0.1
Mild Scatter Treatment	500	Similar area as full scatter. 400 – 650 burns in one single session	0.1
Confluent Local Treatment	200 - 1000	Smaller specific area, not exposed to possible complication	0.1 – 0.5
Local Full Scatter (Grid Treatment)	<200	Used in area nearer to the macula	0.1

Table 2: Summary of recommended protocols in treatment methods for diabetic retinopathy[8].

In order to reduce the unintentional destruction of neighbouring healthy retina, there is a preference to deliver laser with smaller spot size albeit a higher number of spots while **creating a similar intended total area of lesion on the retina**.

The above protocol can be used as a general guideline for the treatment of diabetic retinopathy. However as retina tissues are heterogeneous, there is a need to observe for

the development of a white lesion after irradiation to ensure consistency of the treatment throughout the retina. While there were previous attempts to automate such tissue reflectance feedback control, it is not within the scope of this thesis. Further investigation and research would be necessary for such an integration.

Spot Size

Most ophthalmologist recommends spot size of **200 µm to 300 µm** for the purpose of a full scatter treatment. The present benchmark of the PASCAL photocoagulator has a spot size range of 60 µm to 400 µm at the corneal plane, before magnification by the fundus lens. Taking into account of this information and the power density threshold of the cornea (refer to Section 3.4.3), the proposed design should be capable of delivering a spot size to the retina within a range of **100 µm to 400 µm**. This would satisfy the requirement for a full scatter treatment, while enabling smaller spot sized treatment of the area near the macula.

Imaging of the retina through a fundus lens

The slit lamp viewing setup of the photocoagulation system is not able to focus directly on the patient's retina because of the optical properties of the patient's eye which projects the retina at near infinity[43]. However, the use of fundus lens placed adjacent to the eye enables the retina image to be condensed and projected for viewing at a focal plane. This similar optical setup will help direct the laser beam to the target retina. In general, there are 3 classification of fundus lens: positive non-contact (indirect), positive contact, and negative contact[44].

The physician's view of the retina is restricted by the aperture of the pupil. Hence the closer the proximity of the lens is to the pupil, the larger the field of view of the retina. In panretinal photocoagulation, a positive contact lens is used to provide the widest field of view. A contact lens is also used in practice to keep the eyelids apart, to keep the cornea moist (with gel application) and to stabilize the eye[45] by reducing involuntary movements. The lens design also determines the resulting projected image by varying the viewing angle within the eye and spot size magnification.

The laser beam is focused onto the front focal plane of the fundus lens as noted in Figure 3.1. Different techniques can be used to vary the spot size of the beam; the laser beam's focus point may also be shifted away from this plane. Further details of the optics involved are found in Section 3.4.3.
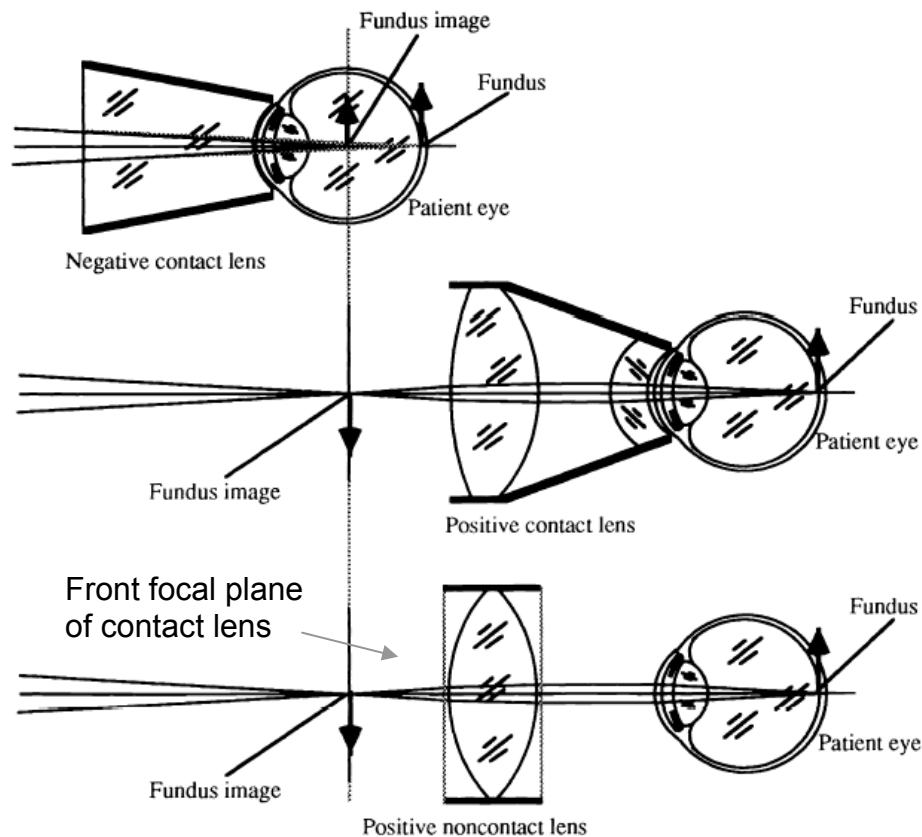
Figure 3.1: Propagation of a focused laser beam through the various type of fundus lens onto the retinal. Adapted from Dewey D. (1991)[44].

A layer of gel is routinely placed between the contact lens and the cornea such that it act as a medium f or continual magnification and to stabilize the lens on the eye by creating suction between the contact element and the cornea using standard flange on the lens posterior. It also allows for easier removal of the lens from the cornea and reduce patient discomfort during the procedures[46].

During photocoagulation, **high resolution and magnification are particularly critical when it is being performed near the macula[43].** When **pan retinal photocoagulation** is carried out at the peripheray, high resolution, though desirable, is not mandatory. Instead, lenses with **wider field of view will be more relevant**. Although the main objective of the proposed design is to automate the time consuming

procedure of a full pan retinal treatment, considerations should also be given in utilizing the system for the treatment of other pathologies such as macular edema. Hence a **variable magnification vision system** should be incorporated in the design.
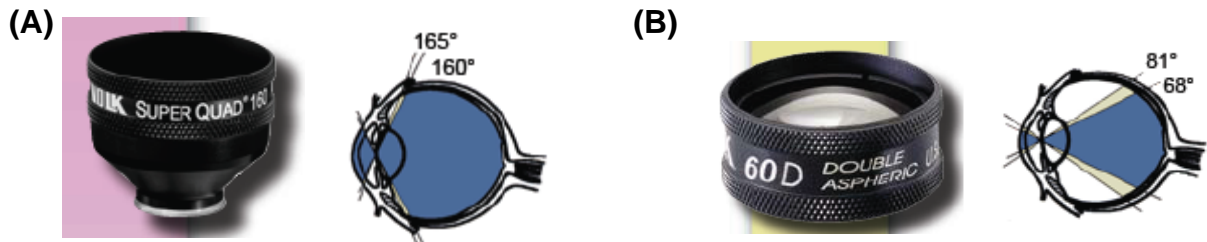
Figure 3.2: Comparison of the field of view provided by a (A) positive contact lens and (B) non-contact lens. Adapted from VOLK catalogue 2006.

In most circumstances, a viewing angle of 150° is sufficient to treat most retinal pathologies. As such, the **VOLK Super Quad 160** (Figure 3.2A) is the lens of choice for the proposed design. It is a positive contact lens that projects an **inverted real image** and has a static viewing angle of 160°. When combined with the optical system of the eye, the fundus lens-eye system will have an **image magnification power of 0.5**, and **laser spot magnification power of 2**.

As the spot size on the retina has a range of **100 to 400 μm**, the laser beam that is delivered to the lens will have a diameter of **50μm to 200μm.**

Direction of treatment

The initial treatment is usually at the inferior (lower) retina. Subsequent treatment will move progressively upwards. This to prevent visual obstruction of the untreated area in the event of vitreous hemorrhage (gravitational forces will pool blood inferiorly) between treatment episodes. When using a positive fundus lens (e.g. VOLK Super Quad 160), the image formed will be inverted. Therefore, the laser delivery will begin at the superior (upper) aspect of the lens and move downwards during treatment.
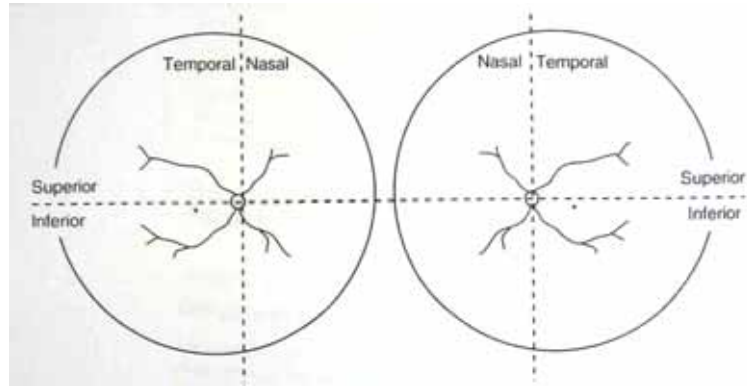
Figure3.3: Orientation of the retina.

Illumination

As mentioned previously, trans-sclera illumination is the method of choice to replace the present use of the slit illumination for laser photocoagulation.

The slit lamp method utilizes the same travel path for the incident beam and the reflected beam. This creates 'hot' spots that induce glare formation when the light intensity or width of beam of the slit lamp is increased. This phenomenon limits the illumination source to a small slit of light, providing the observer with only a small illuminated view of the retina, and prevents the lighting up of the entire retina through the fundus lens.
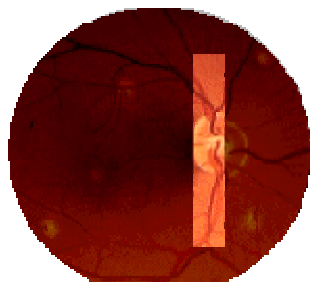
Figure 3.4: A typical slit view of the fundus as seen with a Biomicroscopic Indirect Ophthalmoscope.

Figure 3.5: A view of the retina, seen through the Panoret 1000 Camera using a transscleral illumination method. Adapted from Panoret 1000, Wide Angle Digital Retinal Camera Catalogue.

Correspondence from Medibell had advised the level of illumination of **100mW to 250mW** for trans-sclera illumination to be applied near the limbus, where the sclera is thinnest. The lack of pigment in this region reduces the absorption of light from the illumination source.

Treatment Area
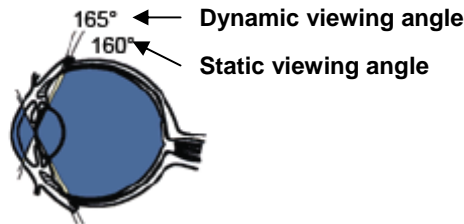
Figure 3.6: Viewing angle for the VOLK Super Quad 160

The VOLK Super Quad 160 has a **static viewing angle of 160°** and a dynamic viewing angle of 165°. Dynamic viewing angle is the total viewing angle obtained by shifting the lens to a different location on the cornea to view different parts of the retina. In this case the movement required is minimal.

In general, the retina covers 72% of the inner globe of the eye, where the average diameter of this inner globe is 22mm [47].

Therefore, the estimated area of the retina $= 0.72 \times 4\pi (11mm)^2 = 1094.7822 \ mm^2$

There are two regions where laser treatment cannot be carried out without detrimental effect to the patient's vision; these are the optic disc and the fovea centralis. For safety reasons, scatter treatment should only be conducted outside the boundary area shown in Figure 3.7[8].
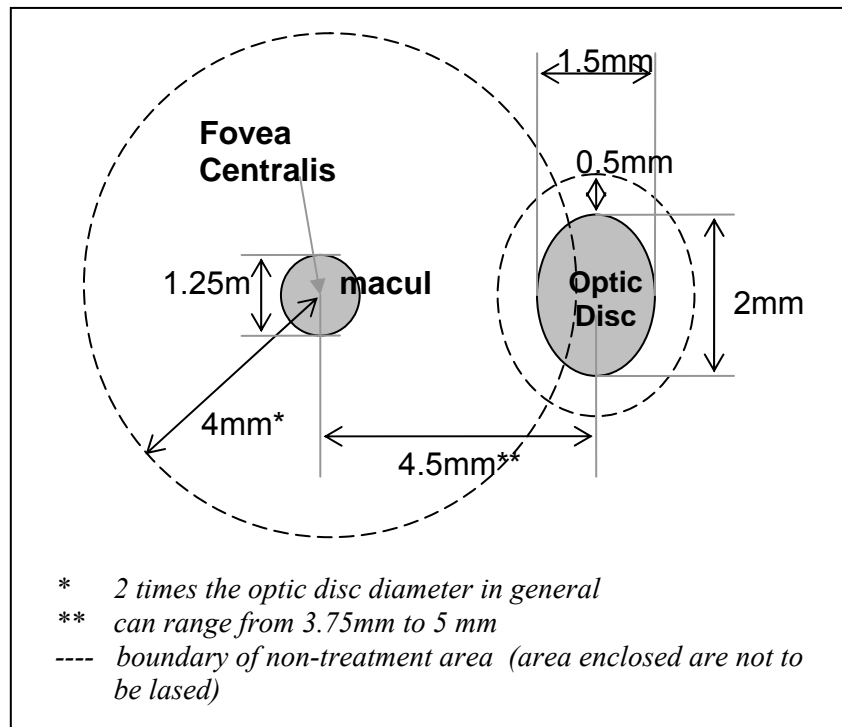
Figure 3.7: Non-treatment area on the retina[8].

By assuming that the retina is a flat surface, the area enclosed by the dotted line can be estimated as shown

$$= \pi(4mm)^2 + \pi(1.5mm)(1.25mm)$$
$$= 56.16 \, \text{mm}^2$$

Therefore, the **total area for treatment** is 1094.78 mm^2 - 56.16 mm^2 = **1,038.62 mm^2**. The term "total area of treatment" is used here to define the span of the retina that will be treated during laser photocoagulation. Generally, laser burns can be irradiated on any point within this area.

It is important to note that the size and structure of the eye differs from individual to individual, hence the value obtained here is only an approximation. Nonetheless, the purpose of this calculation is to estimate the scanning area required by the system and the number of laser burns required to irradiate the region based on the recommended spot size and distance between the laser burns.

Number of burn spots and displacement required for scatter treatment on the retina

In scatter treatment (pan retinal photocoagulation), a spot size of **200 μm to 300 μm** is usually recommended. These spots are placed apart with a distance of **half to one time the diameter** of the spots.
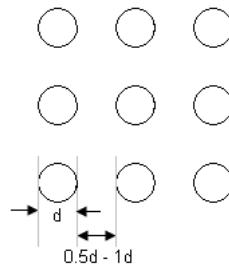
Figure 3.8: Distribution of burns on the retina for a scatter treatment.

From Table 2, the recommendation for full scatter treatment is 1200 to 1600 burns with a spot size of 500 μm, where the area of a 500 μm spot $= \pi(\frac{0.5mm}{2})^2 = 0.19635mm^2$. A prescribed treatment of 1200 to 1600 spots that is 500 μm in diameter implies that the required area to be irradiated **ranges from 235.62 mm² to 314.16 mm²**. With this information, it is possible to estimate the number of laser burns required if a spot size of 250 μm is used. The optimum spacing between the laser burns can also be determined (Refer to Appendix 4 for the method of calculations).

Spacing diameter (mm)	0.5d	0.6d	0.7d	0.8d	0.9d	1.0d
Area per spot (mm²)	0.0491	0.0491	0.0491	0.0491	0.0491	0.0491
Total area (mm²)	1038.63	1038.63	1038.63	1038.63	1038.63	1038.63
Number of spots required	7385.79	**6491.41**	**5750.18**	**5129.02**	**4603.33**	4154.50
Total area covered by spots (mm²)	362.5489	318.6465	282.2613	251.7701	225.9654	203.9338

Table 3: Summary of number of spots required and the optimum spacing between spots on the retina surface if a 250 μm spot size is used. The Figures highlighted are those within the recommended total area of burns based on the data in Table 2.

From Table 3, a 250 μm spot size should be applied at a distance of **0.6d to 0.9d** apart to cover the total treatment area required by the protocol with **4600 to 6500 spots**. It is noted that the selection of spot size has implication to scanning resolution and number of laser spots, thereby influencing the total treatment time.

<u>**Scanning Area of the VOLK Super Quad 160`**</u>

The area for scanning on the VOLK Super Quad 160 is a circle of 22mm in diameter, as this is the maximum aperture of the lens (refer to Section 3.2).
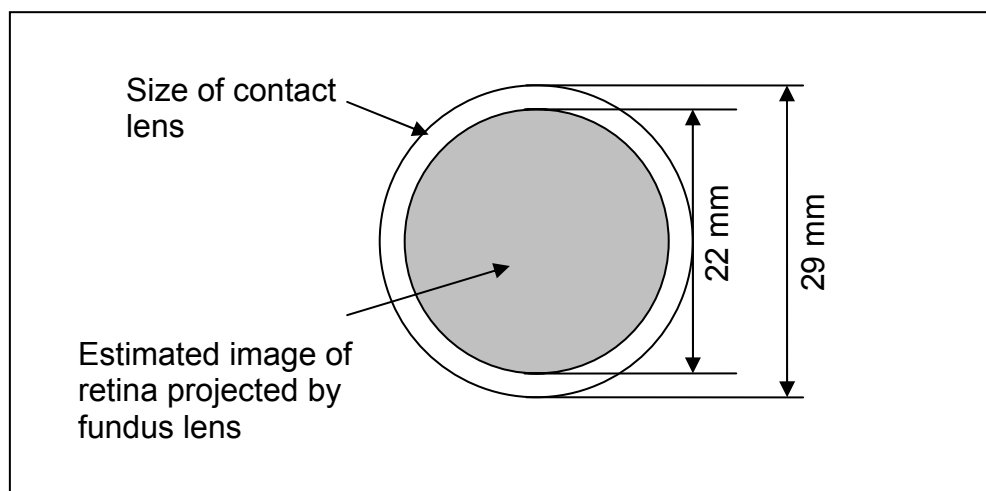
Figure 3.9: Size of the anterior lens and the estimated scanning area.

<u>**Scanning Resolution on the Fundus Lens**</u>

Based on the calculation shown in previous sections,
- the estimated area of the retina projected by the lens for scanning =

$$\pi \left(\frac{22mm}{2} \right)^2$$

= 380.13 mm^2
- the maximum number of spots the treatment will require = 6500

The resolution is calculated by envisioning the image as an imaginary square that have the same area as the image of the retina (380.13 mm^2), and the spots are assumed to be arranged in equal rows and columns within the square.

$$Length\ of\ square = \sqrt{380.13mm^2} = 19.497mm$$

$$Number\ of\ spots\ per\ unit\ length = 80.62$$

$$resolution\ required = \frac{19.497mm}{80.62} = 0.24mm$$

Therefore the scanning resolution required by the system is **0.24mm** on the image plane of the fundus lens**.**

Target Time

The number of spots required ranges from **4600 to 6500** spots. Currently, treatment pattern using pulse duration of 20ms followed by a rest period of 20ms, or even 10ms is possible[2]. Therefore, the system should be able to deliver a full scatter treatment across the entire retina in **3 minutes to 4.33 minutes** if using a 20ms rest time**,** or **2.30 to 3.25 minutes** if a 10ms rest time is used, assuming that the whole treatment is carried out without interruption. This will also meet the requirement of having the eye placed **under suction for not more than 10 minutes**.

In current clinical practice, ophthalmologist takes about 15 to 30 minutes to treat half of the retina in one session. This is because the positioning of the laser is done manually and the involuntary movement of the patient's eye has to be compensated. Treatment is also carried out with pulse duration of 100ms.

Spot diameter on retina, d=0.25mm

Spacing diameter	0.6d	0.7d	0.8d	0.9d
Number of spots required	6491.41	5750.18	5129.02	4603.33
Total treatment time (minute):				
(a) 20ms pulse + 20ms rest	4.33	3.83	3.42	3.07
(b) 20ms pulse + 10ms rest	3.25	2.88	2.56	2.30

Table 4: Total treatment time for different pulse durations and total number of spots using a 250μm spot size. It is assumed that the whole treatment is carried out in one single session non-stop.

Nonetheless, one point of contention is the viability of carrying out scatter treatment for the whole retina in one session. ETDRS (1987)[8] recommended that no more than 900 applications be applied per session. And sessions were typically separated by 2 weeks because of concerns relating to the potential complications of macular edema, choroidal detachment, exudative retinal detachment, and shallowing or closure of the anterior chamber angle[17]. Nonetheless, this system will be designed based on the assumption that it is possible to conduct the whole scatter treatment within one session. This is to allow for future development in the system where usage of an 810nm laser may be used to replace the 532nm. The 810nm laser has the advantage of causing less damage to the retina. However it does not leave a lesion on the retina, thereby making it difficult to detect the area that had been treated.

Laser pulse duration, power and energy threshold based on treatment requirement

In treating the retina, the proposed system has to provide just the right amount of energy required to prevent any wastage of capacity. In current clinical practice, the normal procedure is to use laser with pulse duration of 100ms to 200ms. However, studies have shown that even for light burns at 10 – 100 ms the damage is confined to the outer retina and retinal pigment epithelium[2] , and not reaching the choroid (refer to Appendix 6). Furthermore, significant diffusion of heat is occurring in pulse duration of more than 20ms with less localized homogenous lesions. Diffusion of heat is not desirable as only the treatment area should be exposed to the laser burns.

This implies that smaller pulse duration will result in less thermal diffusion yet providing for an acceptable burn effect. On another note, for very short pulse durations (e.g. 1 ms) the power range between producing a light burn and a photodisruptive result is small; **therefore a 20 ms pulse duration for peripheral treatment and 10 ms for macular treatment is recommended** to increase the power level range between a threshold photocoagulation burn and photodisruptive phenomena[2]. Based on experimental data from Blumenkranz (2006), the pulse duration and laser power required for creating a clinically visible light retinal burn on rabbit eyes using a 514nm wavelength argon ion laser (Novus 2000, Lumenis) is summarized in the table below:

Pulse Duration (ms)	Laser Power (mW)	Pulse Energy (mJ)
10	190-240	1.9-2.4
20	**110-120**	**2.2-2.4**
50	75	3.8
100	50-60	5.0-6.0

Table 5: Range of Power Settings and Corresponding Pulse Energies at Various Pulse Durations Required to Achieve Clinically Visible Light Retinal Burn on rabbit eyes using a 514nm laser for a 130 µm spot size on the retina.

In the proposed design, a 532nm laser will be used instead of the 514nm mentioned in the experiment above. In general, damage threshold scales with wavelength, therefore the damage threshold at **532 nm** will be higher then the **514nm**[48], which implies the need for a higher amount of power to produce the same burn effect. However as the difference here is less than 4% and the power used for calculation is the maximum value in the given range, the wavelength difference is assumed to be negligible. The threshold for **haermorrhage** is found to be at 600mW for a 20ms pulse duration using a 130µm spot size, which corresponds to **4520 W/cm^2**.

It had been determined in the later part of this thesis that the **maximum spot size** delivered by the proposed system will be **400 µm** on the retina (see Section 3.4.3). As more power is required to irradiate a larger area, the appropriate power requirement for a maximum spot size of 400 µm can be determined by calculating the power per unit area required for treatment under the different pulse durations. The result is summarized in the table below:

Pulse Duration (ms)	Maximum Laser Power used for a 130 µm spot size on retina (W)	Power threshold required to achieve clinically visible light retinal burn on the retinal surface (W/cm^2)	Calculated maximum power required for a 400 µm spot size on the retina (W)	Energy for the **respective pulse duration** (J/cm^2)
10	0.240	1808.151	2.272	18.082
20	0.120	904.075	1.136	18.082
50	0.075	565.047	0.710	28.252
100	0.060	452.038	0.568	45.204

Table 6: Power requirement for a 400µm spot size on the retina with different pulse duration.

Spot Diameter on retina (μm)	1000	900	800	700	600	500	400	300	200	100
Spot Area on retina (mm^2)	0.785	0.636	0.503	0.385	0.283	0.196	0.126	0.071	0.031	0.008
Pulse Duration (ms)	Power required by the different spot size on the retina (W)									
10	14.201	11.503	9.089	6.959	5.112	3.550	2.272	1.278	0.568	0.142
20	7.101	5.751	4.544	3.479	2.556	1.775	1.136	0.639	0.284	0.071
50	4.438	3.595	2.840	2.175	1.598	1.109	0.710	0.399	0.178	0.044
100	3.550	2.876	2.272	1.740	1.278	0.888	0.568	0.320	0.142	0.036

Legend:

              Pulse duration and spot size combination that requires power below 2 Watt

              Spot diameter 100μm to 400μm

Table 7: Theoretical power requirement matrix for various spot diameters versus pulse duration for creating a light retinal burn. Calculation is based on experimental data by Blumenkranz (2006)[2].

The energy density on the retina shown here is well within the 200J/cm^2 limit which is used as a general guideline for ensuring that the pupillary beam diameter will remain larger than the retinal beam diameter when using a visible light system[49]. Based on the recommended pulse duration of 20ms and the maximum spot size of 400μm, a **power source of 2 Watt** will be sufficient to meet these requirements.

Treatment and aiming laser beam source

The laser source required for treatment is a frequency-doubled **Nd : YAG solid state laser, diode-pumped, continuous wave (cw)** with a wavelength of **532nm** and maximum power of **2 W**. The laser beam for aiming can be a **diode laser, continuous wave (cw)** with a **635nm** wavelength with a maximum power of **0.4 mW**[50,51].

Parameters	Specification
Spot Size on the retina	200 μm to 300 μm
Field of view	At least 150°
Direction of treatment	Bottom part of the retina to be treated first
Transscleral illumination requirement	100mW to 250mW to be applied near the limbus
Total area for treatment	1,038.62 mm^2
Number of burn spots	4600 to 6500 spots
Displacement between spots	0.6 to 0.9 of spot diameter
Scanning resolution	0.24mm
Target Time	20ms per pulse duration
Treatment laser (532nm) power	2 W
Aiming laser (635nm) power	0.4 mW

Table 8: Summary of operation and treatment criteria

3.1.2 Patient's Safety and Comfort

Fixation of the eye

In the current system, a red LED is used as a focus point for patient to fix their gaze on during the treatment process. However the gaze of a patient who is fixating on a point is found to deviate from 6.24 to 8.28 arc minute along the horizontal meridian, and 3.96 to 4.8 arc minute along the vertical meridian within a trial time of 12.8 seconds[52].

The PASCAL system circumvents this problem by delivering a limited number of spot within a patient's reaction time of 1 second[53]. For example, during treatment around the fovea area, the PASCAL system is able to deliver a ring of 12 spots around the fovea area in approximately 132 milliseconds, which is below a patient's reaction time. This would decrease the risk of accidentally placing spots on the fovea.

To achieve this project objective of delivering a whole scatter treatment within 5 minutes, a corneoscleral limbal vacuum device would have to be implemented to reduce unexpected involuntary motion of the eyeball. It is recommended to fix the

suction level at **20mmHg for a maximum duration of 10 minutes**[41] to avoid potential injuries to the eye.

Effect of depression of fundus lens on the scleral of the eye

Feedback from patients and ophthalmologist revealed that the bulk of discomfort generally occurs during the laser shots on the retina, where a sensation similar to being bitten by an ant is perceived. The depression of the fundus lens on the eye does not cause much discomfort if it is performed appropriately.

3.1.3   User requirement

As described previously, the current method of photocoagulation is tedious to carry out. This new laser photocoagulation system should introduce the following concept:

(1) Positioning of the laser beam to be carried out using a computer.
(2) Multiple shots can be carried out with one press of the switch if required.
(3) The treatment of the whole retina can be done automatically after a set of predefined boundary limits is set.
(4) The fundus lens is to be held mechanically.

3.2 EXPERIMENT

3.2.1 Overview

The fundus lens is an integral component in the apparatus used to treat diabetic retinopathy. It focuses the laser beam onto the retina, allowing a linear scanning motion to be mapped on the spherical surface of the retina. Therefore it is vital to understand the relationship between the point of focus on the retina and the point of incidence of the laser at the front of the fundus lens.
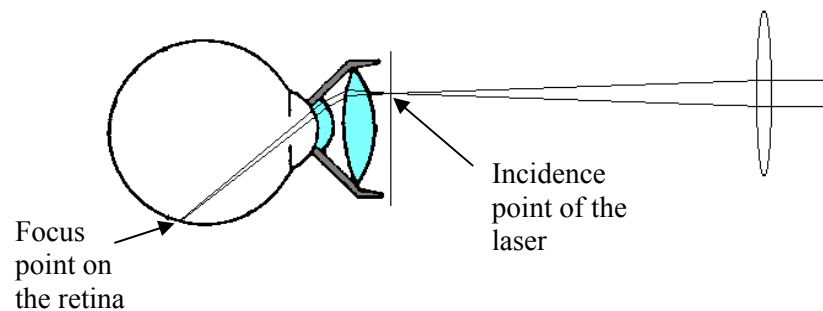
Figure 3.10: Propagation of the laser beam through the fundus lens and onto the retina.

3.2.2 Experiment procedure

1. The laser pointer, focusing lens and VOLK lens were optically aligned to ensure that the optical axis of the focusing lens, VOLK lens and beam propagation is parallel with each other. A common iterative procedure is used by placing a screen close to the laser and moving it about 50cm away while ensuring the beam lands on the exact same spot on the screen by adjusting the alignment of the laser pointer.

2. The focusing lens is placed in front of the laser pointer, and the common iterative procedure is repeated by adjusting the alignment of the focusing lens.

3. Once the laser pointer and the focusing lens are optically aligned, the VOLK lens is placed in front of the focusing lens such that the focused spot of the laser coincides with the front focal plane of the VOLK lens. The common iterative procedure is repeated by adjusting the position of the VOLK lens.
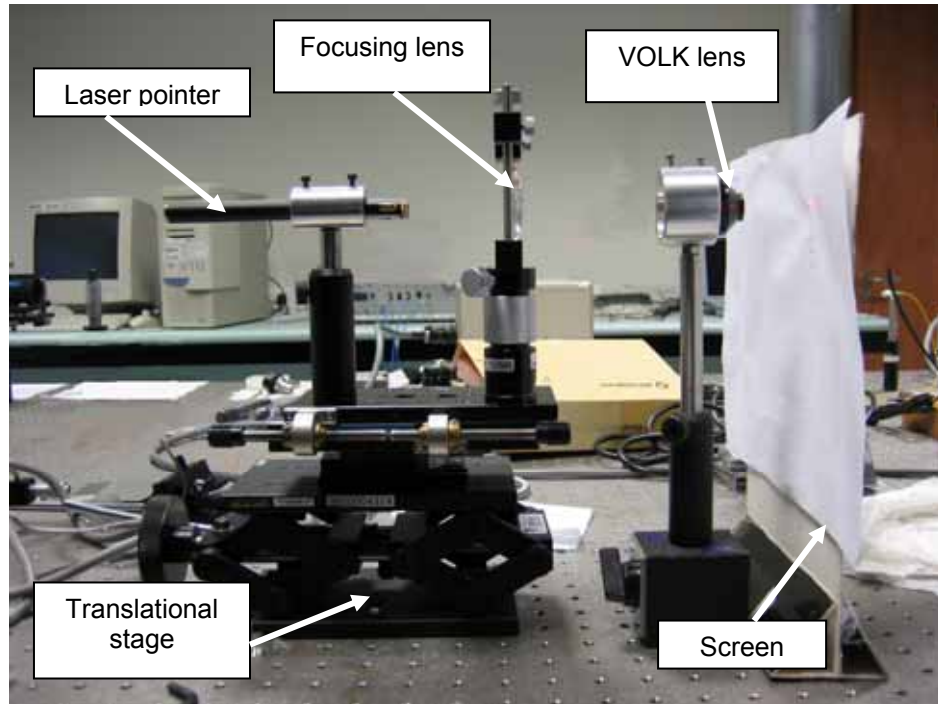
Figure 3.11: Experiment set up for studying the changes in focus position of the VOLK lens with different point of incidence.

4. The screen is then placed in front of the assembly and moved along the optical axis until a focused spot is visible on the screen. The distance between the posterior part of the VOLK lens and the screen position, *d*, is measured.

5. Once the optical apparatus have been optically aligned and centered at the optical axis, the laser pointer is displaced from the optical by *r*=1mm using the translation ramp. The corresponding *D* value is noted down. A 1mm increment is added to the displacement away from the optical axis until the laser is blocked by the VOLK lens aperture. The entire process is repeated for *r*= -1mm. The data collected for this arrangement is known as Set 1.

6. The VOLK lens is then rotated 90° about its optical axis and step 3 to 5 was repeated. The data collected for this arrangement is known as Set 2.

7. From the result of the experiment, the angle α is determined by $\alpha \approx \tan^{-1}\left(\dfrac{D}{d}\right)$
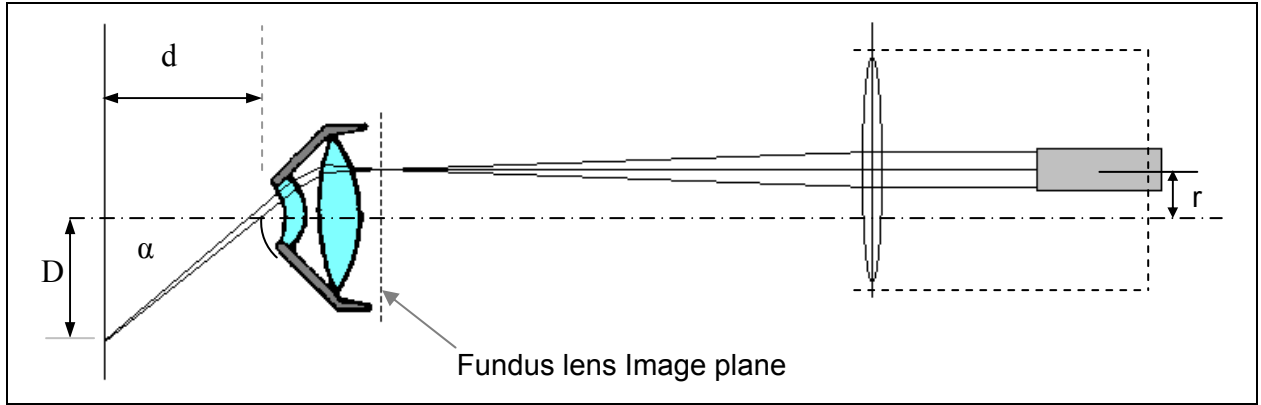
Figure 3.12: Schematics of the experiment set up for studying the changes in focus position of the VOLK lens with different point of incidence.

3.2.3 Result

The result of the experiment is recorded in the table below:

r (mm)	Set 1, d=40.5mm		Set 2, d=37.5 mm		$\alpha = \dfrac{\alpha_1 + \alpha_2}{2}$ (°)
	D (mm)	$|\alpha_1|$ (°)	D (mm)	$|\alpha_2|$ (°)	
11	-121	70.91	-120	72.65	71.78
10	-95	66.47	-87.5	66.80	66.63
9	-74.5	61.47	-67.0	60.76	61.12
8	-58	55.07	-53.0	54.72	54.90
7	-46	48.64	-42.5	48.58	48.61
6	-37	42.41	-33.5	41.78	42.09
5	-28	34.66	-26.0	34.73	34.70
4	-21	27.41	-19.5	27.47	27.44
3	-15.5	20.94	-15	21.80	21.37
2	-10	13.87	-9.5	14.22	14.04
1	-4.5	6.34	-4.5	6.84	6.59
0	-0	0.00	0	0.00	0.00
-1	6	-8.43	4.5	-6.84	-7.63
-2	11	-15.20	9.5	-14.22	-14.71
-3	15.5	-20.94	14.5	-21.14	-21.04
-4	21	-27.41	19.5	-27.47	-27.44
-5	28.5	-35.13	25.5	-34.22	-34.67
-6	36	-41.63	34.0	-42.20	-41.92
-7	45.5	-48.33	42.5	-48.58	-48.45
-8	57	-54.61	53.5	-54.97	-54.79
-9	70	-59.95	66.0	-60.40	-60.17
-10	92	-66.24	85.5	-66.32	-66.28
-11	118	-71.06	116.0	-72.09	-71.57

Table 9: Result of experiment

3.2.4 Analysis

As the lens is symmetrical about the optical axis, the angular displacement of the focus spot from the optical axis is the same for r>0 and r<0, hence the average of the data is summarized in the table below:

r (mm)	Average for r>0 and r<0, $|\alpha_{ave}|$ (°)
11	71.82
10	66.57
9	60.64
8	54.84
7	48.53
6	42.01
5	34.69
4	27.44
3	21.21
2	14.37
1	7.11
0	0.00

Table 10: Average angular displacement of focus point from optical axis with respect to different points of incidence.
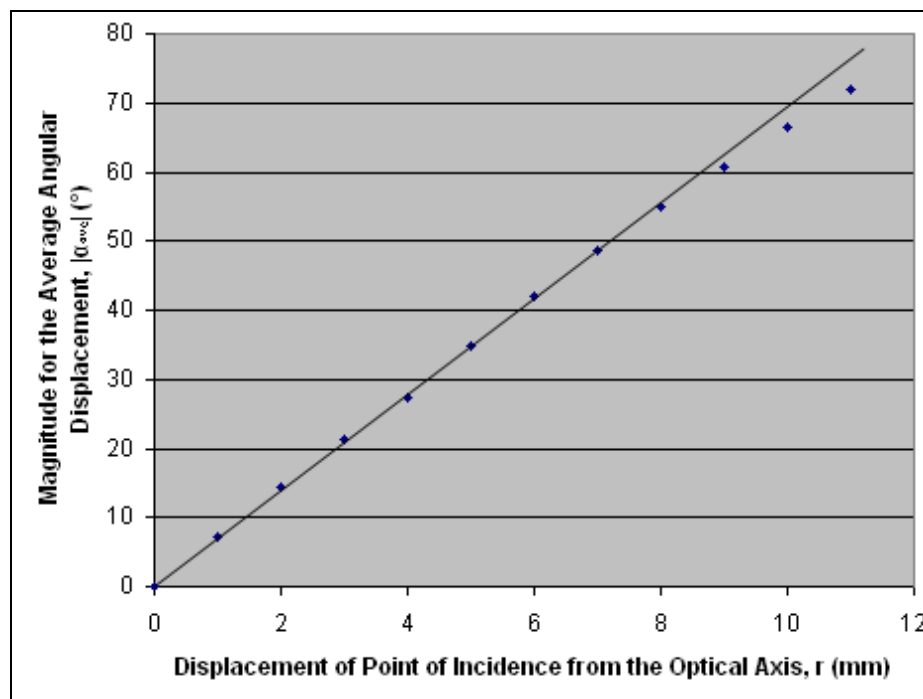
Figure 3.13: Plot of the displacement of the point of incidence from the optical axis, r (mm), against the magnitude of the angular displacement of the point of focus, α_{ave} (°).

From Figure 3.13, the slope of the straight line $= \dfrac{71-0}{10.2-0} = 6.96$

3.2.5 Conclusion

In conclusion, the relationship between the displacement of the point of incidence from the optical axis, **r (mm)**, and the magnitude of the angular displacement of the point of focus, $\boldsymbol{\alpha_{\textbf{ave}}}$ **(°)** is represented by $\boldsymbol{\alpha_{\textbf{ave}}}$ = **6.96r**. If the direction of α_{ave} is considered, then the equation would be $\boldsymbol{\alpha_{\textbf{ave}}}$ = **-6.96r.**

This equation will be used in Section 3.4.2 to relate the rotation of the galvanometers to the positioning of the laser beam on the retina.

3.2.6 Discussion

The equation $\alpha_{ave} = -6.96r$ is derived based on the following assumptions:

(1) **The exit beam is assumed to be emitted from the point of optical axis and from a distance _d_ from the screen for all values of _r_.** However, the point of emission is in fact displaced from the optical axis by a value of ε when $r \neq 0$. The beam is only emitted from the point at the optical axis if r=0mm. In addition, the distance _d_ does not reflect the actual distance of the curved surface of the lens from the screen, creating an error value of Δ.

(2) **The relationship between α_{ave} and _r_ is linear.** The linear relationship of $\alpha = 60.8r$ seems to be valid for r<8mm. For r≥8mm, relationship starts to deviate from linearity. It is not clear whether this is the property of the lens or an effect of error in the measurement of D. As the beam position on the screen moves further away from the optical axis, the shape of the beam image becomes more elongated. This makes it difficult to pinpoint the exact position of the spot. During the experiment, the measurement was taken at the center of each spot.

(3)   **The index of refraction of the eye was not taken into consideration.** The equation $\alpha_{ave} = -6.96r$ relates only the relationship between r and α when the laser beam is propagating in the air. Further refinement of this relationship had to be carried out with regards to the index property of the structures in the eye and its effect on the beam propagation.
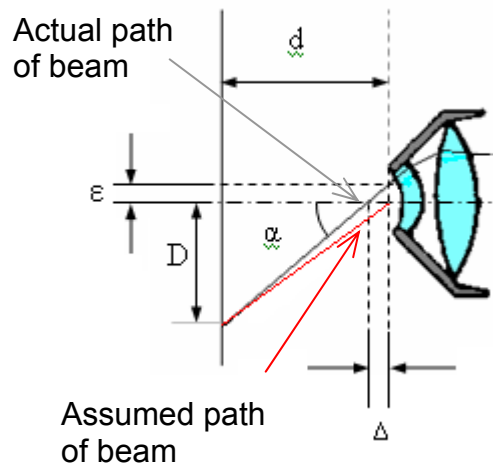
Figure 3.14: Error in calculation of α   **Figure 3.15: Elongation of beam image as D increases**
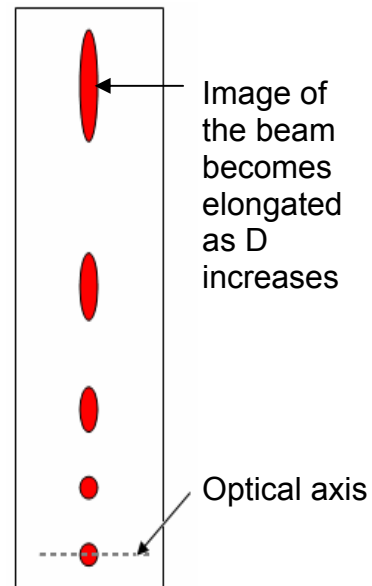
3.3 CONCEPTUAL DESIGN AND DESIGN SYNTHESIS

3.3.1 Overview of Design Objective

The objective is to identify the most suitable mechanism and design concepts to be implemented in the optomechanical system. The key questions can be classified into the following categories:

(1) **Fundus lens-cornea interface** – to determine the mobility required of the fundus lens and the possibility of using a non-contact fundus lens in the design

(2) **Optical Scanning System –** to determine the type of optical system to be implemented

(3) **Type of scanning lens required** – to choose a suitable type of scanning lens

(4) **Methods for varying the spot size of the laser beam** – to choose between the parfocal or defocus method for varying the spot size

In selecting the final concept, the decision criteria will be focused on ensuring **safety of the patient and the ophthalmologist** during operation of the apparatus, **compactness**, and **ease of maneuvering and operation** of the device.

3.3.2 Fundus lens-cornea interface

In the initial part of the investigation, a key question to answer was the mobility required of the fundus lens and the possibility of using a non-contact fundus lens to circumvent the complication of having to position the apparatus on the cornea itself (see Section 3.1.1 for more details about the fundus lens). Three design concepts were evaluated to identify the best concept to be used.

Concept 1:

The fundus lens is fixed and the eye is kept still using a small suction to keep the cornea in place. Positioning of the laser spot on the retina will be done solely by manipulating the laser beam.
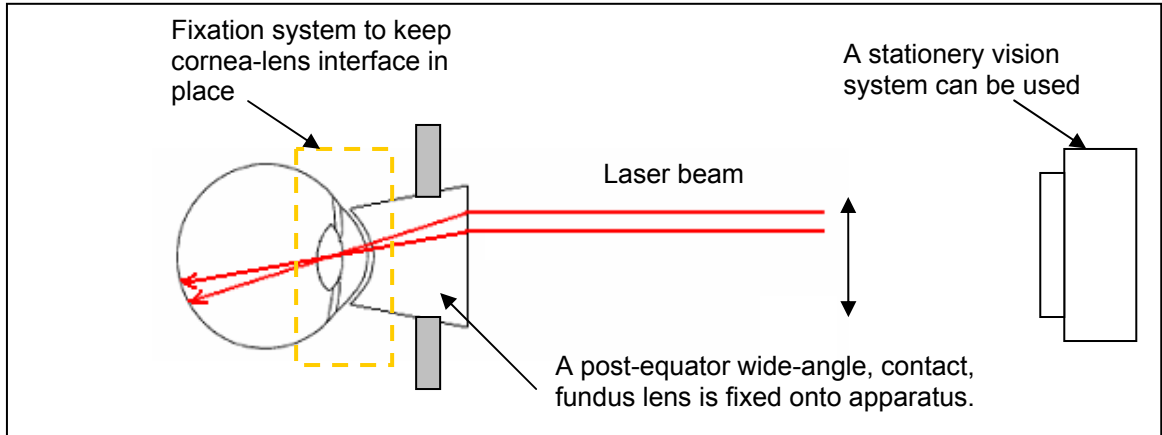
Figure 3.16: Schematics of a design using concept 1

Concept 2:

The fundus lens is mechanically manipulated to emulate the current practice of displacing the lens across the cornea in small movement to obtain the desired view of the retina in instances where the peripheral view is not clear or not in sight. The tilting of the fundus lens will also provide minute steering of the laser onto the retina surface. However the positioning of the laser spot on the retina will be largely done through manipulation of the laser beam itself.
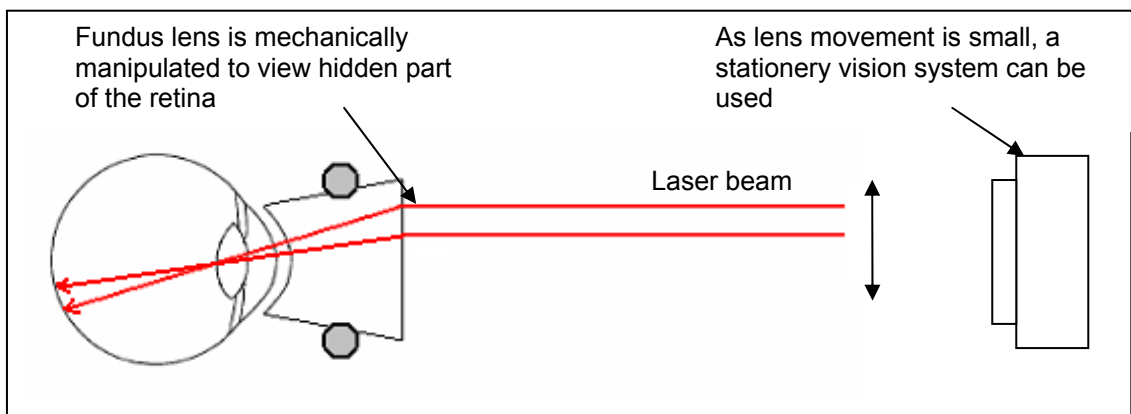
Figure 3.17: Schematics of design using concept 2

Concept 3:

A non-contact fundus lens or a contact lens which is displaced about 5mm from the cornea is used.

The viewing system will have to be aligned perpendicularly to the surface of the lens to obtain the best image

5 mm

If a non contact fundus lens is used, the design would require the patient to shift his or her gaze OR to swing the fundus lens to project the laser into the periphery area of the retina
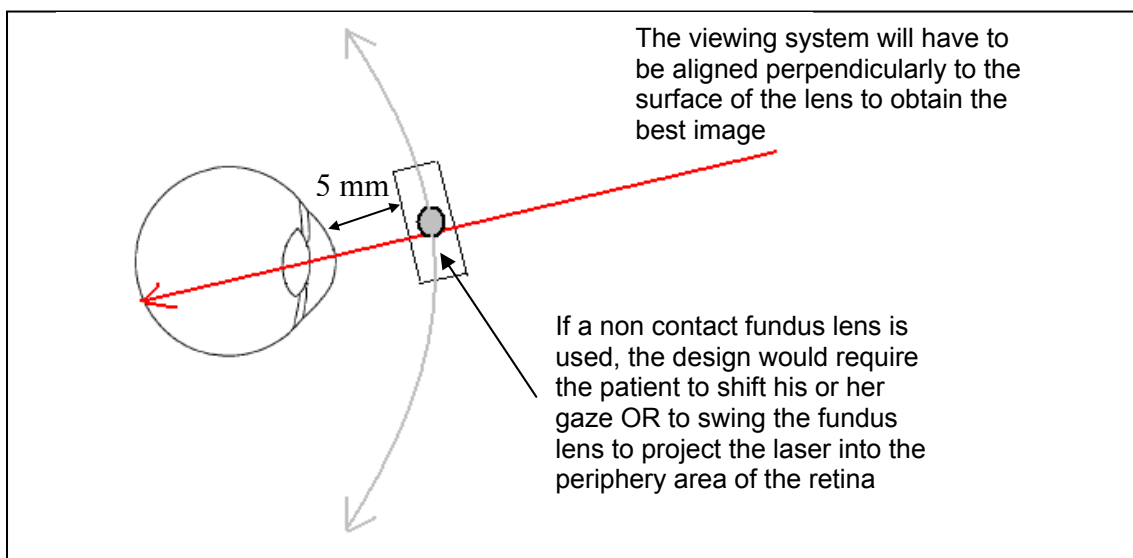
Figure 3.18: Schematics of design using concept 3

The result of the investigation is summarized in the table below:

	Concept 1	Concept 2	Concept 3
Ease of achieving the desired field of view	Good. Current lens can provide view of 160° which will cover all treatment area. Therefore there is no need to utilize the dynamic field of view as proposed in concept 2.	Good. The dynamic field of view for the VOLK Super Quad is 165°.	Difficult. Current non-contact lens offer dynamic field of view up to 124° (for the Super Vitreo Fundus®.)
Patient's safety	Suction system will ensure the eye remains stationery. Concern for safety exists in the design of the suction system.	It is recommended that a suction system also be used to ensure there is no eye movement.	It is recommended that a suction system also be used to ensure there is no eye movement.

Ease and accuracy of beam steering	Stationery lens coupled with a stationery eye ensure that placement of laser beam is controlled only by the scanning system.	Motion of the lens present complication in the scanning system as placement of laser now depends on the scanner and the contact lens movement.	Motion of the lens present complication in the scanning system as placement of laser now depends on the scanner and the contact lens movement.

Table 11: Comparison of the proposed concept.

Based on the investigation, **the best concept to be used is Concept 1**. The most suitable lens to be used is the VOLK Super Quad 160, which is described in Section 3.1.1 The VOLK Super Quad 160 is used in current treatment of proliferative diabetic retinopathy providing a viewing angle of up to 160º which covers the entire treatment area. However the lens had to be held onto the cornea during treatment. In normal cases, the VOLK Super Quad 160 would be able to accommodate all adult eyes so there would be **no need to change to a different lens for different patients**.

3.3.3   Optical Scanning System

In the current laser photocoagulation apparatus, beam steering is done by (1) a laser tower with mirrors (2) galvanometers (proprietary electronic micromanipulator) used by the PASCAL system. The laser tower does not allow for rapid movement and based on the simulation on the PASCAL website, the electronic micromanipulator in the PASCAL systems only allows for scanning within a 4.4mm x 4.4mm on the surface of the corneal (corneal plane). For this system, the objective is to be able to **scan the laser beam over the whole retina** (an area of 22mm in diameter if using the VOLK Super Quad 160) and **complete the treatment within 5 minutes**.

In a general scanning system, the laser beam can be a converging beam, diverging beam or a collimated beam. There are 3 basic scanning conFigurations: objective scanning, post-objective scanning and pre-objective scanning which are differentiated by the different positioning and relative motion of the objective lens, in relation with the scanner and the scanning surface[54].

Concept 1: Objective scanning

The objective lens is rotated from a remote axis or translated in a linear manner across the collimated beam.
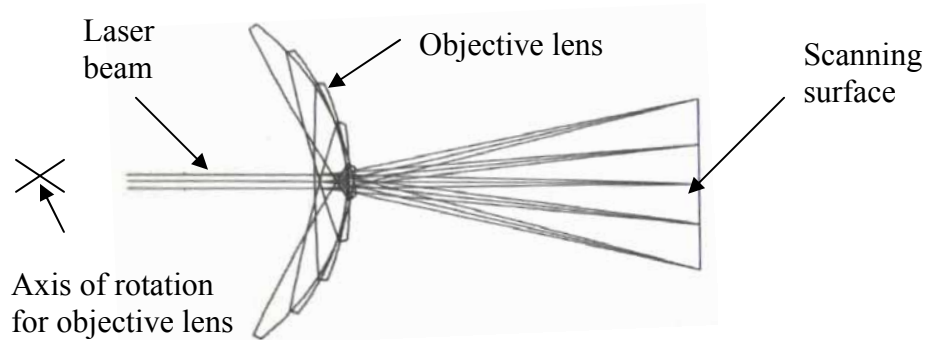
Figure 3.19: Objective scanning

Concept 2: Post-objective scanning

The scanner is located between the objective lens and the scanning surface. The objective lens is required to have a long focal length to accommodate the scanning mirrors; the focal point will approximately paint a sphere. To obtain a large angular excursion on a flat plane scanning surface, the objective lens has to be translated on a linear stage.
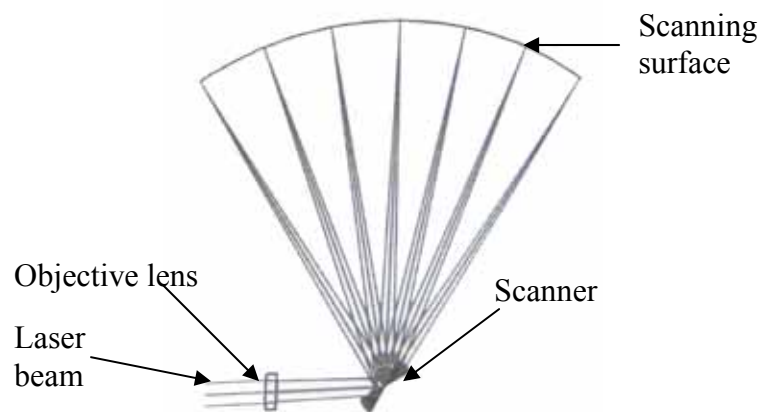
Figure 3.20: Post-objective scanning

Concept 3: Pre-Objective scanning

The objective lens is located between the scanners and the scanning surface. It permits a comparatively small spot size with high energy density. A flat field objective lens is normally used to image the angular scanning field onto a flat surface.
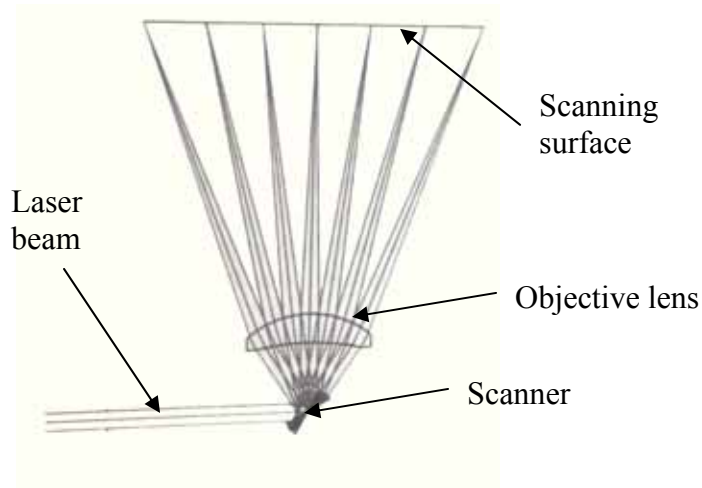
Figure 3.21: Pre-objective scanning

Conclusion:

In the proposed design, a **pre-objective** scanning system with a flat field objective is utilized to ensure that the focus plane of the beam delivery system will coincide or is parallel with the image plane of the fundus lens. The scanning system will consist of **two galvanometer scanners** and a **flat field objective lens**.
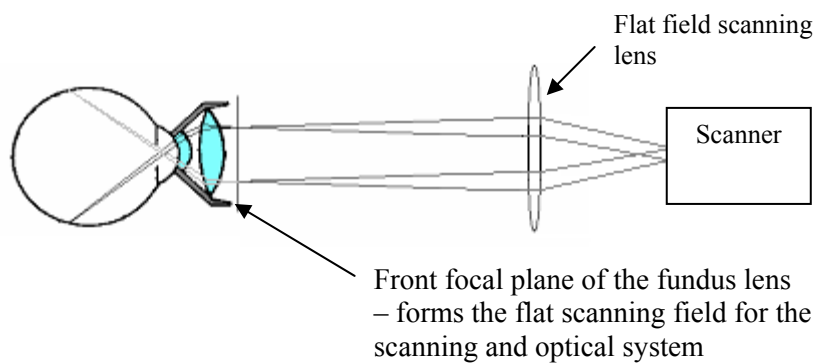
Figure 3.22: Pre-objective scanning system and the fundus lens

3.3.4   Type of scanning lens required

Flat field scanning lens has 2 functions, first to focus the beam onto the desired plane, and second to focus the beam so that the focal plane forms a flat surface as opposed to a curved plane when using a typical focusing lens. A flat field scanning lens is used in

the proposed design so as to ensure that the focused spot has the same size and shape across the whole scanning surface at the front of the fundus lens.
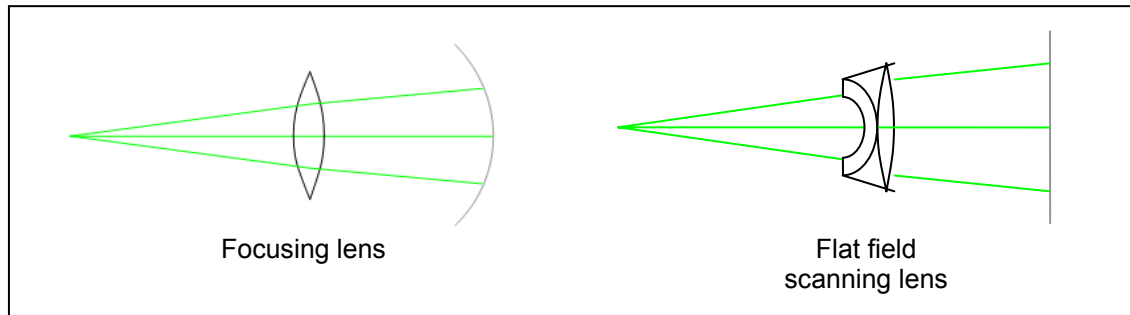
Figure 3.23: Diagram of the focusing plane formed by off axis deflection through a focusing lens and a flat field scanning lens.

There are 3 subclasses to the flat-field scanning lens: a typical flat field scanning lens, an f-θ lens, and a telecentric lens. Based on the notations in Figure 3.24, the difference in the lens characteristic is summarized in the table below:

Properties	Lens type		
	Typical flat field scanning lens	Flat field scanning lens with f-θ characteristic	Flat field scanning lens with telecentric characteristic
Displacement from optical axis, R	R=Ftanθ	R=Fθ	Depends on whether it is has f-θ characteristic or not
Angle of incidence on the scanning plane, Φ	$\Phi \neq 0°$	Depends on whether it is has telecentric characteristic or not	$\Phi = 0°$

Table 12: Comparison of scanning lens.
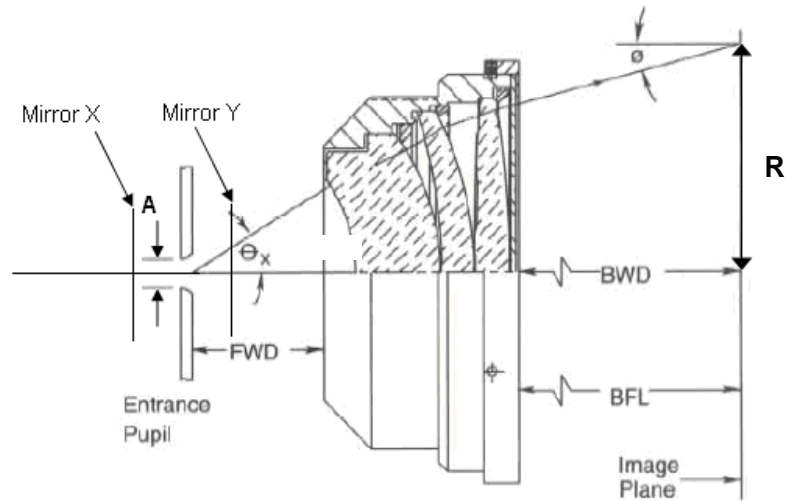
Figure 3.24: Diagram of a general scanning lens.

For a galvanometer beam steering system, an f-θ lens is not necessary as we can control the shaft rotation. A telecentric lens focuses the scanning beam at an incident angle which is normal to the entire flat scanning field. The image of the retina projected by VOLK lens will act as the scanning field (or image plane) in this application.

Depending on the scanning lens property, laser of different wavelength may have different values of R (Figure. 3.24). As we are using laser beams with a wavelength of 635nm and 532nm, choosing a **colour corrected lens** would ensure that both beams falls on the same point with the same deflection of the galvanometer. The scanning lens requirement is summarized in the table below:

Criteria	Required for the design purpose?
Flat field	**Yes**
Telecentric properties	**Recommended** The main advantage is to avoid distortion of the spot size on the scanning field (front image plane of the fundus lens).
F-θ	**Not necessary.** Galvanometer shaft can be controlled to provide the necessary rotation to produce the required position. The linearity provided by the f- θ lens is not a must, just a matter of convenience in the control design.

Colour corrected	**Recommended.** Having the two different lasers falling on the same point with the same deflection of the galvanometer would ensure accurate positioning as there will not be any discrepancy between the location of the aiming beam (635nm) and the treatment beam (532nm).

Table 13: Summary of design requirement for the scanning lens.

3.3.5 Methods for varying the spot size of the laser beam

<u>Overview on the importance of choosing the right method for varying the spot size</u>

In delivering a laser beam to the retina, the laser will also pass through the cornea, aqueous humor, lens and vitreous humor. These structures are exposed to local heating that may result in damage[44]. The cornea particularly has poor thermal conduction on the outer surface and has a damage threshold of **10 W/mm^2** [55].

One method of differentiating the impact of the laser beam through the various structures is by choosing the proper wavelength to take advantage of the differences in spectral absorption. Another method is to adjust the width of the beam, such as focusing the beam into a cone to obtain different energy densities as it passes through different structures. Therefore power can be localized at the desired plane along the axis of propagation[44].
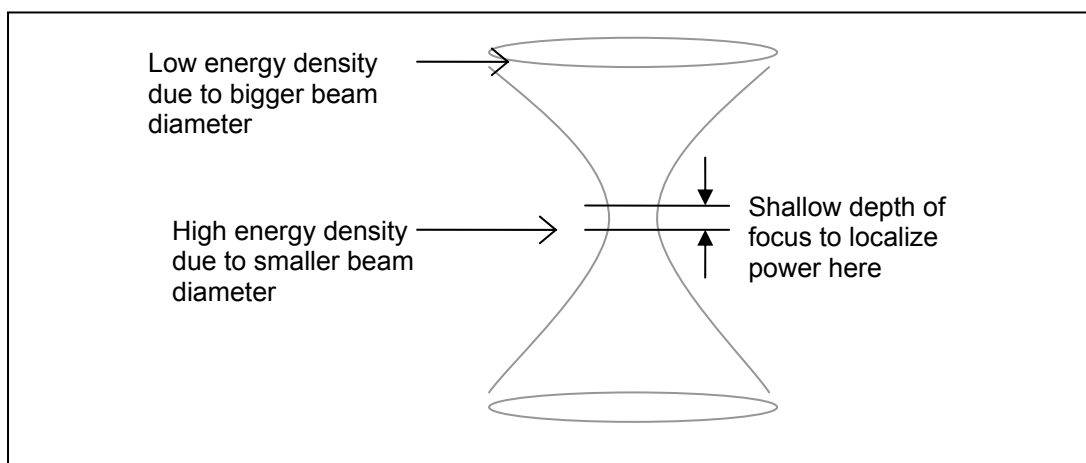
Figure 3.25: Focusing a large diameter beam into a conical shape to obtain lower power density on either side of the focal point.

Method for varying the spot size - Parfocal vs. Defocus

Two different methods have been used by laser system manufacturers to obtain a selection of spot sizes at the slit lamp focal plane. The methods are commonly referred to as "Parfocal", and "Defocus". Some systems are designed with only one method, some systems use a "Parfocal" method for the smaller spot settings and changes to "Defocus" when the spot size increases.

In a "Parfocal" system the size of the spot is changed by varying the magnification while maintaining focus at the retina. This produces a clean round image with relatively even laser intensity over the entire spot. The parfocal approach also changes the beam convergence as the spot size is changed resulting in a long depth of field at large spot sizes (Figure. 3.26). Depth of field is the distance in front of and beyond the subject that appears to be in focus. There is only one distance at which a subject is precisely in focus and the focus falls off gradually on either side of that distance.

In a defocus system the size of the spot is changed while focusing on the retina for only a small range of spot sizes. Beyond that the spot size is changed by shifting the focal point of the beam away from the retina. This will result in a large laser spot size where the out of focus beam is truncated at the slit lamp focal plane (Figure. 3.26). In the defocused mode, the energy density at the cornea decreases as spot size increases. A defocus system can be achieved by shifting the objective lens along the axis of the laser propagation, thereby shifting the focusing point for the laser beam.
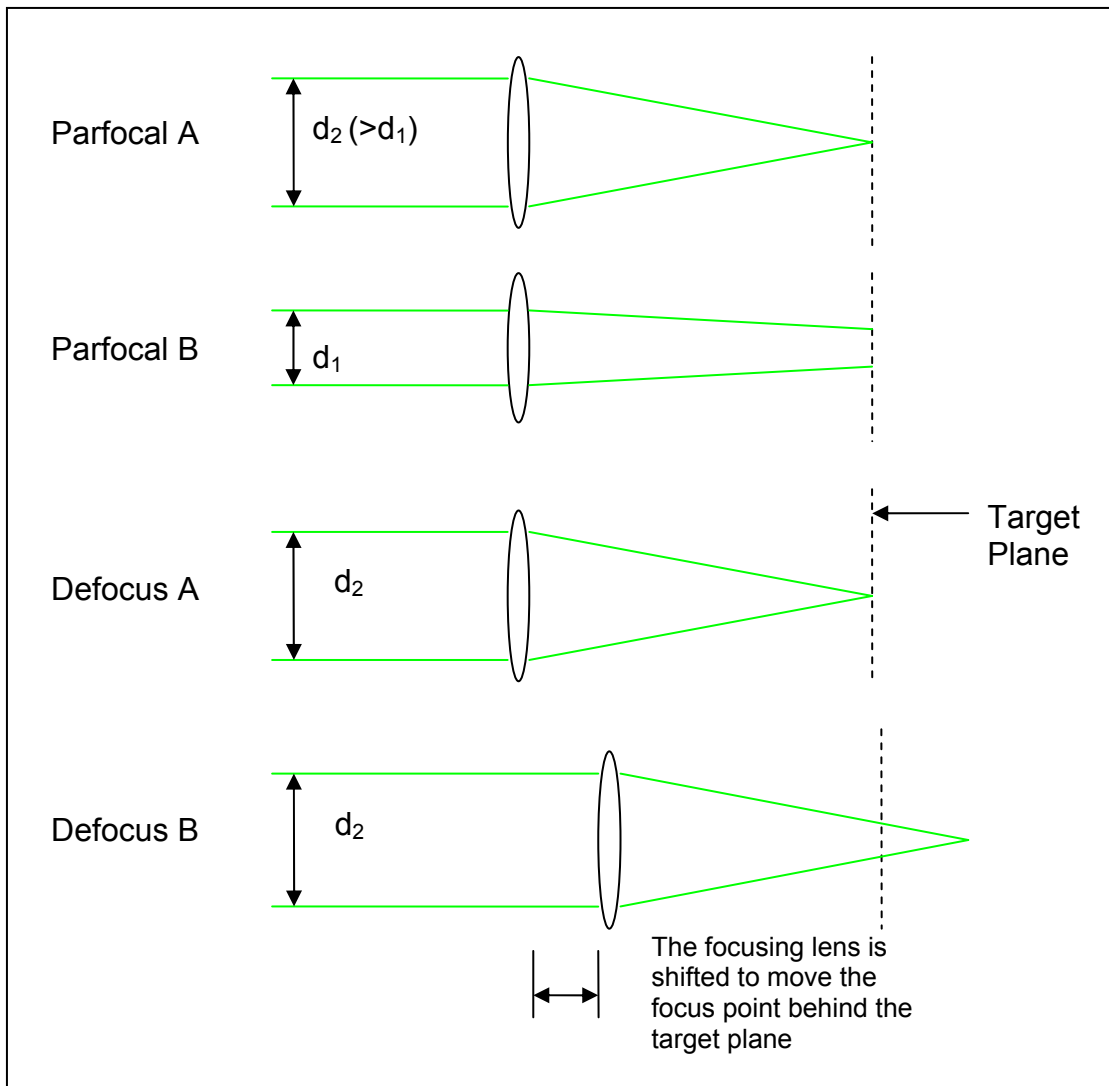
Figure 3.26: Mechanism for parfocal system and defocus system.

Since the far field intensity pattern of the light emerging from the optical fiber has a Gaussian profile, laser spots produced by defocusing have a Gaussian character rather than the sharply defined edges produced by a parfocal system (Figure. 3.28). Therefore, the beam tends to be hotter in the center and thus less evenly irradiated.

(A)

100μm & 500μm Parfocal beam diameters
vs distance from focal plane.
(for a .01 "beam product" beam)

-500 μm Ø

·100 μm Ø

Focal plane
(Retinal position)

Approx. corneal position
(Goldmann contact lens)

Distance from focal point (mm)

(B)

100μm & 500μm defocus beam diameters
vs distance from focal plane
(for a .01 "beam product" beam)

·500 μm Ø Defocus

·100 μm Ø

Focal plane
(Retinal position)

Approx. corneal position
(Goldmann contact lens)

Distance from focal point (mm)

Figure 3.27: Comparison of the difference in beam diameter at the corneal plane for "Parfocal" and "Defocus" method. Adapted from Dewey D. (1991)[44].

In general, the sharply defined edge and evenly irradiated spot of the parfocal beam is preferable to the unevenly irradiated spot created by a defocus beam. However a parfocal beam with a large spot size will produce a high energy density at the cornea due to its small radius. Therefore a parfocal beam is often used together with lower energy setting and smaller spot size and a defocus beam is used when a high energy setting is required for a larger spot size.

The Quadra Aspheric lens is found to maintain less than 2 J/mm^2 pupillary radiant exposure if the true retinal **spot size is kept below 400μm** for **both parfocal and defocus** delivery systems. As the magnification power of the VOLK Super Quad 160 is similar to the Quadra Aspheric, the proposed system should also ensure that the retina spot size is kept below 400 μm. As there is no distinct difference between the parfocal and defocus system within this range, a parfocal system will be implemented in the proposed design to obtain a sharply defined and evenly irradiated therapy area.

Parfocal and Defocus beam profiles for the VariSpot
at 500μm Ø spot size. Perfect "top hat" and gaussian
profiles are also plotted for reference.
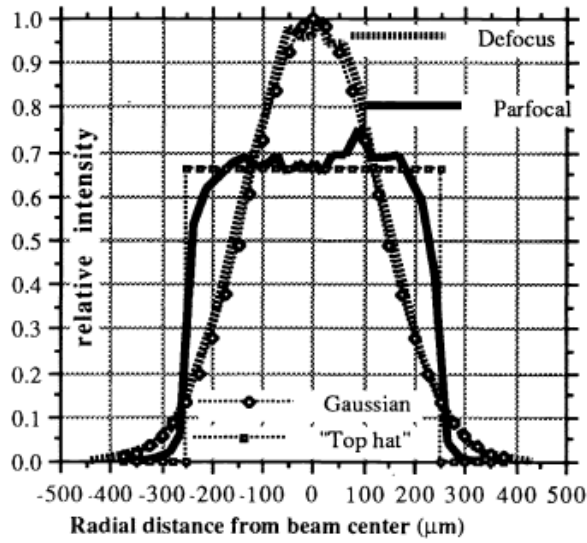
Figure 3.28: Comparison of the intensity profile for a laser spot of the same size created by a "Parfocal" and a "Defocus" method. Adapted from Dewey D. (1991)[44].

Beam diameter at the cornea, cyrstalline lens, & retina.
VariSpot with Quadra Aspheric lens
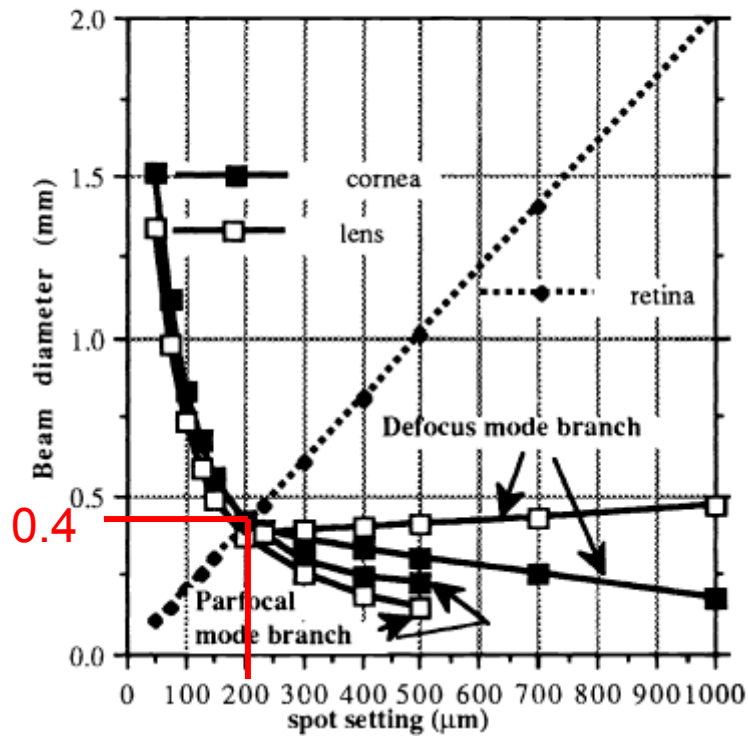
Figure 3.29: Beam diameter at the cornea, crystalline lens & retina with a Quadra Aspheric lens. Adapted from Dewey D. (1991)[44].

3.4   EMBODIMENT AND DETAILED DESIGNS

3.4.1   Overview

Based on the design concepts selected in Section 3.3 and the design specifications listed in Section 3.1, the detailed design for the optomechanical system for laser scanning can be carried out. The relationship between the various concepts discussed in Section 3.3 is illustrated in the diagram below.
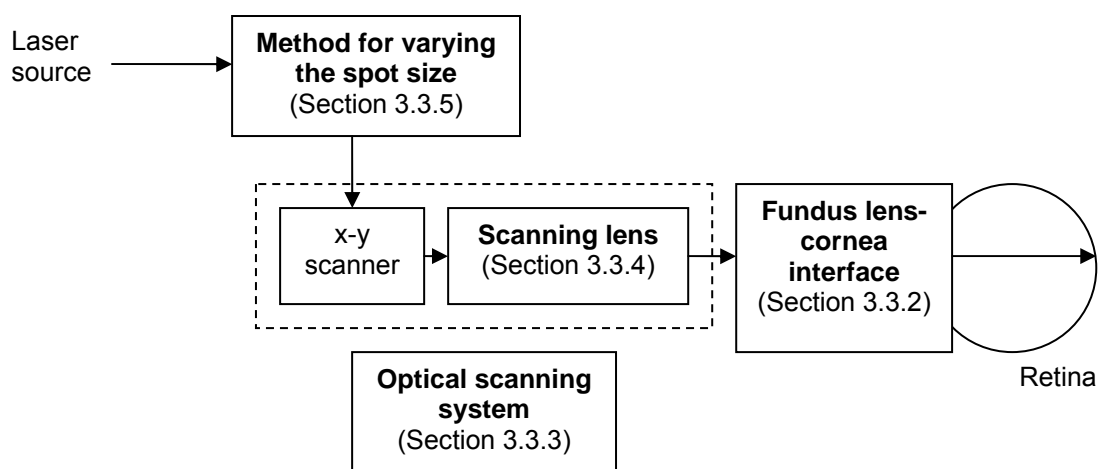
Figure 3.30: Relationship between design concepts discussed in Section 3.3: Conceptual Design

In this thesis, the details of the design for the following system are provided:

- **Laser Beam Steering System** - to position the laser on the retina
- **Laser Delivery System** – to deliver the treatment and aiming laser at the required spot size to the galvanometer and into the retina
- **Laser Source System** – to deliver the treatment and aiming laser at the required power and pulse rate into the optical fiber which connects to the laser delivery system
- **Vision System** – for diagnosis and viewing during treatment

An overview of the systems discussed is shown in Figure 3.31 and Figure 3.32.
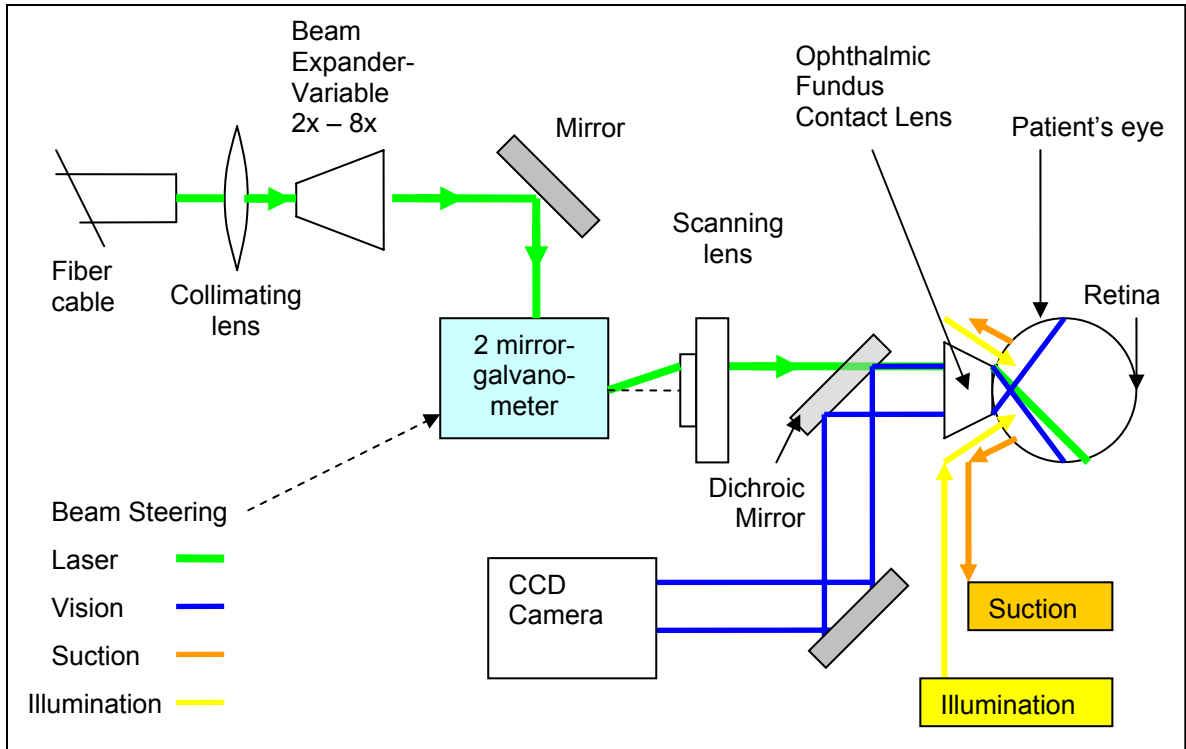
Figure 3.31: Schematics of the overall laser photocoagulation system.
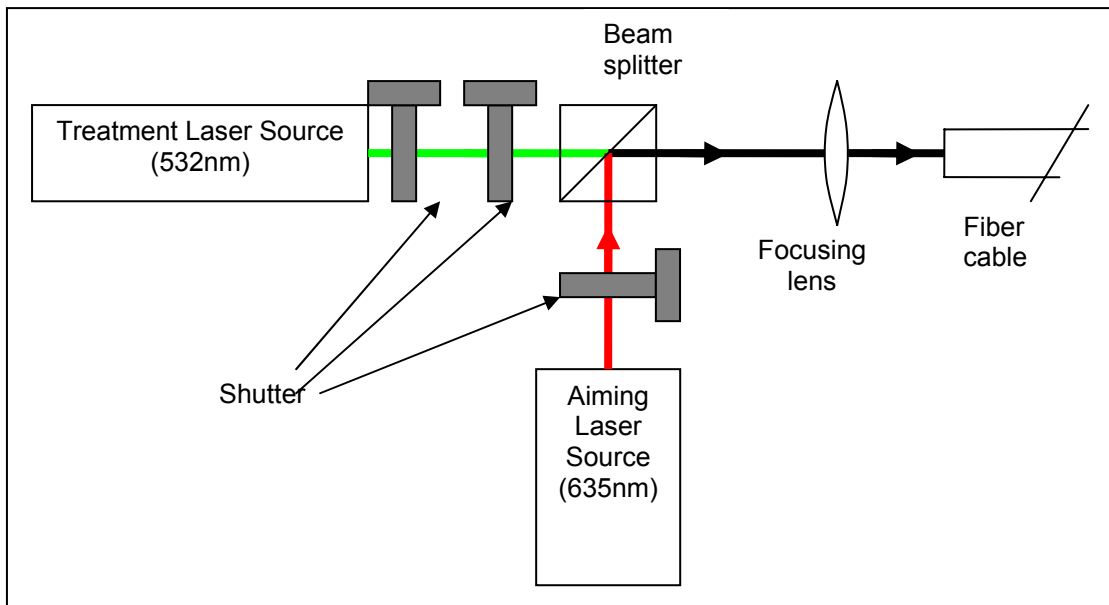
Figure 3.32: Schematics of the laser source system.

3.4.2   Laser Beam Steering System

The laser beam steering system consists of:

1.   2 Galvanometers
2.   Flat Field Scanning lens
3.   Mirrors attached to each galvanometer
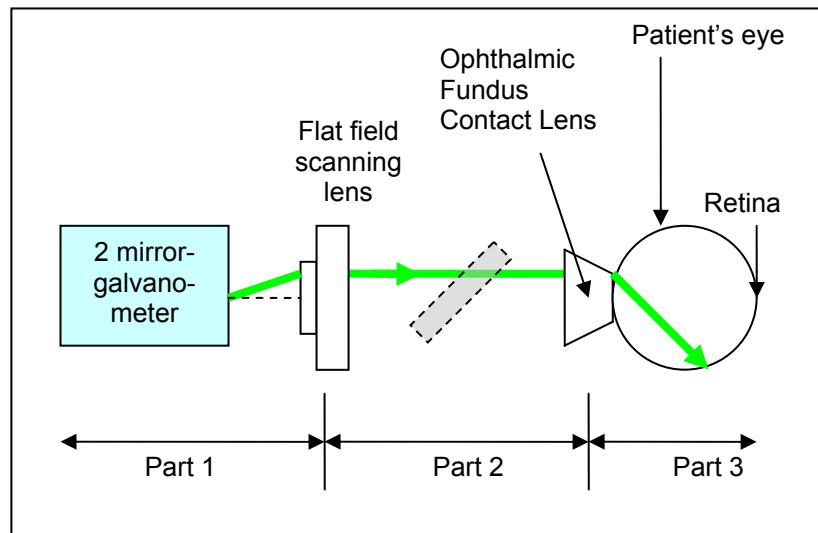
Figure 3.33: Beam steering system.

The galvanometer will steer the beam onto the scanning lens, which will then focus and position the beam onto the fundus lens. The fundus lens will direct and focus the beam onto the retina. The focus of the design will be on the positioning of the treatment beam. The flow of discussion will be separated into Part 1, Part 2, and Part 3 (Figure. 46). This will be followed by a discussion on issue concerning the implementation of the aiming beam for a full scatter treatment.

3.4.2.1 Part 1 – Relationship between the galvanometers and the scanning lens

The X-Y scanner is made up of 2 galvanometers arranged as shown in Figure 3.34.
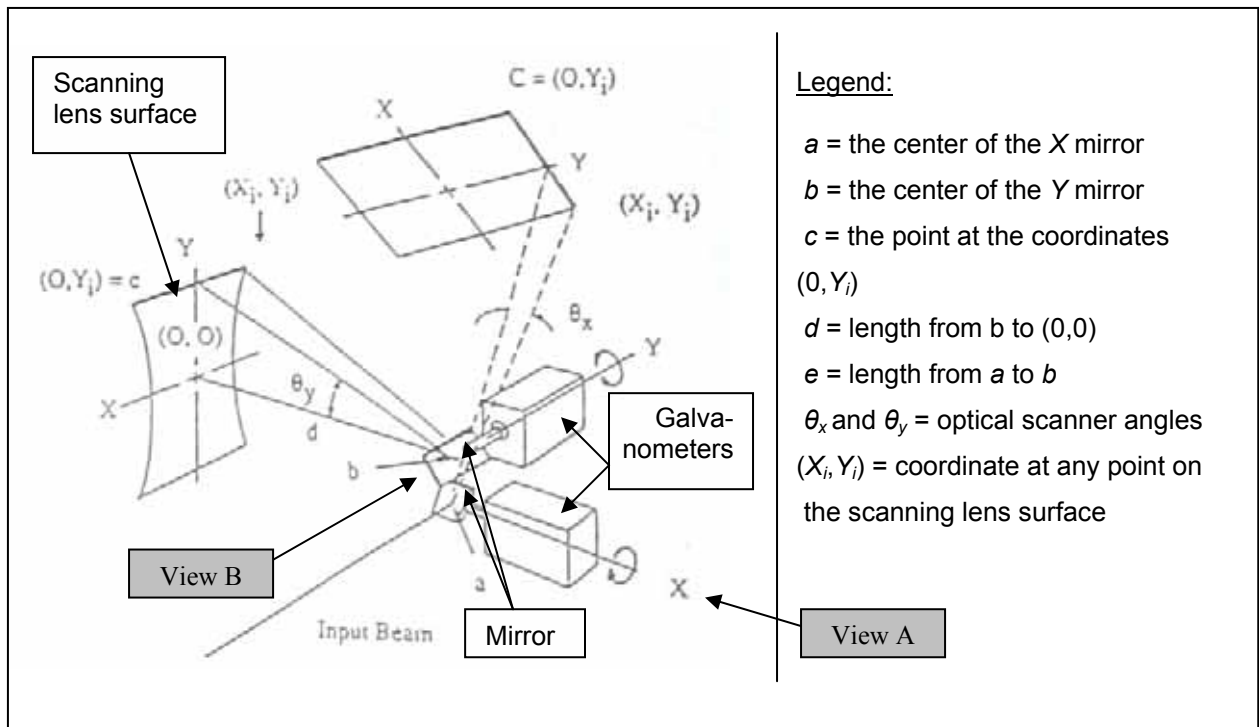
Figure 3.34: Two-mirror, two-axis flat-field assembly[56].
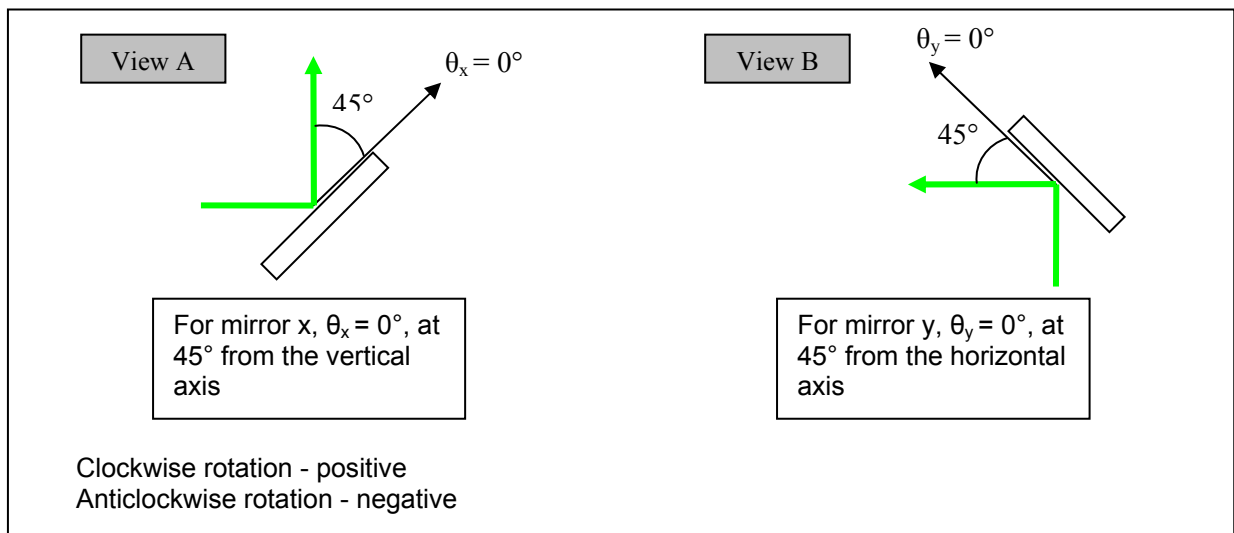
Figure 3.35: Diagram showing position of θx = 0° and θy = 0°.

When $X_i = Y_i = 0$, then $\theta_x = \theta_y = 0$, (See Figure 3.34)

$Y_i = d \tan \theta_y$, and

$X_i = ac \tan \theta_x$.

Since $ac = (d^2 + Y_i^2)^{1/2} + e$ where $e = ab$, the solution is

$X_i = \{(d^2 + Y_i^2)^{1/2} + e\}\tan \theta_x$.

By solving the length from a to (X_i, Y_i) we obtain the equation for the focus length:

$$f_i = \left[\left\{ (d^2 + Y_i^2)^{1/2} + e \right\}^2 + X_i^2 \right]^{1/2},$$

The resulting change in focus length for (X_i, Y_i) is

$$\Delta f_i = \left[\left\{ (d^2 + Y_i^2)^{1/2} + e \right\}^2 + X_i^2 \right]^{1/2} - (d + e).$$

In a two-mirror systems, the pincushion error ε is the ratio of the change in the value of X_i as θ_y changes from zero to a specified value, to the peak-to-peak amplitude $2\,X_i$ at $\theta_y = 0$:

$$\varepsilon = \frac{X_{i\theta_y} - X_{i0}}{2X_{i0}} = (1 - \cos\theta_y)/2(1 + e/d)\cos\theta_y$$

This error can be corrected by the control system.

Shape expected based on calculations

Shape produced due to error in a two mirror scanning system
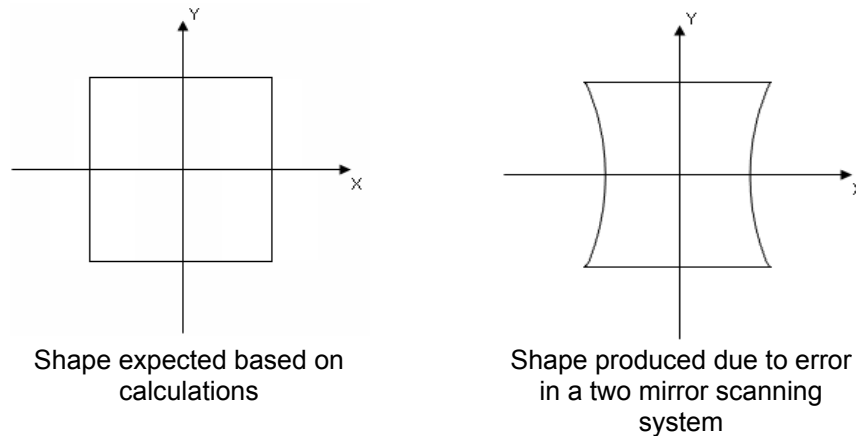
Figure 3.36: Pincushion effect caused by a two-mirror beam steering system.

3.4.2.2 Part 2 – Relationship between the scanning lens and the fundus lens

Table 13 shows the properties of a **flat field**, **colour corrected scan lens, F-θ, telecentric scan lens** chosen for the design. Although F-θ is not a necessary property, it is inherent in this lens design. Based on these properties, the equations relating the scanning lens to the front surface of the fundus lens can be determined.

Wavelength	Focal Length (mm)	Scan angle (±)	Scan length (mm)	Entrance Pupil (mm)	Spot Φ (μm)	Front Working Distance (mm)	Flange Distance (mm)	Back Working Distance (mm)
450-650nm	60	15°	28	6	10	25.6	49.5	72.4

Table 14: Scanning lens property chosen for design
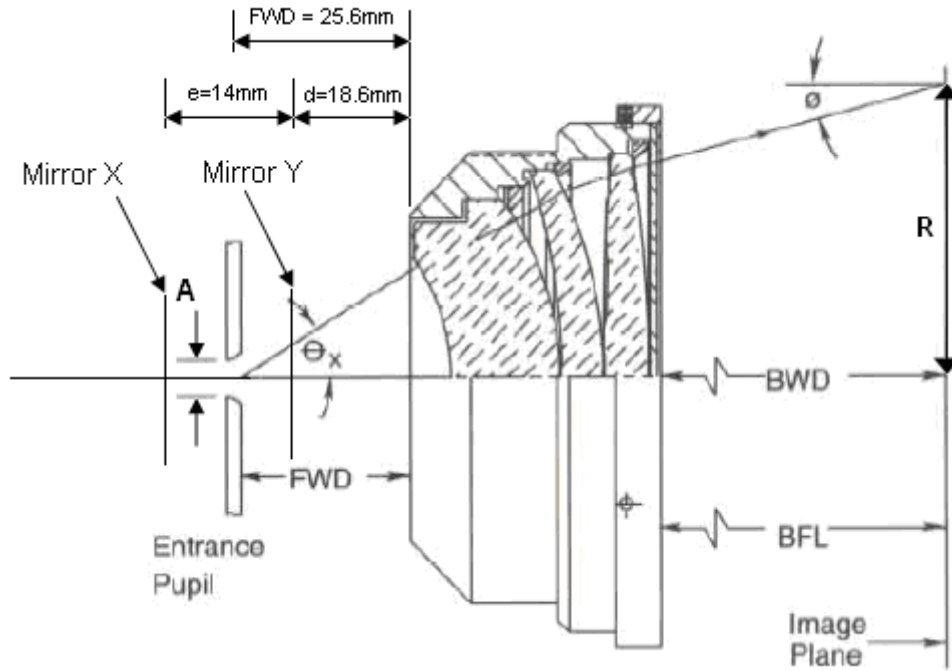
Figure 3.37: Diagram of a general scanning lens.
For a telecentric scanning lens, =0.

θ_x = maximum deflection angle allowed before vignetting occurs

ϕ = incident angle on the work surface or image plane.

A = Diameter of entrance pupil

FWD = the distance from the entrance pupil to the lens housing (Front Working Distance)

BWD = the distance from the work surface to the output side of the lens housing (Back Working Distance)

From Table 14, the FWD of the lens is 25.6mm, therefore the value of d and e can be chosen. The value is chosen such that the mirrors are placed as close as possible as long as the mirrors do not hit each other as they rotate. In this case, the value chosen is e = 14mm and d = 18.6mm. The definition for e and d can be found in Section 3.4.2.1

The entrance pupil is located at the front focal point of the scanning lens. In general, the position where the beam is deflected from the axis is positioned at the entrance pupil. For a two mirrors system, the origin of beam deflection is in between the mirrors[57]. It is best to position the mirrors as close together as possible; however most lens manufacturers have a recommended distance to be used for their lens.

If the origin of the beam deflection is moved off the entrance pupil location and away from the lens system, the allowable beam diameter and deflection angle will be reduced, if it is moved towards the lens system, the allowable beam diameter and deflection angle will be increased. For a two axis deflection system which has been displaced a distance L from the entrance pupil, and away from the lens system, the maximum laser diameter is A', where

$$A' = A[1 - (2L/A)\tan\theta],$$

θ = half the maximum deflection ,
L = offset distance of the beam deflection origin from the entrance pupil (focal point),
A = Diameter of entrance pupil.

Determining the spot size

The spot size on the image plane depends on: **input laser beam diameter**, **divergence** of the laser source and the **effective focal length** of the lens system.

If a Gaussian source is used, the spot size, $S = \dfrac{4M^2 \lambda f}{\pi D}$,

If a "tophat" intensity beam is used, $S = \dfrac{2.44 \lambda f}{D}$.

λ = wavelength
f = lens focal length
D = input beam diameter at the lens ($1/e^2$ point)
M^2 = beam mode parameter (Measures the ratio of divergence angles of the actual and ideal beams)

In the proposed design, a multimode step-index fiber is selected; therefore the beam emitted from the fiber will be of a "tophat" profile[58].

For non-telecentric lens, the off axis spot will be elongated proportionally to the output scan angle (ϕ), where:

Elongated off axis spot size, $S_e = \dfrac{S}{\cos\phi}$
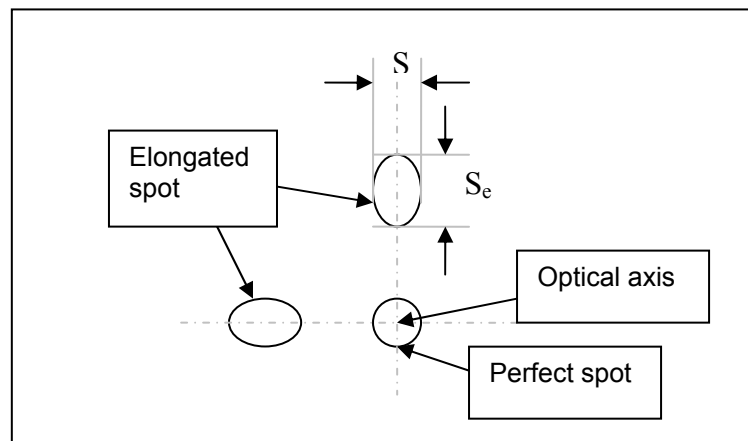
Figure 3.38: Changes in off axis spot shape and size for non telecentric lens.

Determining position of the focused spot

The displacement of the beam from the optical axis on the scanning plane, Y, for

      (i)   A F-θ lens is, $r = F\theta$ _____(1)

      (ii)   a lens without the F-θ characteristic is, $r = F\tan\theta$ _____(2)

where,   F = Effective Focus Length of the lens,

           θ = Half of the divergence angle from the stop plane

Using the same symbol as in Section 3.4.2.1, the formulas for relating the scanning coordinates by the galvanometer to the position of the incident beam on the fundus lens is shown below:
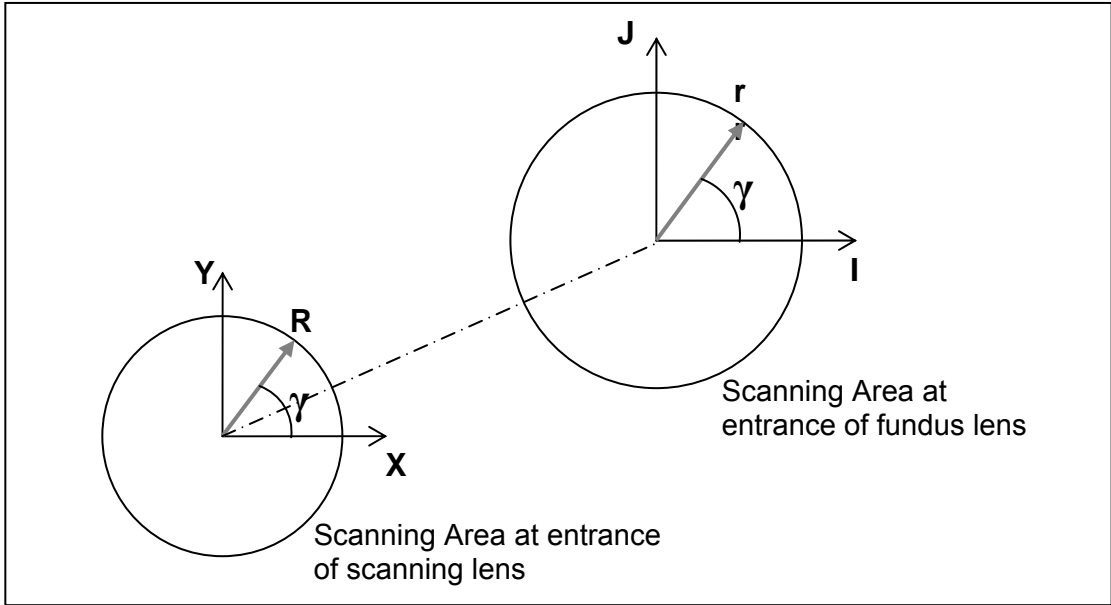
Figure 3.39: Relationship between scanning area at entrance of the scanning lens and entrance of the fundus lens.

$$R_i = \sqrt{X_i^2 + Y_i^2}$$

$$L = d + \frac{1}{2}e$$

$$\tan\theta_i = \frac{R_i}{L_i}$$

$$\theta_i = \tan^{-1}\left(\frac{R_i}{L_i}\right)$$

As a F-θ lens is used, $r_i = F\theta_i$

Assuming that there is no distortion, and γ is the same at the scanning lens entrance and at the fundus lens entrance. Therefore $I_i = r_i\cos\gamma_i$ and $J_i = r_i\sin\gamma_i$, where

$$\gamma_i = \tan^{-1}\left(\frac{Y_i}{X_i}\right).$$

Based on these calculations, a plot of the relationship between θ_x and I, and θ_y and J is shown below:
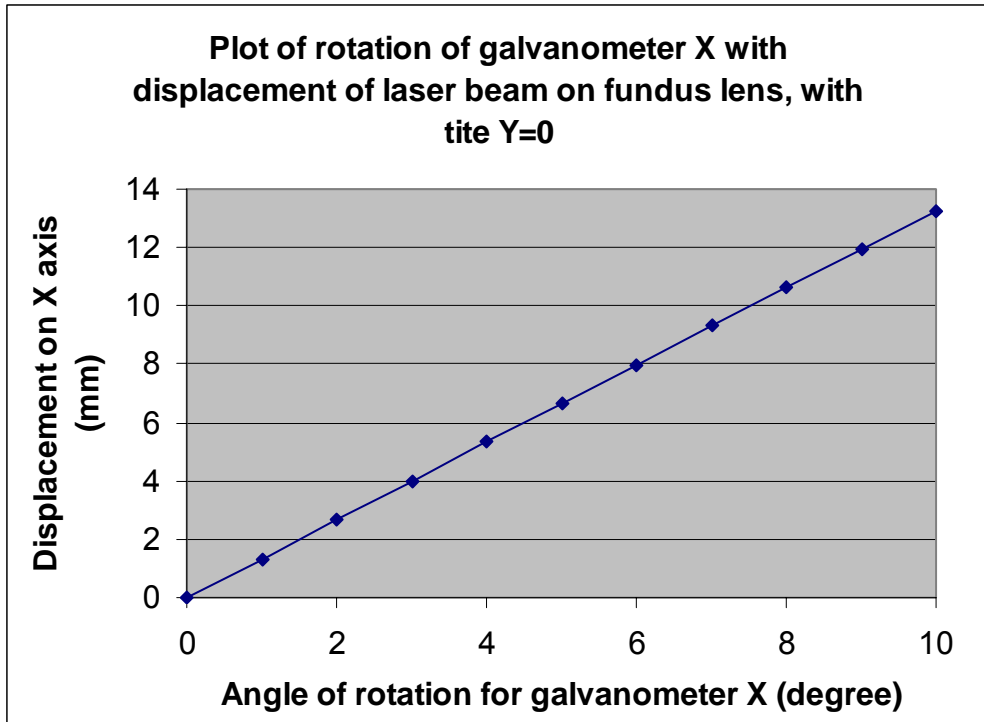
Figure 3.40: Plot of rotation of galvanometer X with displacement of laser beam on fundus lens, with θy=0°.
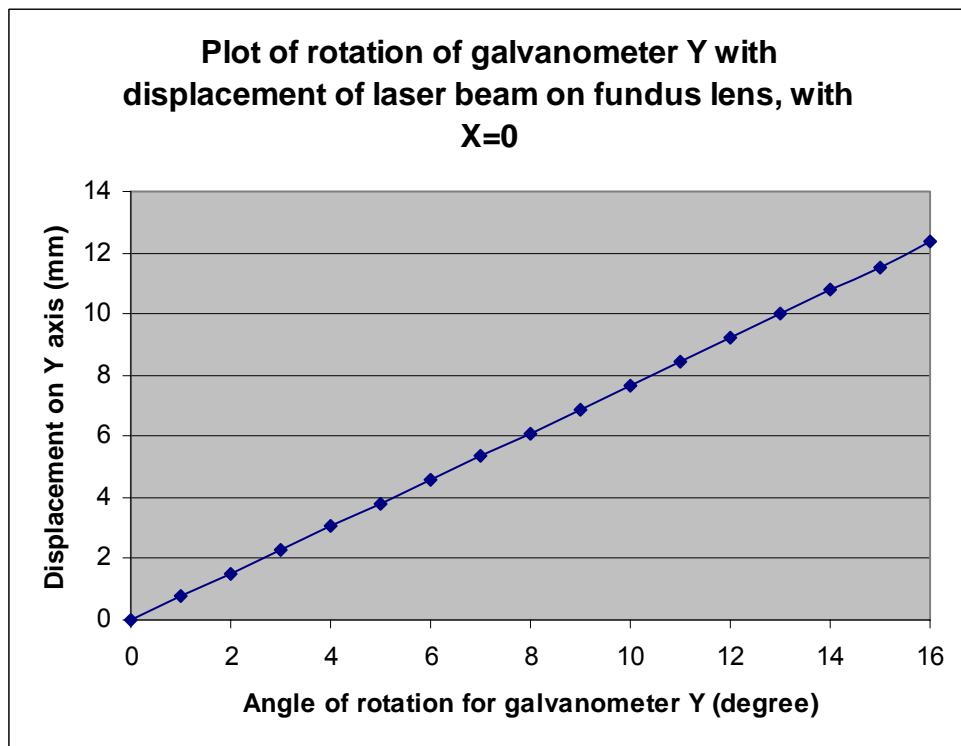
Figure 3.41: Plot of rotation of galvanometer Y with displacement of laser beam on fundus lens, with θx=0°.

θ-x in °	I (mm)
0.000	0.00
1.000	1.33
2.000	2.67
3.000	4.00
4.000	5.33
5.000	6.65
6.000	7.98
7.000	9.30
8.000	10.62
9.000	11.94
10.000	13.25

Table 15: θx (°) versus I (mm).

θ-y in °	J (mm)
0.000	0.00
1.000	0.76
2.000	1.52
3.000	2.29
4.000	3.05
5.000	3.81
6.000	4.58
7.000	5.34
8.000	6.11
9.000	6.88
10.000	7.65
11.000	8.43
12.000	9.20
13.000	9.98
14.000	10.76
15.000	11.55
16.000	12.33

Table 16: θy (°) versus J (mm).

From Figure 3.40 and Figure 3.41, the maximum rotation angle required by the galvanometer to achieve **I=11mm** is **θ_x=9.049°**, and to achieve **J=11mm** is **θ_y=15.576°** when the value of d=. I=11mm and J=11mm are the maximum displacement from the optical axis required in the system as the maximum aperture of the VOLK Super Quad 160 is 22mm.

3.4.2.3 Part 3 – Relationship between the fundus lens and the retina

From the result of the experiment in Section 3.2, the equation $\alpha_i = -6.96 r_i$ is obtained, where α_i is the angular displacement from the optical axis in degree, and r_i is in mm.

The position of the focused beam on an imaginary retina plane can be defined by α and γ. However it should be noted that this equation applies only to a plane in air as the index of refraction of the cornea and vitreous fluid were not taken into consideration.

$$\gamma = \tan^{-1}\left(\frac{Y}{X}\right)$$

$$= \tan^{-1}\left(\frac{d \tan \theta_y}{\left(d^2 + d^2 \tan^2 \theta_y\right)^{1/2} + e\right) \tan \theta_x}\right)$$

$$\alpha = -6.96 r$$
$$= -6.96(F\theta), \quad \text{where } \theta \text{ is in radian}$$

$$= -6.96 \times 60 \times \left\{\tan^{-1}\left(\frac{\sqrt{X^2 + Y^2}}{d + \frac{1}{2}e}\right)\right\}^C$$

$$= -417.6 \times \left\{\tan^{-1}\left(\frac{\sqrt{(d \sec \theta_y + e)^2 \tan^2 \theta_x + d^2 \tan^2 \theta_y}}{d + \frac{1}{2}e}\right)\right\}^C$$
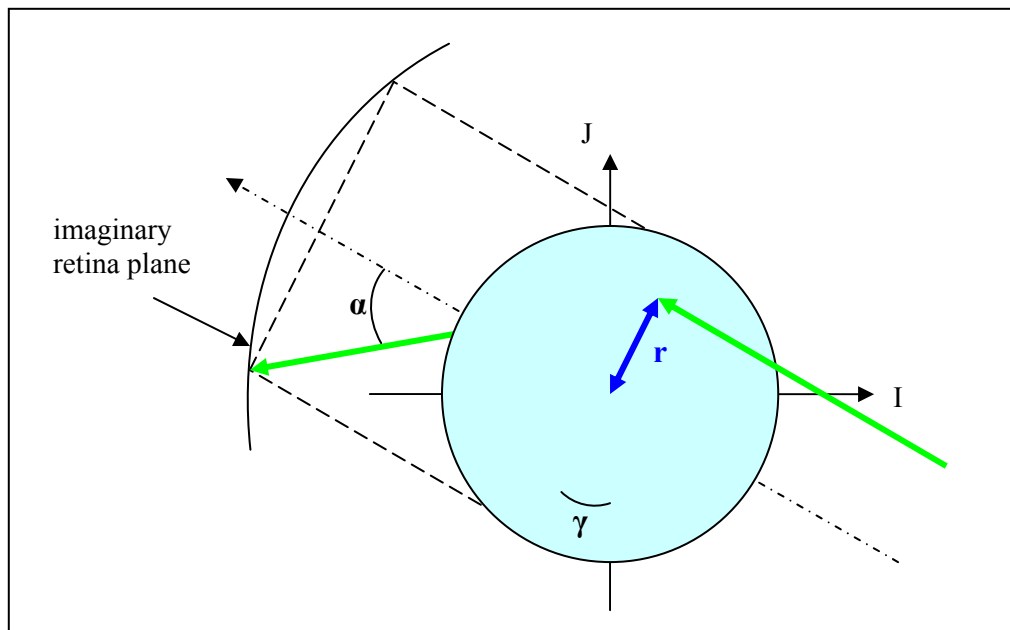
Figure 3.42: Diagram of the relationship between r, α and γ.

3.4.2.4 Discussion on aiming beam and summary

In current systems, the aiming beam positions the laser at the intended treatment area for validation by the ophthalmologist before the switch for the treatment laser is pressed. However if all 5000 spots are to be illuminated within the eye detection time, compared to only 56 spots used by the PASCAL system, the galvanometers would have to scan at a faster speed than what is specified above. Therefore the parts chosen for the system have to be reevaluated for their suitability. This factor will also influence the choice of shutter, described in Section 3.4.3.1

Future investigation to produce a surgical planner will be conducted on the treatment sequence and method. As it had not been ascertained how the treatment should be conducted and what role will the aiming beam plays, further development on this part of the system will have to be carried out as well. To conclude this section, a comparison of the design requirement and the system capability is shown in the table below.

Parameter	Design Requirement	System design Capability
Object work area (Fundus lens front image plane)	Area of 22mm in diameter	Maximum lens scan area of 28mm in diameter
Field of view of retina	150°	160° provided by VOLK lens
Number of scanning axes	2	2 axis galvanometer
Optical wavelength	532nm and 635nm	A colour corrected scanning lens is used (450nm to 650nm)
Spot size and shape	Constant throughout whole scanning area	A telecentric lens is used to obtain a constant spot shape when scanning onto the fundus lens. However the changes in spot shape caused by the VOLK lens had not been ascertained.
Maximum range of motion (Optical)	For Y = ± 16° For X = ± 10°	For Y = ± 80° For X = ± 80°
Maximum range of motion (Mechanical)	For Y = ± 8° For X = ± 5°	For Y = ± 40° For X = ± 40°

Maximum mirror damage threshold	420 W/cm^2 continuous wave	0.2MW/cm2 continuous wave
Minimum Optical Resolution	**50** μm (Smallest spot size in air)	10 μm (Property of lens)
Small Angle Step Response	10 ms (Based on minimum pulse duration available in current photocoagulation system)	0.130 ms with 3mm Y mirror, settled to 99%. Less than 0.130 ms with 3mm X mirror due to smaller inertia.

Table 17: Summary of design specification and the system capability in meeting the requirements.

3.4.3   Laser Delivery System

The laser beam delivery system consists of:

1.   Laser beam expander used as a beam reducer

2.   Flat Field Scanning lens

3.   Fundus lens
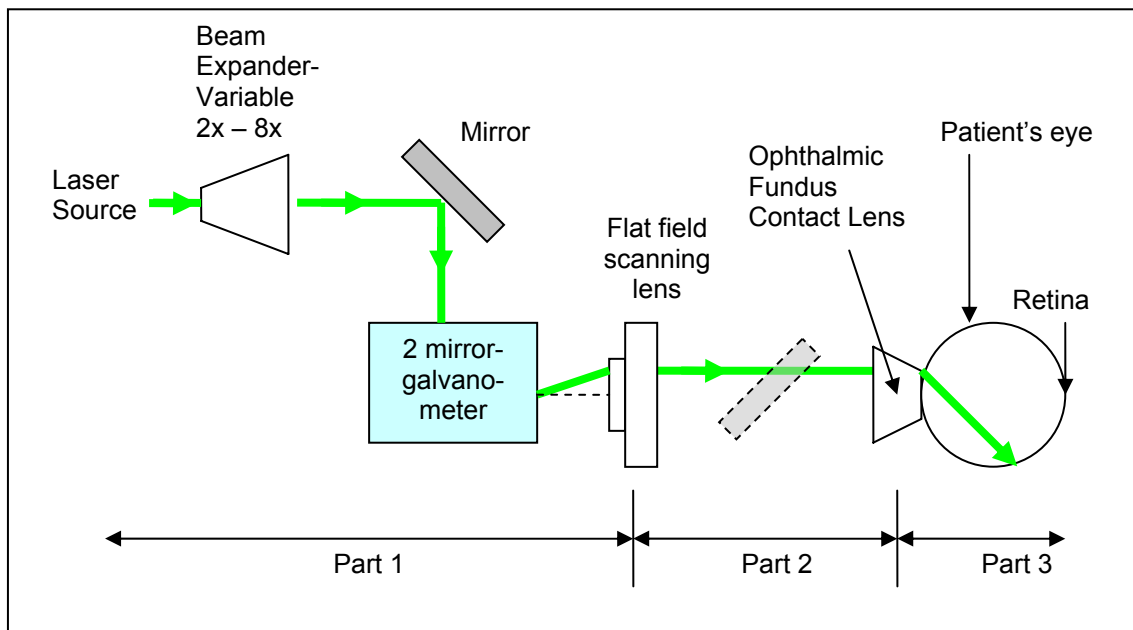
Figure 3.43: Laser delivery system

The laser delivery system consists of similar components as the beam steering system. The additional component is a beam expander/reducer to manipulate the diameter of the beam required. The focus of the design will be on calculating the changes in beam

diameter as the laser propagates through the system. The input beam diameter required from the laser source will also be determined. In this section, the flow of the discussion will start with Part 3 and Part 2, and then followed by Part 1 (Figure. 3.43).

3.4.3.1 Part 3 and Part 2 - Spot size calculation on fundus lens image plane

In using a parfocal system, as explained in Section 3.3.5, the input beam diameter to a stationery scanning lens is changed to obtain a different spot size. As we are using the near field Gaussian vs. tophat analysis:

The required input diameter for a "top hat" intensity beam to produce a spot size of S is,

$$D = \frac{2.44\lambda \times EFL}{S} \; .$$

λ (nm)	532	532
f (mm)	60	60
S (μm)	50	200
D (μm)	**1557.7**	**389.4**

Table 18: Required input beam diameter for the scanning lens for 532nm wavelength

λ (nm)	635	635
f (mm)	60	60
S (μm)	50	200
D (μm)	**1853.4**	**463.4**

Table 19: Required input diameter for the scanning lens for 635nm wavelength

The input beam diameter of the treatment beam at the scanning lens will range from **389.4 μm** to **1557.7 μm**, and for the aiming beam will range from **463.4 μm to 1853.4 μm**. This difference in beam diameter is not critical as the human eye would not be able to resolve the difference in spot size. In this system, the treatment beam takes precedence over the aiming beam, therefore parts will be chosen based on the treatment beam properties.

3.4.3.2 Part 1 - Apparatus for varying the spot size

From the range of spot size calculated above (389.4 μm to 1557.7 μm), the apparatus will require a magnification of at least 4x. In this design, a beam reducer function will be utilized to reduce the size of the beam emitted from the fiber delivery system. A motorized 2x to 8x laser beam expander is used to reduce the beam size by using the exit position as the entrance. However as the designed wavelength for the beam expander selected is at 532nm, there might be a slight variation in magnification with the 635mm aiming beam. This slight variation is assumed to be negligible in this design.

D_{output} (μm)	1557.7	389.4
Magnification	1/2	1/8
D_{input} (μm)	3115.392	3115.392

Therefore the beam diameter required from the fiber delivery system is **3115.392μm**. A summary of the design goals in term of the changes in beam diameter as it propagates through the system is illustrated in Figure 3.44. To achieve this, the collimated output beam from the fiber cable has to have a diameter of 3155 μm. This will be discussed in Section 3.4.4
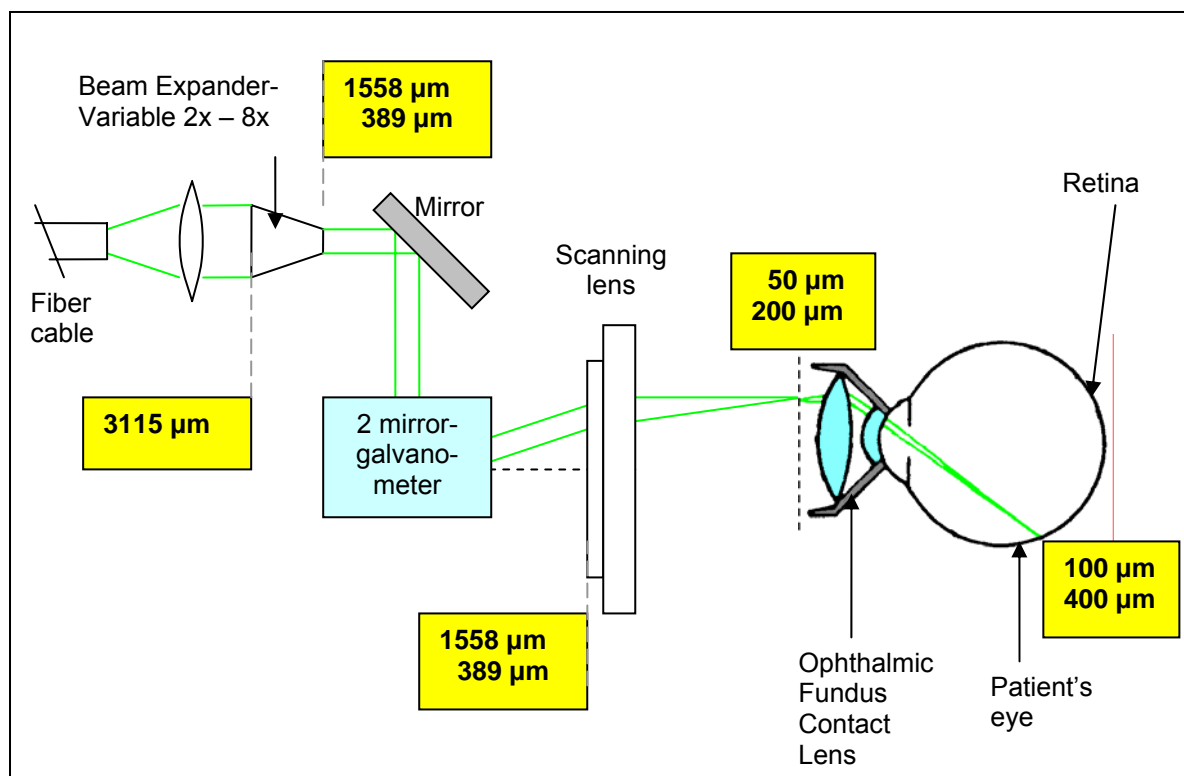
Figure 3.44: Overview of the desired changes in beam diameter as the 532nm beam propagates through the system

3.4.4 Laser Source System

The laser source system consists of the following components:

1. Laser source – treatment beam and aiming beam, shutter and beam splitter
2. Input Coupler
3. Fiber Optic Cables
4. Output Coupler

These components control the power of the laser, the pulse duration and the switching between the treatment laser and aiming laser.
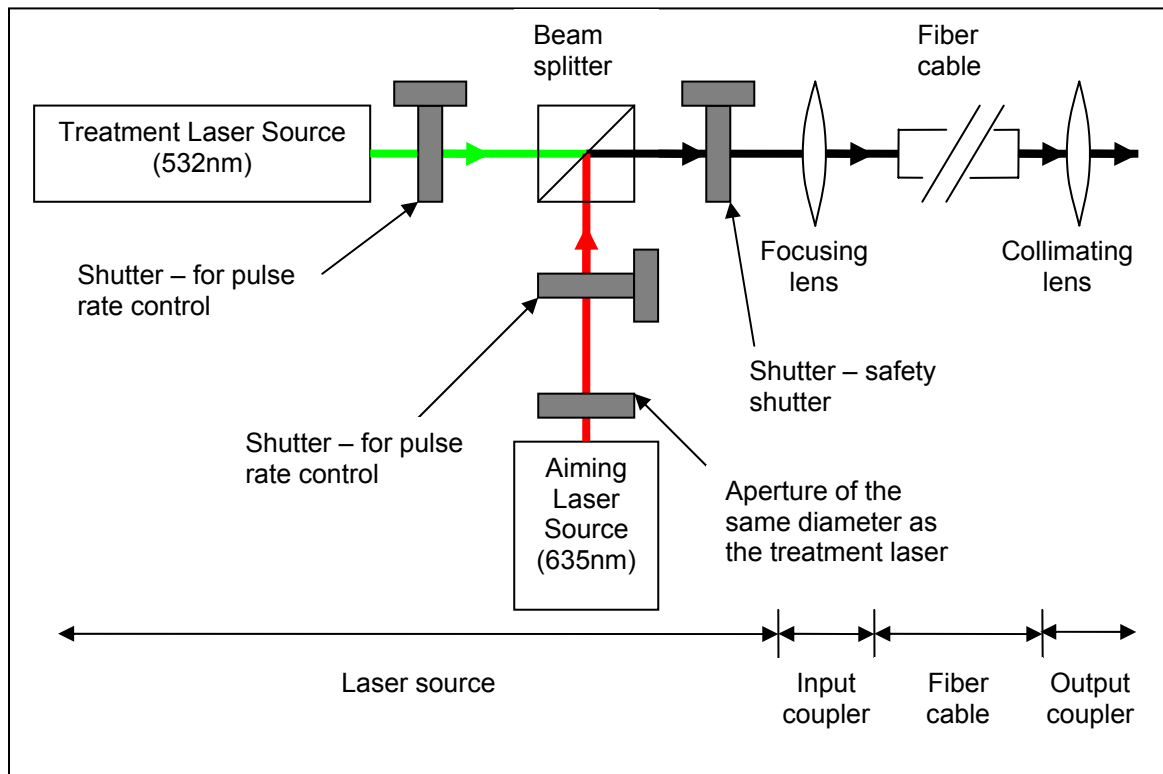
Figure 3.45: Laser source system

3.4.4.1 Laser Source

Overview on Gaussian laser beam

The laser beam emitted from the laser source has a Gaussian beam profile. Normally diameter of a laser beam is described using the diameter where the intensity falls to $1/e^2$ of its peak value. It encompasses 86.5 percent of the beam power and is about half of the actual beam diameter.
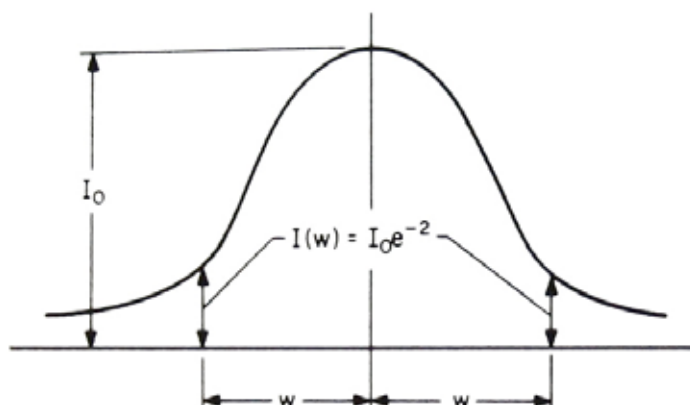
Figure 3.46: Gaussian beam intensity profile

The distribution of intensity in a Gaussian beam is illustrated in Figure 3.46 and can be described by equation[59]:

$$I(r) = I_0 e^{-2r^2/w^2}$$

where
      I(r) = the beam intensity at a distance r from the beam axis
      I_0 = the intensity on axis
      r = the radial distance
      e = 2.718…..
      w = the radial distance at which the intensity falls to I_0/e^2

In selecting mirrors and aperture for the laser system, incidence of beam truncation have to be taken into account to ensure that the desired power is transmitted across.

By integrating $I(r) = I_0 e^{-2r^2/w^2}$, we find the total power in the beam to be given by:

$$P_{tot} = \frac{\pi I_0 w^2}{2}$$

The power passed through a centred circular aperture of radius a is given by

$$P(a) = P_{tot}(1 - e^{-2a^2/w^2})$$

From this equation, the following table can be obtained:

a/w	0.8	1	1.2	1.4	1.6	1.8	2	3	4
Loss (%)	27.8037	13.5335	5.6135	1.9841	0.5976	0.1534	0.0335	0.0000	0.0000

Table20: Percentage of power transmitted due to different aperture to beam diameter ratio

Therefore an acceptable ratio would be **1.6** or more to ensure a **loss of less than 1%**.

Treatment Laser

A 532nm, continuous wave (CW), solid state diode-pumped laser will be used as a treatment beam. In Section 3.1.1, it has been ascertained that a 2W power source would be suitable for the proposed design. The laser source chosen emits a beam with a diameter of 2.25mm ± 10% ($1/e^2$ diameter) and $M^2<1.1$. M^2 is a measurement of beam quality where $M^2=1$ denotes an ideal Gaussian beam.

To account for beam truncation and ensure that at least 99% of the power is transmitted, the required minimum diameter for any aperture is 2.25mm x 110% x 1.6 = **3.96mm**.

As the laser source is a continuous wave source, a shutter is used to mechanically chop the laser beam to create the required pulses.

Aiming Laser

The laser beam for aiming can be a **diode laser, continuous wave (cw)** with a **635nm** wavelength with a maximum power of **0.4 mW**[60,61]. As the laser source is a continuous wave source, a shutter is used to mechanically chop the laser beam to create the required pulses.

Beamsplitter

A standard cube beam splitter is used to combine the optical path of the treatment laser and the aiming laser beam[62].

<u>Shutter</u>

Three shutters will be used in the system – two will be used to control the laser pulses for the treatment and aiming beam while the third is positioned just before the input coupling optics to provide a safety measure against accidental irradiation of the patient's eye. The design requirement and system capability of the shuttle is summarized in the table below:

Parameter	Design Requirement	System design Capability
Minimum exposure time	10 ms	2 ms
Maximum power threshold	0.621 Watt/mm^2 based on minimum treatment laser beam diameter of 2.25mm – 10%, and maximum power of 2 watt	5W/mm^2
Wavelength	532nm and 635nm	Aluminum coated plate for visible light range
Frequency required	If pulse rate of 10ms duration is used, therefore 1/ 10 ms = 100Hz	150 Hz
Beam width	3.96mm for power transmission of 99%	Aperture 6mm

Table 21: Design specification and system capability of shuttle
(See Appendix 6 for catalogue)

3.4.4.2 Input Coupling Optics

The purpose of this optical assembly is to couple the energy from the laser into the core of the fiber. To function properly, the system must meet the following criteria:

1. The cone angle of the input beam must be less than the acceptance angle of the fiber. Any energy arriving at a greater angle will not be completely reflected at the first core-clad intersection; the energy escaping into the cladding will be lost, and may also cause catastrophic failure.

2. The energy focused on the fiber should be lower than the power threshold of the fiber.

3. **$D_s < D_f$** , the diameter of the focused spot (D_s) must be smaller than the core diameter of the fiber (D_f), and the spot must be aligned to the center of the core to prevent losses and failure of the fiber cladding[63].
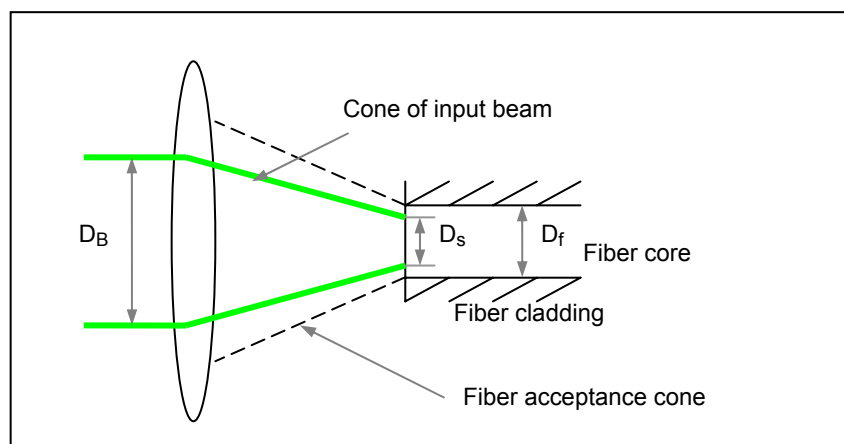
Figure 3.47: Focusing laser beam into the fiber core

To achieve condition 1:

$$f_{lens} \geq \frac{D_B}{2NA_f}$$

Where, D_B = Diameter of laser beam,

         NA_f = Numerical aperture of fiber.

Therefore, $f_{lens} \geq \frac{3.96mm}{2(0.22)} = 9mm$

Therefore the focus length of the lens must be **more than 9mm.**
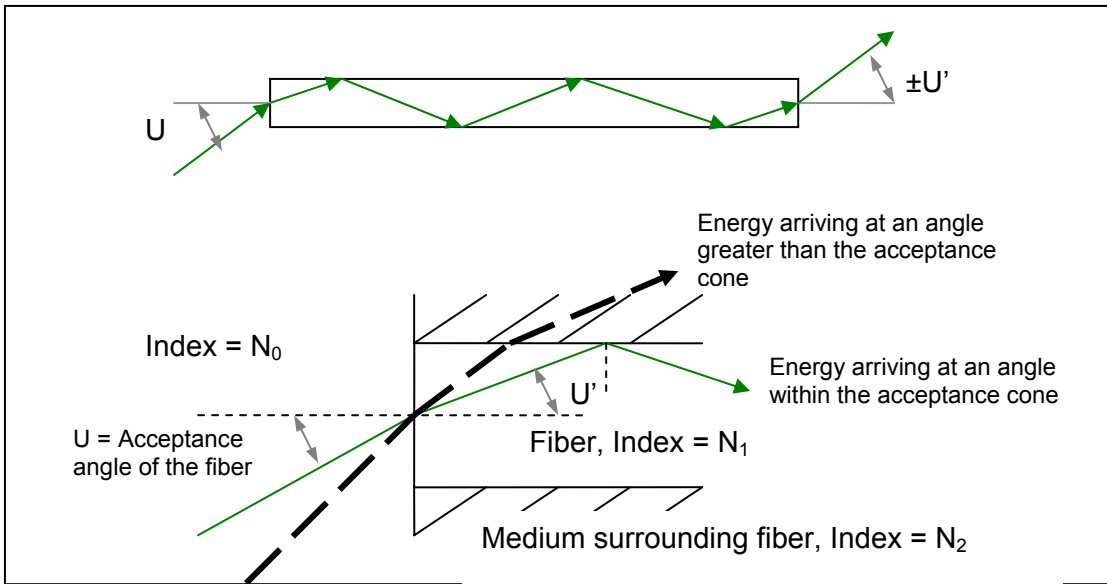
Figure 3.48: Angle of incidence on fiber surface

To achieve condition 2:

Energy threshold of the fiber chosen is **1GW/cm^2 CW**. This is to ensure that a small enough spot can be focused on the fiber without causing damage, thereby allowing a more compact design for the input coupling optic. For laser beams with a Gaussian intensity profile, multiplying the power density of the laser by two for safety is required to accommodate the peak power density at the center of the beam[64]. Therefore, to ensure that the energy focused on the fiber is less than the energy threshold:

$$2 \times \left(\frac{2\,W}{\pi \left(\dfrac{D_s}{2} \right)^2} \right) \leq 1\,000\,000\,000\;W \cdot cm^{-2}$$

$$0.714\;\mu m \leq D_s$$

Therefore the focused spot size should be **more than 0.714 μm** in diameter.

To achieve condition 3:

In focusing a collimated laser beam, $y_1 \approx f\theta_2$ [65]
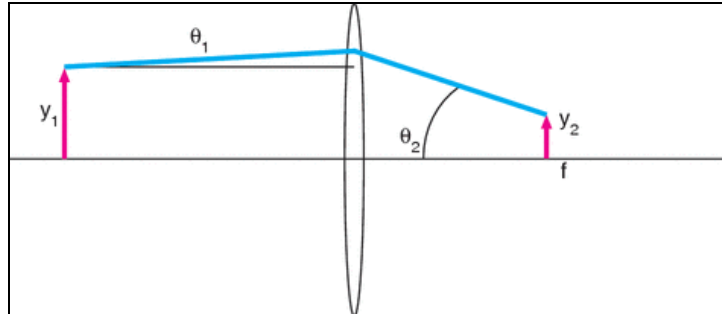
Figure 3.49: Focusing a collimated laser beam

From the concept of optical invariant, $\dfrac{y_1}{\theta_2} = \dfrac{y_2}{\theta_1}$ because the product of radius and divergence angle must be constant.

Therefore, $y_2 = f\theta_1$

$$\frac{D_s}{2} = f_{lens}\theta_B$$

Where, f_{lens} = focal length of lens ,

                    θ_b = divergence of laser beam

From the previous section, it had been determined that the minimum focused spot diameter (D_s) is **0.714 μm**

Therefore,

$$2f_{lens}\theta_B \geq 0.000714 \quad mm$$
$$f_{lens} \geq \frac{0.000714 mm}{2(0.25 mrad)}$$
$$f_{lens} \geq 1.428 \quad mm$$

Conclusion:

Taking into account all the three conditions stipulated in the previous section, the lens focal length should be **more than 9mm** and have a clear aperture of more than **3.96mm.**

The focusing lens chosen have a focus length of **11mm** and a clear aperture of **5.5mm**, and the collimator head uses a **SMA connector**. Therefore the fiber cable should also use a SMA connector for ease of assembling. However the lens chosen is not achromatic hence a slight adjustment had to be made to the distance between the lens and the fiber when setting up the prototype.

In this design, a fiber with high energy threshold is chosen. If a fiber with moderate energy threshold of 100kW/cm^2 CW is used, the calculated minimum focus spot diameter is 71.36 μm, and the required focal length of the lens would be 142mm in diameter-which would not allow for a compact design

3.4.4.3 Fiber Optic Cables

For medical laser power delivery, a multimode step-index fiber will be suitable, especially if high power densities are required[66]. The core of a step-index fiber has a uniform index of refraction right up to the cladding interface where the index changes in a step-like fashion, producing a top hat beam at the output[45].

The fiber chosen have a core diameter of **365μm,** numerical aperture of **0.22** and a power threshold of **1 GW cm^{-2}**. From the previous section, a lens of 11 mm focal length is chosen.

$$D_s = 2 f_{lens} \theta_B \quad = \quad 2 \times 11 mm \times 0.25 mrad \quad = \quad 5.5 \mu m$$

The focused spot is 66 times smaller than the fiber core which will ensure the safety of the design.

From the manufacture chart, attenuation in fiber is 0.018db/m for a wavelength of 532nm. This would mean a power loss of 0.4% for every meter. If a length of 5 meters is used, this would translate to a **power loss of 2%**.

$$A(dB) = 10 \log \left(\frac{P_{in}}{P_{out}} \right)$$

For this choice of fiber, future designs consideration have to ensure that the minimum bend radius is kept above 47mm to ensure long term usability of up to 20 years. For short tem bending (less than 60 minutes), the minimum bending radius is 29mm.

3.4.4.4 Output Coupling Optics
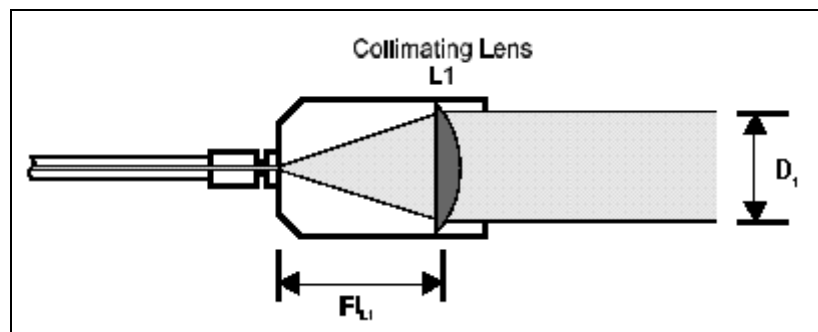
**Figure 3.50: Output Optical Assemble. Adapted from
http://www.uslasercorp.com/envoy/fobdstep.html**

The laser beam exiting from the fiber core will be rapidly diverging and has to be straightened by a collimating lens ($L1$), positioned at a distance of Fl_{L1} from the exit face of the fiber, where Fl_{L1} is the focal length of lens $L1$.

As the laser energy is delivered through a step index fiber, the beam will expands to fill the fiber core as it passes through the fiber. Therefore, the beam profile, at the exit face of the fiber, is a top hat, with a diameter equal to the fiber core diameter. This phenomenon is independent of the diameter of the beam when it enters the fiber.

The selection of the focal length and clear aperture of the collimating lens ($L1$) depends on the numerical aperture (NA) of the fiber. The diameter of the lens should be about 2 mm bigger than the clear aperture of the lens to allow for mechanical mounting.

$$NA = N_0 \sin U_{max}$$

Where, N_0 = index of the medium where the image lies (For air, assume N_0=1)

U_{max} = half of the angle of "acceptance cone" of the fiber core

For a fiber with NA=0.22

$$\sin U_{max} = 0.22$$

$$U_{max} = \sin^{-1} 0.22 = 12.71°$$
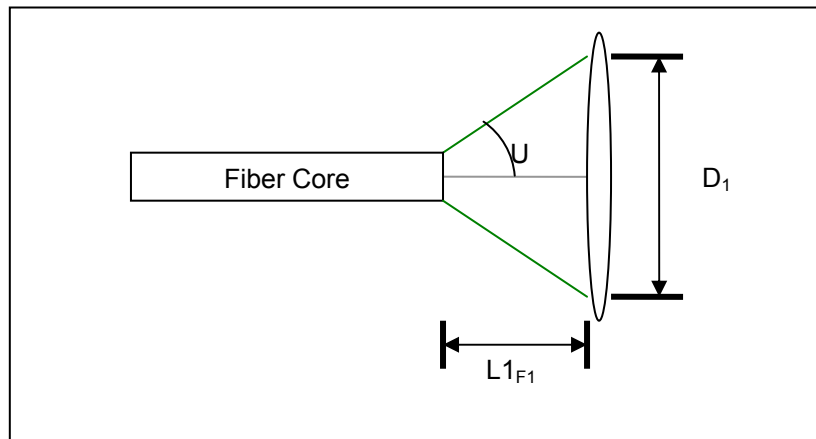
Figure 3.51: Relationship between the focus length and clear aperture of the collimating lens with the angle of acceptance of the fiber

From the Figure above,

$$\tan U \approx \frac{D_1}{2(L1_{F1})}$$

Where, U = half the angle of the cone formed by the lens aperture and focal length.

D_1 = Clear aperture of the collimating lens

To ensure that the beam from the fiber is transmitted without loss,

$$U \geq U_{max}$$

Therefore, $\quad NA_{lens} \geq NA_{fb}$

As the required output beam diameter required is **3115.392μm** (refer to Section 3.4.3), the focal length required for the lens can be determined.

Assuming sin U ≈ tan U, (for small angle approximation)

$$\frac{D_1}{2(L1_{F1})} \approx 0.22$$

$$L1_{F1} \approx \frac{3.12mm}{2(0.22)}$$

$$L1_{F1} \approx 7.09mm$$

In conclusion, the collimating lens required must have a **numerical aperture of more or equal 0.22**, a **focal length of about 7.09mm**, **and a clear aperture of more than 3115.392μm**. An achromatic lens is desired as to accommodate the usage of 2 different wavelengths.

The lens selected for the current system has a **focal length of 8mm**, numerical aperture of **0.5**, and a **clear aperture of 8mm**.

The beam diameter emitted from a lens with a focal length of 8 mm is **3.5mm**. To obtain the desired beam diameter of 3.1mm, a lens of 7.09mm focal length has to be custom made.

With an output collimated beam diameter of 3.5mm, the actual changes in beam diameter as the treatment beam propagates through the systems is shown in Figure 3.52.
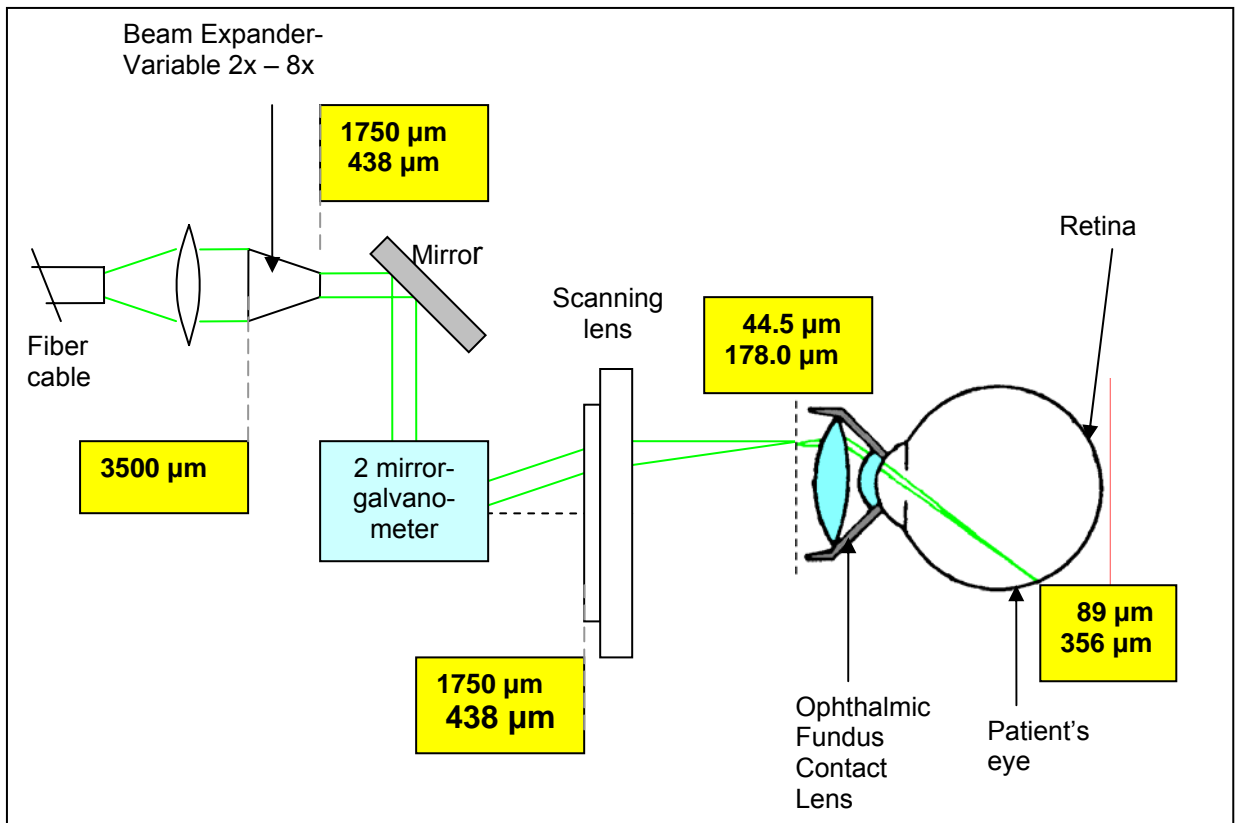
Figure 3.52: Overview of the actual changes in diameter as the 532nm beam propagates through the system

4 DISCUSSION, CONCLUSION AND RECOMMENDATION

4.1 DISCUSSION

4.1.1 Integration of Medical – Engineering expertise

The development of this novel system required intensive research in both medical and engineering disciplines. It was essential to understand the anatomy and physiology of the eye, background of diabetic retinopathy and past and present treatment procedures. After identifying the medical requirements, further research that required engineering expertise was integrated to help develop the most appropriate solution. During this process, there was a need to acquire in-depth understanding of the principles of optics, various existing imaging methods, scanners and laser delivery systems. Further review and analysis of various eye treatment techniques were also performed to determine the suitability of suggested solutions. A vast selection of alternative treatment methods was made available, taking into account of the advantages and disadvantages.

The collaboration with engineering staff from the Computer Integrated Medical Intervention Laboratory has helped solved much of the technical challenges faced throughout the entire development process. Experiments and simulations were performed while recommendations and opinions were suggested at regular meetings. The planning of the proposed system was reviewed and revised before it was confirmed in this final report.

4.1.2 Comments on the relevance of the development of a Controllable Laser Delivery System for Diabetic Retinopathy

Currently, a company called Optimedica has already developed a method for scanning the laser onto the retina in the PASCAL® system[53]. However the PASCAL system only delivers up to a maximum of 56 spots within a space of 4.4mm x 4.4mm in a predetermined array at one press of the switch. Therefore the novelty of this project lies in the following area:

(1) The overall system contains a suction device for eye fixation.

(2) The system uses trans-sclera illumination instead of a slit lamp.

(3) The laser beam can be scan onto the whole treatment area using the galvanometer scanners.

(4) A CCD camera is used in place of a slit lamp (biomicroscope), which would allow the system to be used for diagnosis and for capturing the image of the retina.

A CCD camera with the relevant resolution (4) was also selected and implemented in the engineering drawings in Appendix 4.

<u>Comments on the proposed observatory device design</u>

The observatory device was designed with an average human sized eyeball as reference. During the process of drafting the plans of the suction and illumination ring, a constraint of placement area over the cornea was noted. To overcome the limitation, CAD software was used to provide an excellent overall view of the observatory device before decisions were made on final design and dimensions.

When vacuum forces are applied, the coupling gel will likely be sucked into and obstruct the outlets on the suction ring. To overcome this complication, the suction ring has to be positioned in place and activated prior to the assembly of the gel coated VOLK® lens.

This system was designed to ease the fabrication process and avoid the need for costly molding. As such, the use of sheet metal bending and assembly technique was proposed for the various components such as the suction and illumination chamber and the general encasement of the device. The suction chamber was also designed for easy dismantling so as to allow regular servicing and maintenance.

Comments on the proposed optomechanical system

The optomechanical system is designed using off the shelf parts available from distributors and suppliers. The parts are chosen so as to closely meet the design specification of the system. However some difficulties were faced in obtaining an exact match for parts such as the beam expander/reducer and collimating lens.

The motorized beam expander/reducer used for the system is too large, as it is able to accommodate a laser beam of up to 8mm, whereas the system only requires a beam diameter of up to 3.5 mm. A more compact system could be custom made to create a smaller scanning system.

The spot size delivered is not an exact match of the design goals set up in Section 2. The system delivered a spot size range of 89μm to 356μm onto the retina as opposed to the desired range of 100μm to 400 μm for the treatment beam (532nm wavelength). Nonetheless, it is able to meet the requirement to perform a scatter treatment that requires a spot size range of 200μm to 300 μm (Section 3.1.1).

In addition, the proposed system has a footprint of 250cm x 430cm x 120cm. This is still quite bulky and patient may not feel safe enough to lie under the scanning device as it is lowered toward the eye.

In the design of the housing for the optomechanical system, care had been taken to ensure all parts are optically aligned. Any changes to the design in the future have to ensure that the conditions (1) and (2) illustrated in Figure 4.1 is adhered to, as these conditions are determined by the properties of the lens (Table 14 and Figure 3.37). These conditions refer to the distance between the mirror and the lens, and the Back Working Distance of the lens.

<u>Safety and feasibility</u>

The proposed integrated system addresses the reliability and safety issues concerning the selection of various solutions. Every proposed implementation has to withstand rigorous evaluation and the safety margins of critical components such as the vacuum pressure for the suction ring, illumination level for trans-sclera imaging and laser parameters had to be determined through animal testing as conducted by various researchers.

Finally, the design was reviewed by a panel of ophthalmologists and engineers to ensure its feasibility.

4.2   CONCLUSION

In general, the proposed system has been conceptualized to minimize any discomfort that may be experienced by the patient undergoing the procedure of photocoagulation. This is achieved by allowing the patient to rest comfortably in a supine position and in a close proximity with the ophthalmologist for a sense of assurance. Such a posture will also reduce an additional plane of potential movement (anterior – posterior motion while in the upright position as encountered in existing photocoagulation slit lamp units). All these factors will contribute to the ease of performing the laser photocoagulation procedure with greater success and faster recovery.

The novel setup will allow the ophthalmologist to carry out the laser operation with greater efficiency due to the improved ease of handling the observatory device. The manual manipulation of the VOLK$^{®}$ lens is minimized such that its primary function is the provision of the primary magnification for trans-sclera imaging without the need to function as a 'laser beam director'. Hence, the improved imaging coupled with a precise control of the laser delivery sequence will reduce tremendously the duration for each treatment and increasing the efficacy many folds.

The general design of the system allows for flexibility and ease of performing the treatment over a wide range of patients with different needs and requirement.

Furthermore, the need for manufacturability, safety and ease of maintenance has also been taken into account.

An optomechanical system has been designed to perform laser scanning in the treatment of diabetic retinopathy and is illustrated in Figure 4.1. Additional illustration of the final design can be found in Appendix 8. A housing to assemble the different parts had also been designed for the system. In Figure 4.1, it can be seen that the observatory device can be attached to the scanning system using 4 screws. Detailed engineering drawings of the different parts and the assembly of the system can be found in Appendix 7.

Parts for the laser source system had also been selected. However the housing for the parts had not been designed. A schematic illustrating the arrangement of the parts for the laser source system can be found in Figure 4.3. A list of all parts used in the laser delivery and beam steering system, laser source system and vision system has been compiled in Appendix 5 for reference.

This system is able to meet the design specification stated in Section 3.1. A comparison of the system capabilities and specification required can be found in Table 22.

A flowchart to illustrate the role of each part as the system is put into operation is shown in Figure 4.2. For the convenience of the reader, a schematic of the parts mentioned in the flowchart is illustrated in Figure 4.3.
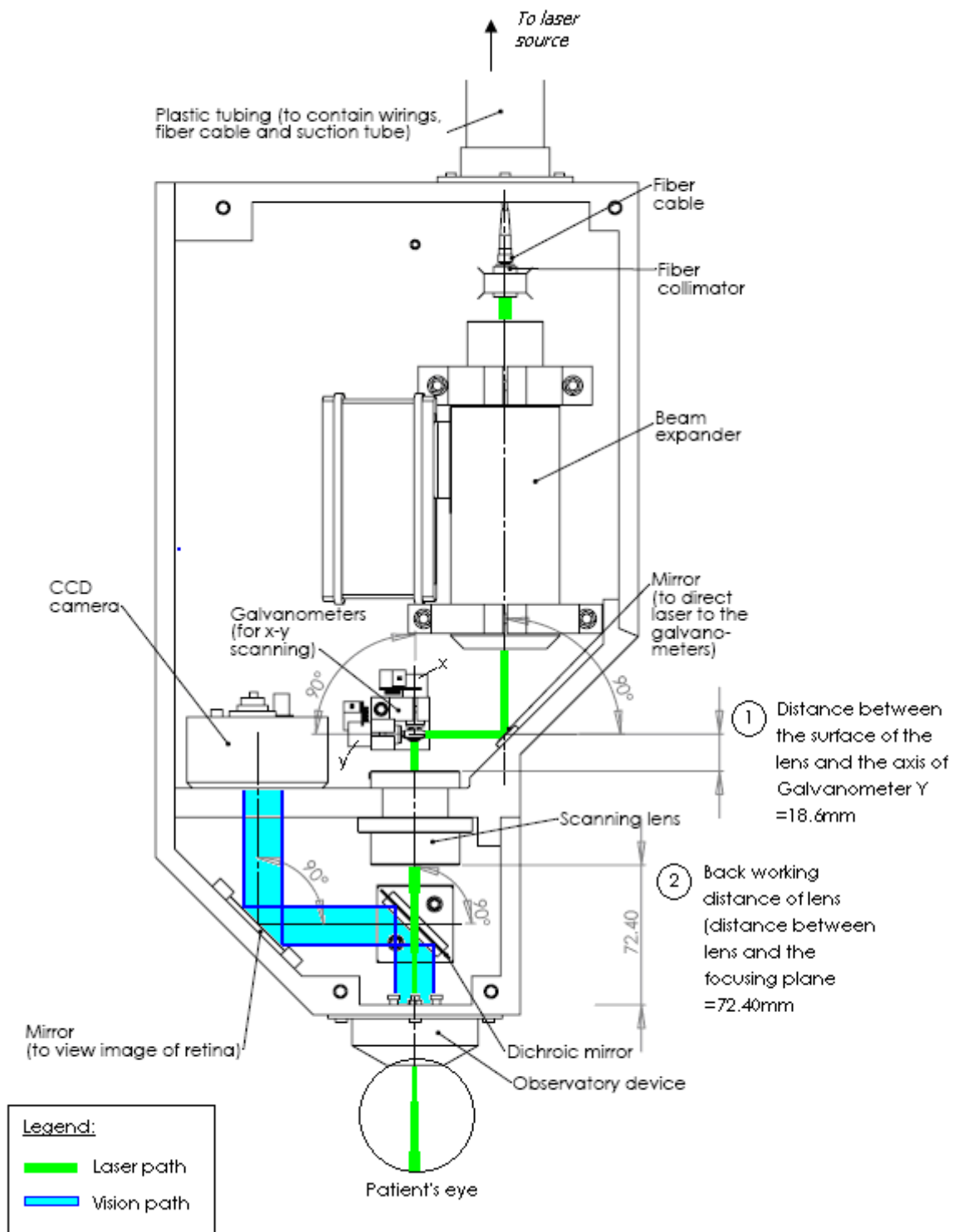
Figure 4.1: Optomechanical system to perform laser scanning for treatment of Diabetic Retinopathy. An exploded view of the drawing can be found in Appendix 7.

	Parameter	Design Requirement	System design Capability
Optome-chanical scanning system	Object work area (Fundus lens front image plane)	Area of 22mm in diameter	Maximum lens scan area of 28mm in diameter
	Number of scanning axes	2	2 axis galvanometer
	Maximum range of motion (Optical)	For Y = ± 16° For X = ± 10°	For Y = ± 80° For X = ± 80°
	Maximum range of motion (Mechanical)	For Y = ± 8° For X = ± 5°	For Y = ± 40° For X = ± 40°
	Maximum mirror damage threshold	420 W/cm^2 continuous wave	0.2MW/cm2 continuous wave
	Small Angle Step Response	10 ms (Based on minimum pulse duration available in current photocoagulation system)	0.130 ms with 3mm Y mirror, settled to 99%. Less than 0.130 ms with 3mm X mirror due to smaller inertia.
Vision system	Field of view of retina	150°	160° provided by VOLK lens
Laser delivery system	Optical wavelength	532nm and 635nm	A colour corrected scanning lens is used (450nm to 650nm)
	Spot size and shape	Constant throughout whole scanning area	A telecentric lens is used to obtain a constant spot shape when scanning onto the fundus lens. However the changes in spot shape caused by the VOLK lens had not been ascertained.
	Spot size on retina	100μm - 400 μm	89 μm - 356 μm
	Spot size in the air	50μm - 200 μm	44.5 μm - 178.0 μm
	Minimum Optical Resolution	50 μm (Smallest spot size in air)	10 μm (Property of lens)
Laser source system	System Power	2W	2W
	Frequency of treatment pulses	If pulse rate of 10ms duration is used, therefore 1/ 10 ms = 100Hz	150 Hz
	Minimum pulse duration	10 ms	2 ms
Overall	Footprint	-	250cm x 430cm x 120cm

Table 22: Summary of design specification and the system capability of the overall design
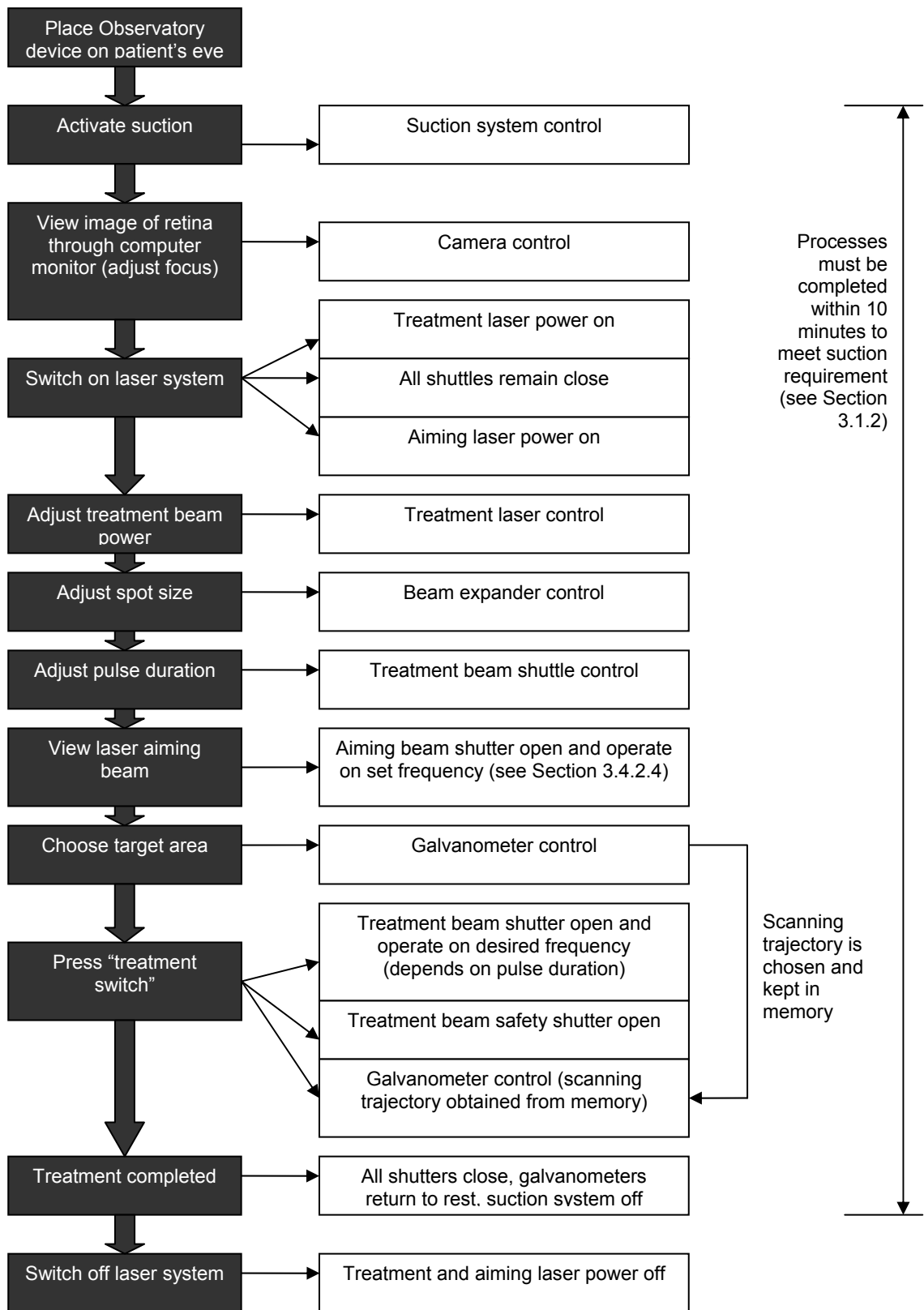
Figure 4.2: Flowchart of treatment procedure and function of the parts used

Flowchart content:

- Place Observatory device on patient's eye
- Activate suction → Suction system control
- View image of retina through computer monitor (adjust focus) → Camera control
- Switch on laser system → Treatment laser power on / All shuttles remain close / Aiming laser power on
- Adjust treatment beam power → Treatment laser control
- Adjust spot size → Beam expander control
- Adjust pulse duration → Treatment beam shuttle control
- View laser aiming beam → Aiming beam shutter open and operate on set frequency (see Section 3.4.2.4)
- Choose target area → Galvanometer control
- Press "treatment switch" → Treatment beam shutter open and operate on desired frequency (depends on pulse duration) / Treatment beam safety shutter open / Galvanometer control (scanning trajectory obtained from memory)
- Treatment completed → All shutters close, galvanometers return to rest, suction system off
- Switch off laser system → Treatment and aiming laser power off

Processes must be completed within 10 minutes to meet suction requirement (see Section 3.1.2)

Scanning trajectory is chosen and kept in memory

111

Figure 4.3: Schematics of laser photocoagulation system

## 4.3   RECOMMENDATION AND AREAS FOR FURTHER DEVELOPMENT
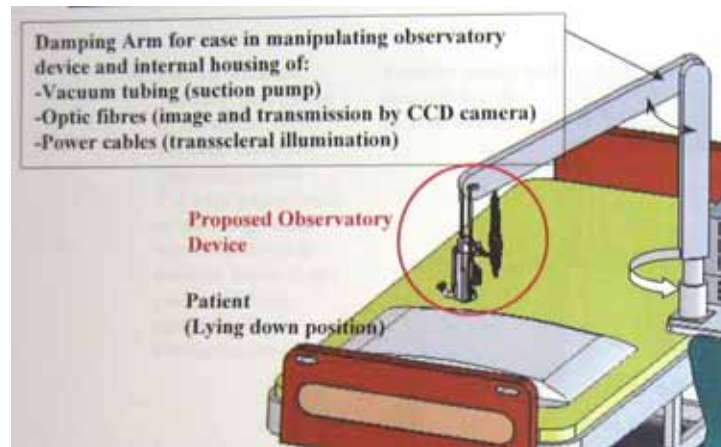
Figure 4.4: Damping arm

A damping arm has yet to be designed to allow for maneuverability of the scanning system and observatory device onto the patient's eye. A thorough investigation has to be conducted to understand the maneuverability required to place the entire system on the patient's eye as such a design could be intimidating to the patient.

Attempts should also be made in the future to test the observatory (illumination and suction system) and optomechanical (laser delivery system) as proposed in this report.

A central coordinating control system would also have to be implemented to control all the various functions in the system such as the scanning system, the shutters, the laser power, the beam expander, the CCD camera, the illumination system and the suction system.

The development of this laser delivery device has many other clinical applications beyond diabetic retinopathy. It can be particularly useful in uncooperative patients such as toddlers and the elderly, accident victims (who are unable to sit upright), patient with nystagmus and other circumstances whereby the usage of conventional slit lamp and lenses is considered suboptimal. The device can also facilitate and improve existing treatment modalities of various clinical conditions such as glaucoma (the use of gonio lenses can be restrictive), macula treatment that requires utmost precision and

'leaking' vessels in real time angiography. Further research will certainly help realize the potential of this novel trans-sclera laser delivery system.

5. REFERENCES

[1] Diabetic Retinopathy. Retrieved from: http://www.discoveryfund.com/diabeticretinopathy.html

[2] Fong D. S., et al. 2003. Diabetic Retinopathy. Diabetes Care. 26 (1): 599.

[3] Klein R., et al. 1984. The Wisconsin epidemiologic study of diabetic retinopathy II. Prevalence and risk of diabetic retinopathy when age at diagnosis is less than 30 years. Arch. Ophthalnol. 102: 520-526.

[4] Klein R., et al. 1984. The Wisconsin epidemiologic study of diabetic retinopathy III. Prevalence and risk of diabetic retinopathy when age at diagnosis is 30 or more years. Arch. Ophthalnol. 102: 527-532.

[5] Diabetic Retinopathy. Retrieved from: http://www.stlukeseye.com/Conditions/DiabeticRetinopathy.asp

[6] Finally, a silent killer gets some recognition. 2007, January 10. The Straits Times Interactive.

[7] Ministry of Health, Singapore, Epidemiology and Disease Control Department. 1998. National Health Survey 1998. Singapore: Ministry of Health.

[8] The Early Treatment Diabetic Retinopathy Study Research Group. Techniques for scatter and local photocoagulation treatment of diabetic retinopathy: Early Treatment Diabetic Retinopathy Study Report no. 3. Int Ophthalmol Clin. 1987; 27(4):254-64.

[9] Early Treatment Diabetic Retinopathy Study Research Group. Treatment techniques and clinical guidelines for photocoagulation of diabetic macular edema. Early Treatment Diabetic Retinopathy Study Report Number 2. Ophthalmology. 1987; 94(7):761-74.

[10] The Diabetic Retinopathy Study Research Group. Photocoagulation treatment of proliferative diabetic retinopathy. Clinical application of Diabetic Retinopathy Study (DRS) findings, DRS Report Number 8. Ophthalmology. 1981; 88(7):583-600.

[11] Fong DS. Changing times for the management of diabetic retinopathy. Surv Ophthalmol. 2002; 47 Suppl 2:S238-45.

[12] Aiello LP. The potential role of PKC beta in diabetic retinopathy and macular edema. Surv Ophthalmol. 2002; 47 Suppl 2:S263-9.

[13] Lund-Andersen H. Mechanisms for monitoring changes in retinal status following therapeutic intervention in diabetic retinopathy. Surv Ophthalmol. 2002; 47 Suppl 2:S270-7.

[14] Klein R. Prevention of visual loss from diabetic retinopathy. Surv Ophthalmol. 2002; 47 Suppl 2:S246-52.

[15] Gardner TW, Antonetti DA, Barber AJ, LaNoue KF, Levison SW. Diabetic retinopathy: more than meets the eye. Surv Ophthalmol. 2002; 47 Suppl 2:S253-62.

[16] Beetham W.P., et al. 1969. Rubylaser photocoagulation of early diabetic neovascular retinopathy: preliminary report of a long-term controlled study. *Trans Am Ophthalmol Soc.* 67: 39–67.

[17] L'Esperance F. A. Jr. 1972. Clinical photocoagulation with the krypton laser. *Arch Ophthalmol.* 87: 693–700.

[18] Little HL, Zweng HC, Peabody RR. 1970. Argon laser slit-lamp retinal photocoagulation. *Trans Am Acad Ophthalmol Otolaryngol.* 74: 85–97.

[19] JT Schwartz, GR Williams: Proceedings of Workshop on Television. Ophthalmology. Public Health Service Publication No 1490, 1965.

[20]Kelly DH, Crane HD. Research study of a fundus tracker for experiments in stabilized vision. NASA CR-1121. NASA Contract Rep NASA CR. 1968 May;1-45.

[21]Cornsweet TN, Crane HD. Accurate two-dimensional eye tracker using first and fourth Purkinje images. J Opt Soc Am. 1973; 63(8):921-8.

[22]Crane HD, Steele CM. Accurate three-dimensional eyetracker. Appl Opt. 1977; 17(5):691-705.

[23]Timberlake GT, Crane HD. Eyetracker-stabilized laser photocoagulation. Invest. Ophthalmol. Visual Sci. 1985; Suppl. 26, 38

[24]Bantel T, Ott D, Rueff M. Global tracking of the ocular fundus pattern imaged by scanning laser ophthalmoscopy. Int J Biomed Comput. 1991; 27(1):59-69

[25]Wornson DP, Hughes GW, Webb RH. Fundus tracking with the scanning laser ophthalmoscope. Appl. Opt. 1987; 26, 1500-1504

[26]Markow MS. The preliminary development of a robotic laser system used for ophthalmic surgery. Ph.D. dissertation 1985, The University of Texas at Austin

[27]Birngruber R, Gabel VP, Hillenkamp F. Fundusreflectometry:. A step toward optimization of retina photocoagulation. Mod. Prob. Ophthalmol. 1979; 18 383-390.

[28]Weinberg WS, Birngruber R. Lorenz B. The change in light reflection of the retina during therapeutic laser-photocoagulation. IEEE J Quan Elec. 1984, 20 1481-1489.

[29]Yang Y, Markow MS, Rylander HG 3rd, Welch AJ. Automatic control of lesion size in a simulated model of the. Eye. IEEE J. Quan Elec. 1990; 26 2232-2239.

[30]Jerath MR, Chundru R, Barrett SF, Rylander HG 3rd, Welch AJ. Preliminary results on reflectance feedback control of photocoagulation in vivo. IEEE Trans Biomed Eng. 1994; 41(2):201-3.

[31]Maharajh N. Use of reflectance for the real time feedback control of photocoagulation, Master's thesis 1996, The University of Texas at Austin.

[32]Inderfurth JH, Ferguson RD, Frish MB, Birngruber R. Dynamic reflectometer for control of laser photocoagulation on the retina. Lasers Surg Med. 1994; 15(1):54-61.

[33]BarrettSF, Jerath MR, Rylander HG 3rd, Welch AJ. Digital tracking and control of retinal images. Opt. Eng. 1994 33(1) 150–159

[34]Barrett SF, Jerath MR, Rylander HG 3rd, Welch AJ. Automated lesion placement in the rabbit eye. Lasers Surg Med. 1995; 17(2):172-7.

[35]Barrett SF, Wright CH, Oberg ED, Rockwell BA, Cain C, Rylander HG 3rd, Welch AJ. Development of an integrated automated retinal surgical laser system. Biomed Sci Instrum. 1996; 32:215-24.

[36]Barrett SF, Wright CH, Jerath MR, Lewis RS, Dillard BC, Rylander, HG 3rd, Welch AJ. Computer-aided retinal photocoagulation system. J. Biomed Opt. 1996; 1(1) 83-91

[37]Ferguson RD, Wright CH, Rylander HG 3rd, Welch AJ, Barrett SF. Hybrid tracking and control system for computer-aided retinal surgery. Proc. SPIE. 1996; 2673 32-41

[38]Wright CH, Barrett SF, Ferguson RD, Rylander HG 3rd, Welch AJ. Initial in vivo results of a hybrid retinal photocoagulation system. J Biomed Opt. 2000; 5(1):56-61.

[39]Naess E, Molvik T, Ludwig D, Barrett S, Legowski S, Wright C, de Graaf P. Computer-assisted laser photocoagulation of the retina--a hybrid tracking approach. J Biomed Opt. 2002; 7(2):179-89.

[40]Blumenkranz, M. S., Yellachich, D., Andersen, D. E., et al. 2006. Semiautomated patterned scanning laser for retinal photocoagulation. Retina, the Journal of Retinal and Vitreous Diseases. 26 (3): 370 – 376.

[41]Wei-Li Chen et al: "Ultrasound Biomicroscopic Findings in Rabbit Eyes undergoing Scleral Suction during Lamellar Refractive Surgery", Invest Ophthalmol Vis Sci, 2002; 43 (12) 3665-3672

[42]B.Ben Dor, A.S. Solomon, E.Svetliza, M.Kuszpet: "A New High-Resolution Retinal Camera: Pre Clinical Study", ARVO 2001, 3676-B818; IOVS 42(4), S683.

[43]Das T. 1991. Retinal laser optical aids. Indian Journal of Ophthalmology. 39:115-117. Retrieved from: http://www.ijo.in/article.asp?issn=0301-4738;year=1991;volume=39;issue=3;spage=115;epage=117;aulast=Das

[44]Dewey D. 1991. Corneal and retinal energy density with various laser beam delivery systems and contact lenses. SPIE Ophthalmic Technologies. Vol. 1423: 105-116.

[45]Fankhauser F., et al. 1996. Lasers, optical systems and safety in ophthalmology: a review. Graefe's Arch Clin Exp Ophthalmol. 234:473-487.

[46]Volk Optical Inc. 2006. Ophthalmic Catalog.

[47]Friedman E., Miller J. L. 2003. Photonics rules of thumb. SPIE Press: McGraw-Hill.

[48]Laser Damage threshold. Retrieved from: http://www.newport.com/Laser-Damage-Threshold/144932/1033/catalog.aspx

[49]Goldblatt N. R. 1990. Designing ophthalmic laser systems. In: The Photonics Design and Applications Handbook, Book 3, 36th Ed. Laurin Pittsfield Mass, 280-282.

[50]Original premarket 510(k) notification for the Nidek green laser photocoagulator model GYC-1000, issued by the Department of Health and Human Services, FDA US, to Nidek Incorporated in 2003.

[51]Selecta® glaucoma and cataract treatment catalogue. 2005. Lumenis group of companies.

[52]Kosnik, W., Fikre, J., Sekuler, R. 1986. Visual fixation Stability in Older Adults. Investigative Ophthalmology & Visual Science. 27: 1720-1725.

[53]Blumenkranz et al. May 2006. Patterned laser treatment of the retina. US Patent Application US2006/0100677 A1.

[54]Sagan S. F. 2004. Optical systems for laser scanners. In Marshall G. F. (ed.), Handbook of optical and laser scanning. New York: Marcel Dekker, 71-138.

[55]Dewey et al. December 1992. Combination lens system for retinal photocoagulator laser system. US Patent No. 5,171,242

[56]Montagu J. 2004. Galvanometric and resonant scanners. In Marshall G. F. (ed.), Handbook of optical and laser scanning. New York: Marcel Dekker, 417-476

[57]Scanning Lens Theory. Retrieved from http://www.specialoptics.com/Theory/Scanning%20Lens%20Theory.pdf

[58]Leong K.H., et al. 1996. Selecting a High-Power Fiber-Optic Laser Beam Delivery System. Laser Institute of America. Proceedings ICALEO. 81E: 173-182.

[59]Smith W. J. 1991. Modern optical engineering. McGraw-Hill International Edition.

[60]Maya R. Jerath, et al. 1992. Dynamic optical property changes: implications for reflectance feedback control of photocoagulation. J. Photochem. Photobiol. B: Biol., 16:113-126.

[61]Reis W. December 1989. Apparatus for treatment of the eye with the use of a laser. US Patent 4,884,884.

[62]Sagehashi et al. March 2005. Ophthalmologic photocoagulator and photocoagulation method therof. US Patent 6,869,428 B2.

[63]Optical Source to Fibre Coupling and Fibre Output. Retrieved from http://www.ics.trieste.it/TP_FibreOptics/FibreOptics2.aspx

[64]Laser Damage Threshold. Retrieved from http://www.newport.com/Laser-Damage-Threshold/144932/1033/catalog.aspx

[65]Focusing and Collimating. Retrieved from http://www.newport.com/Focusing-and-Collimating/141191/1033/catalog.aspx

[66]Fiber Optics. Understanding the Basics. Retrieved from http://www.photonics.com/content/handbook/2006/fiber/82240.aspx